PERFORMANCE EVALUATION AND OPTIMIZATION OF THE 600 KWP GRID-TIED SOLAR PHOTOVOLTAIC SYSTEM AT STRATHMORE UNIVERSITY, KENYA

AYORA EMMANUEL

REG NO.: J104/39125/2016

A THESIS SUBMITTED IN PARTIAL FULFILLMENT OF THE AWARD OF MASTER OF SCIENCE (RENEWABLE ENERGY TECHNOLOGY) IN THE SCHOOL OF ENGINEERING AND ARCHITECTURE OF KENYATTA UNIVERSITY

MARCH, 2024

DECLARATION

I declare that this Thesis is my original work and has not been presented for a degree in any other university or for any other award.

Signature …….. Date……

AYORA EMMANUEL

J104/39125/2016

SUPERVISORS

We confirm that the work reported in this thesis was carried out by the student under our supervision.

Signature…… Date: …….

Dr. Mathew Munji

Kenyatta University

Signature ……... Date: …….

Dr. Keren Kaberere

Jomo Kenyatta University of Agriculture and Technology

DEDICATION

This work is dedicated in a special reverence to God, who has been the wellspring of wisdom, knowledge, and comprehension. As my guiding light and protective refuge, His glory shines.

I also extend this dedication to my beloved wife Jilian Kerubo and my cherished children: Daniel Benjamin, Josiah Ayora, and Hadassah Grace. Their unwavering support and fervent prayers have propelled me to reach this milestone.

To my colleagues, the dedicated technicians of the EGP department, and all those who have contributed positively to this study, I extend my heartfelt gratitude. May divine blessings be upon each of you.

ACKNOWLEDGEMENT

The successful completion of this thesis owes its gratitude to several vital factors: robust health, boundless inspiration, and the blessings bestowed by the Almighty God. All praise to Him.

I extend heartfelt appreciation to my esteemed supervisors Dr. Keren Kaberere and Dr. Mathew Munji whose unwavering guidance has been instrumental throughout the journey of this research. Their ceaseless commitment to reviewing my work and providing comprehensive supervision has been pivotal in realizing this achievement.

A debt of gratitude is also owed to Dr. Francis Njoka, the Chair of the Energy, Gas, and Petroleum Engineering Department at Kenyatta University, for his invaluable support in realization of this research endeavour.

A special acknowledgment goes to Thomas Bundi from Strathmore University for enabling access to their PV system. Without this cooperation, the completion of this research would not have been conceivable.

A special acknowledgement goes to DAAD for supporting my academia through the scholarship granted without which this research would not have been successful.

To my family, I extend sincere thanks for being my steadfast support throughout my Master's Studies. Your unwavering presence provided the much-needed foundation during this academic journey.

TABLE OF CONTENTS

LIST OF TABLES

LIST OF FIGURES

LIST OF APPENDICES

LIST OF SYMBOLS, ACRONYMS AND ABBREVIATIONS

∅	Latitude of the location
AC	Alternating Current
COE	Cost of Energy
CRF	Capital Recovery Factor
DC	Direct Current
FiT	Feed in Tariff
GHG	Green House Gases
Gsc	Solar Constant
HOMER	Hybrid Optimization Model Electric Renewable
IEC	International Electrotechnical Commission
I_{SC}	Short circuit current
kW	Kilo Watt
kWh	kilo watt hour
LAN	Local Area Network
L_C	Array capture Losses
LCOE	Levelized Cost of Energy
L_S	System losses
L_T	Total system collection losses
MAE	Mean Absolute Error
MPP	Maximum Power Point
MPPT	Maximum Power Point Tracking
MW	Mega watts
MWh	Mega Watt hour

NASA	National Aeronautics Space Administration
NPC	Net Present Cost
PV	Photovoltaic
RMSE	Root Mean square Error
SPP	Simple Payback period
SSE	Surface Meteorology and Solar Energy
STC	Standard Test Conditions
V_{OC}	Open Circuit Voltage
W	Watt
Y_A	Array yield
Y_F	Final yield
Y_R	Reference yield
δ	Declination angle
ω	Sunset hour angle

ABSTRACT

Kenya boasts of abundant solar irradiation across its expansive regions, averaging between 4.5 kWh/m^2 and 6 kWh/m^2 per day. Despite this advantageous condition, solar energy's contribution to the national energy mix remains relatively low. This is partly occasioned by the solar PV systems degradation over time due to aging and other environmental factors. To boost solar energy contribution to the national grid, it is crucial to assess the performance of existing grid-tied solar PV systems and develop strategies to improve their energy yields and further help in designing and installing new plants. This study presents a technical performance analysis of a 600 kWp grid-tied solar PV system at Strathmore University, monitored over one year between January and December 2019. Economic and thermographic analysis of the solar PV system was done. In addition, tilt angle optimization was done and experimentally validated. The performance indices studied according to IEC 61724 standard include performance ratio, capacity utilization factor, array yield, reference yield, final yield, total collection losses, and total energy yield. This solar plant generated 735 MWh in 2019. The annual average monthly performance ratio, capacity factor, and annual specific energy yield were 57.4%, 13.97%, and 1,225 kWh/kWp, respectively. The annual average monthly final yield, array yield, reference yield, and total system collection losses were 3.37 kWh/kWp, 4.49 kWh/kWp, 5.9 kWh/kWp, and 2.53 kWh/kWp, respectively. The thermographic analysis done showed that the system exhibits normal temperature distribution. The economic analysis demonstrated Levelized Cost of Energy and simple payback period of US$ 0.143/kWh and 9.1 years, respectively. The optimal tilt angle obtained through experimental validation was 11°. Further analysis on the effect of air gap on the PV performance indicated that by increasing the air gap of the solar panel from 100 mm to 150 mm, the back sheet temperature of the module decreased by 7.5% due to the increased flow of cooling convection air currents. The study reveals that the Strathmore University system's performance is comparable to other solar plants worldwide.

CHAPTER ONE

INTRODUCTION

1.1 Background to the study

The demand for energy in Kenya is ever on the rise due to an expanding economy. The country has heavily relied on petroleum fuels to provide peak loads. Globally, the overreliance on fossil fuels for power generation has contributed to the rapid exhaustion of the fuels and caused adverse environmental degradation. Kenya has made tremendous steps to scale up the share of electricity generated by the renewable energy sources such as geothermal (44%), wind (11%), hydro (36%), and solar (1%), all constituting 92.3% of the total contribution to the grid as shown in figure 1.1.

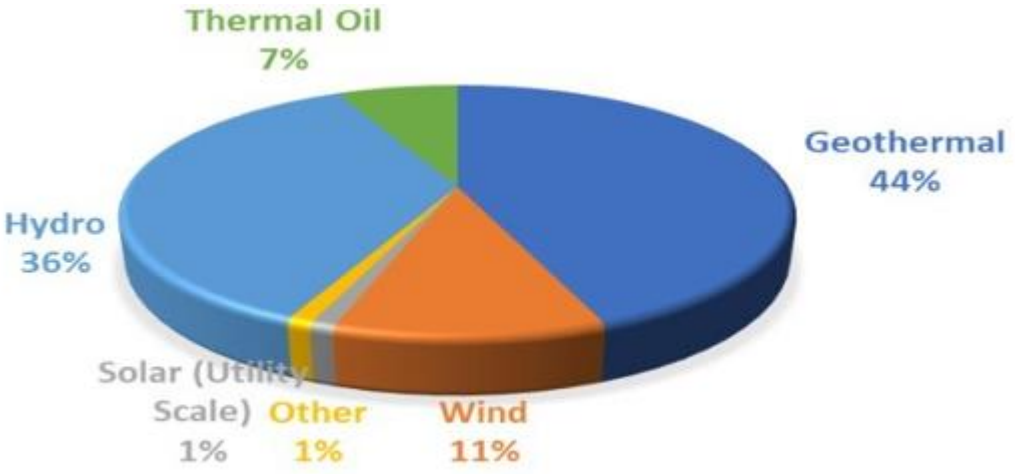

Figure 1.1: Kenyan Electricity Installed generation capacity share in 2020 (Cleantechnica, 2021)

In 2016, 310 MW wind power turbines were installed in Turkana, thus, increasing the wind energy contribution to the national electricity mix. In 2021, 100 MW Kipeto Wind Power project was commissioned, further increasing wind power generation capacity contribution. The government installed a 55 MW solar plant in 2018 at Garissa County, further boosting renewable energy contribution to electricity

generation. Figure 1.1 shows the Kenyan electricity installed generation share in 2020. Kenya has made tremendous progress towards decarbonization by increasing developments in renewable energy. Despite these developments in renewable energies, Kenya still relies on fossil fuels for power generation, constituting 7% in 2020, which adversely contributes to climate change (Akpolat *et al*., 2019). Of the renewable energies, solar energy is the least exploited, representing 1% of the total electricity generation share despite Kenya's massive potential with vast annual solar radiation potential of above 5 kWh/m^2/day (Francis *et al*., 2017). The vast solar energy potential is critical in encouraging local and international investors to engage in this developing area. Notably, solar energy generation is expected to significantly contribute to the national grid owing to the ever-conducive tropical climatic conditions. The government of Kenya has formulated policies critical in supporting the future expansion of Solar PV to contribute towards the global agenda for clean and sustainable energy in line with the sustainable development goals initiatives. Therefore, Kenya has a clear plan to boost solar PV contribution toward the national grid. Such enabling policies have encouraged Solar PV investments, with many homes adopting small standalone solar home systems mounted on rooftops. For instance, Kenya has enacted laws that zero rate all solar generation equipment imports to incentivize exploiting this green energy resource. Many private and government institutions have installed solar PV systems on rooftops, a move that will see some exporting their surplus power outputs to the grid in the future. The performance of such solar photovoltaic systems is affected by factors like the installation configuration such as tilt angle, orientation, the array technology deployed, system parameters such as inverter efficiency, and other environmental factors like ambient temperature, soiling losses, and solar irradiation (Mamun *et al*., 2022; Singh *et al*.,

n.d.; Babatunde *et al*., 2018; Qadourah, 2022).The performance of PV systems gradually degrades over time, highlighting the importance of monitoring their performance and implementing strategies for improved energy yields. Performance monitoring and evaluation of existing PV systems is also crucial for determining the suitability for solar energy harnessing an area.

Notably, the performance of solar photovoltaic systems is analysed using standard test conditions (STC), which do not accurately represent module operations. This is because the degradation, aging and environmental factors, design, and installation configurations affect the efficiency of the solar PV modules. Such studies are essential in monitoring the performance of the installed systems and provide the basis for improvement. Such studies have not been done extensively in Kenya, so monitoring these systems' performance is imperative. Therefore, this study analyzed the performance of the 600 kWp grid-tied solar photovoltaic systems for Strathmore University based on the IEC 61724 standard performance indices. These indices include performance ratio, capacity factor, reference yield, final yield, annual yield, and system losses which are crucial in establishing baseline information for grid-tied PV system for electricity production (Srivastava *et al*., 2020). Further, economic and thermographic analysis of the solar PV system is studied. Additionally, tilt angle optimization for the Strathmore's 600 kWp grid tied solar PV systems is done. Performance analysis and tilt angle optimization for this system is crucial since it provides a good model replicated across the country to boost sustainable energy development.

1.2 Problem Statement

As Kenya grapples with the challenges of global warming and the escalating prices of petroleum products, there is a pressing need to explore alternative and sustainable energy sources. Kenya, being strategically located near the equator with abundant solar irradiation levels of 4-6 kWh/m^2/day throughout the year, holds great potential for solar energy exploitation. The Kenyan government has shifted its attention towards de-carbonization thus complementing the global agenda for clean and reliable energy for all. Kenya has increased its investment in harnessing solar resources to complement the grid energy supply. To supplement the national grid, institutions such as Strathmore University have installed solar PV systems and entered into power purchase agreements with Kenya Power Company. However, the long-term performance of these solar photovoltaic systems is subject to degradation, necessitating the establishment of optimal configurations and solar plant performance improvement strategies to ensure their efficiency and hence enhance their contribution to the national grid. In Kenya, many developers install solar PV systems on their roofs without considering the tilt angle of installation, air gap and other environmental factors. Optimizing these parameters affects the performance of solar PV system. This research project evaluated the performance of the Strathmore University roof top grid tied solar PV system and developed optimal operational parameters.

1.3 Justification of the study

The investigation into the performance of the 600 kWp grid tied solar PV plant at Strathmore University and the establishment of optimal configurations for electricity supply have the potential to alleviate strain on the national grid and generate

substantial savings on electricity bills. Such studies have not been done extensively in Kenya, so monitoring these systems' performance is imperative. The Strathmore University grid tied solar PV plant is one of the firsts in the country and therefore, the performance analysis and optimization of this system forms a benchmark for other PV systems throughout the country. By assessing the project's performance, valuable insights will be gained, informing the implementation of strategies to enhance the system’s efficiency and effectiveness. This, in turn, will contribute to an increased power supply to the grid and significant reductions in electricity bills for both the institution and the wider community. The findings have practical implications for other institutions within the country, as well as off-grid areas. These findings offer a feasible solution for power generation, highlighting the viability and potential benefits of implementing similar solar energy systems. By showcasing the positive outcomes and successful operation of the Strathmore University system, this research paves the way for the replication and adoption of such systems in other institutions, as well as in areas lacking access to the national power grid. The results contribute to the broader goal of promoting sustainable and clean energy sources, facilitating a more environmentally friendly and economically viable approach to power generation across the country.

1.4 Objectives of study

1.4.1 General objective

The general objective of this research was to conduct a performance evaluation and tilt angle optimization of the 600 kWp Grid Tied roof top Solar Photovoltaic plant at Strathmore University

1.4.2 Specific objectives

i. To investigate the performance of Strathmore University's roof top grid-tied solar PV system based on the IEC 61724 standard.

ii. To carry out economic, thermographic and environmental (Greenhouse Gas savings) performance analysis of the system.

iii. To conduct a tilt angle optimization analysis for the 600 kWp rooftop grid-tied system at Strathmore University using PV Syst Software simulation and carry out experimental validation.

iv. To investigate the effect of air gap and irradiation on the solar PV panel back surface temperature and power output performance respectively across different tilt angles

CHAPTER TWO

LITERATURE REVIEW

2.1 Introduction

This chapter explores theories on the solar resource assessment and exploitation. The solar energy resource exploitation and the solar photovoltaic system operation is presented. The factors affecting solar radiation reaching the solar PV panel in a given area such as the tilt angle and orientation is explained. In addition, factors affecting the solar module power performance are illustrated. The scientific principle of maximum power point tracking (MPPT) and the algorithms enabling MPPT is discussed. The grid tied Solar PV system is explained including the existing grid connection topologies. The application of PVsyst software in designing and simulating grids and performing optimization is illustrated. The solar PV systems optimization techniques are explained. The thermographic analysis aspects of solar Photovoltaic is discussed. Further, the performance analysis case studies is presented. This chapter further discusses other related studies that informed the approach in this study and the existing gap.

2.2 Theoretical Background

2.2.1 Solar Energy

Solar energy refers to sun's heat and the light rays that supports the existence of life and influences the earth's climate and the weather. The sun generally accounts 99% of the flow of the earth's renewable energy. Solar energy is highly abundant, environmentally friendly and easily harnessed though the use of available simple technologies. This makes solar energy more popular as compared to the other renewable energy technologies. Kenya lies within the tropics and as such receives

daily insolation of between 4 kWh/m^2 and 6 kWh/m^2, which if efficiently harnessed will help in enhancing the universal access to energy (Francis *et al*., 2017).

Solar energy technologies available can be broadly divided into solar thermal and solar photovoltaic. For the solar thermal energy, the solar heat energy is harnessed to generate thermal energy for use in industrial applications, commercial or residential. Alternatively, the solar Photovoltaic systems can be used to tap light energy into electricity directly. Also, solar technologies can be categorized into passive and active depending on how they harness, convert and distribute light.

2.2.2 Principle of Operation of Solar Photovoltaics

A Solar PV cell is composed of a semi-conductor material that is able to transform the sun's radiations into electricity. The solar PV cell is composed of a p-type and n-type semi-conductor materials. P-N junction separates the n-type and P-type semi-conductor materials. Solar energy is composed of particles of solar energy or commonly referred to as photons. The sunlight photons contain various levels of energy depending on the wavelengths of the existing solar spectrum. When the sunlight photons hit the surface of the PV cell, free electron-holes pairs are created from the semiconductors atoms that flow to form dc electricity (Kumar et. al, 2020). The negative charge carrying electrons flow to the negative terminal (n-type material) of the PV cell whereas the holes flow to the positive terminal (p-type material) creating potential difference as illustrated in Figure 2.1.

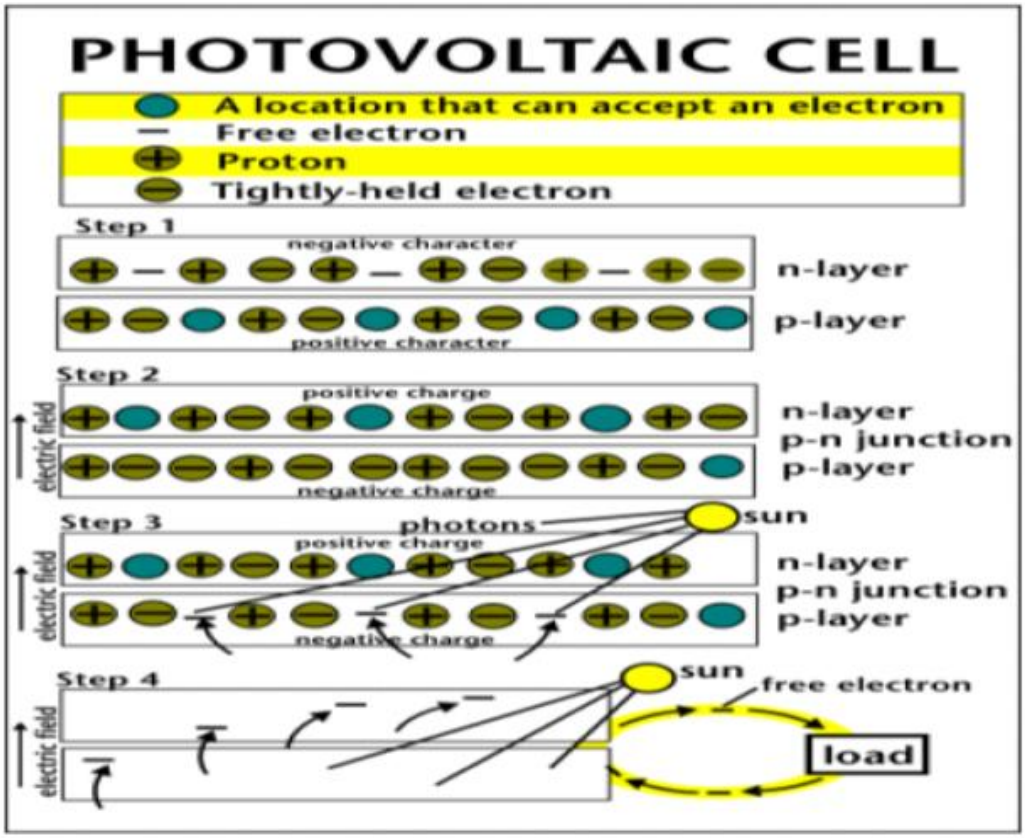

Figure 2.1: Illustration of photoelectric Effect of the solar Cell (Kumar *et. al*, 2020)

2.2.3 Characteristic I-V and P-V curves of solar cells

The solar photovoltaic cell electrical characteristics is represented by the current against voltage (I -V) and P-V for the different conditions. Figure 2.2 shows I-V and P-V characteristic curves. The curve depicts a non-linear current -voltage relationship. At V_{OC}, the current is zero while at short circuit (I_{SC}) the voltage is zero. The P-V characteristic curve depicts increasing power with the increase in Voltage. The power output is maximum at point MPP and decreases significantly on further increasing voltage.

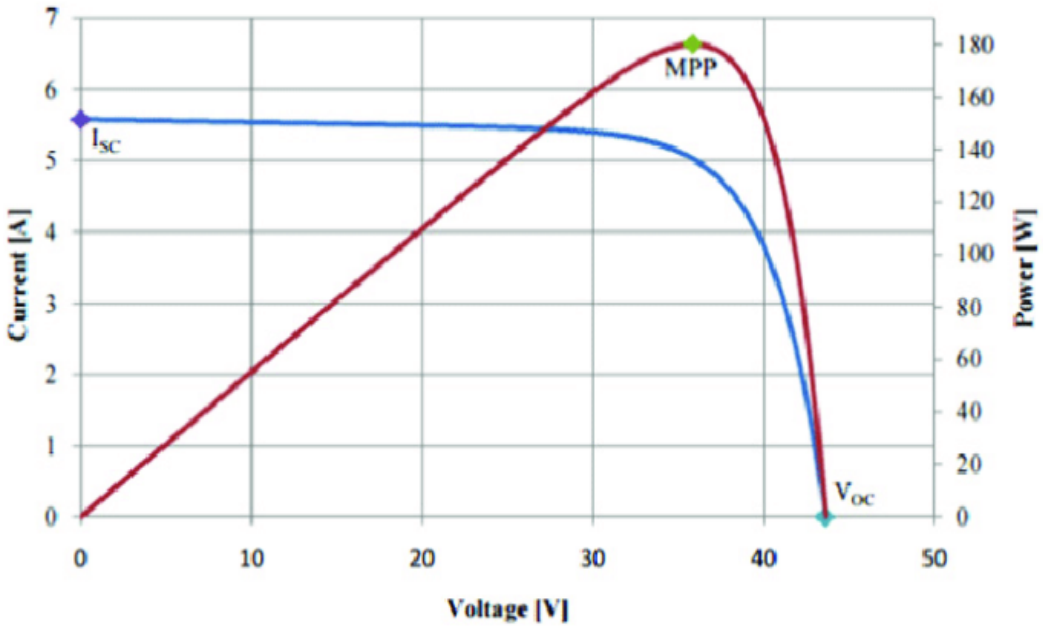

Figure 2.2: Solar cell I-V and P-V characteristic curve

2.2.4 Silicon based solar cell types

Solar panels are composed of a series connections of solar cells that generate electricity. They are made of silicon and use the photovoltaic effect to transform energy from the sun (photons) directly to direct current electricity. The photovoltaic modules are either crystalline cells or thin film. The crystalline panels are the most popular technology and has been around for about 50 years and hence widely adopted in homes. As such, they are the best choice for residential solar energy systems. The crystalline cells are manufactured in two varieties: Monocrystalline cells and Polycrystalline.

Monocrystalline cells are composed of the single-crystal wafer cell materials that is cut from a cylindrical continuous crystal ingot (see Figure 2.3). They are made from single crystal which are uniform and deep blue in colour (Sharma *et. al*, 2015). The efficiency of monocrystalline semi-conductors is between 18-22% and is more expensive than polycrystalline cells.

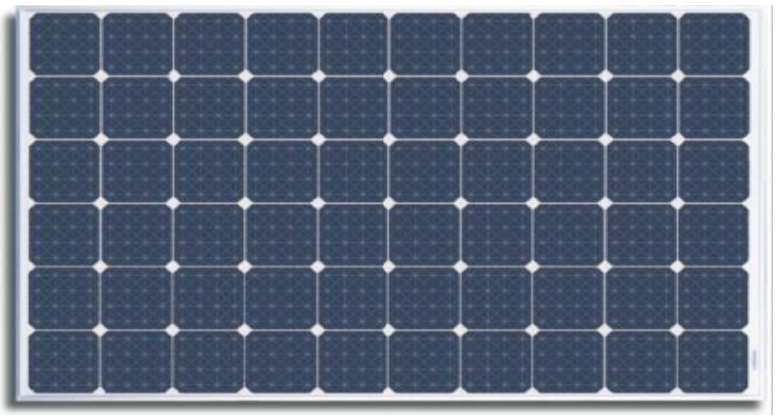

Figure 2.3: Monocrystalline cells (Sharma *et. al*, 2015)

Polycrystalline cells are composed of multiple crystal wafer cells (See Figure 2.4). They are created by moulding molten silicon to form an ingot. In this manner, they are cut into square wafers resulting in random crystal formations (Sharma *et. al*, 2015). The polycrystalline is less efficient as compared to monocrystalline cells. Has efficiency of between 12-15%.

Figure 2.4: Polycrystalline cells (Sharma *et. al*, 2015)

Thin film modules are made by depositing extremely thin layers of photovoltaic materials on substrates such as metal, glass or plastic (See Figure 2.5). Amorphous thin film solar cells utilizes a non–crystalline (amorphous silicon) silicon material which is deposited on the substrate to produce solar panels of any shape to suit the surface (Shah, 2020). Currently, researchers are focusing their studies on these solar PV technologies. Amorphous silicon cells have efficiencies of 10-12%.

Figure 2.5: Amorphous silicon cells (Shah, 2020)

2.2.5 Solar Resource Assessment

The solar resource assessment entails the accurate determination of the availability of solar irradiation resources for deploying, developing and operating cost effective solar energy technologies. Solar resource assessment ensures solar resource data is availed to cost effectively integrate high levels of solar power into the grid (Perez *et al*., 2013).

The sun is the primary source of all the forms of energy on the earth's surface and other planets. The sun is predominantly composed mainly of hydrogen gas, helium and other trace elements. A massive nuclear fusion reaction during conversion of hydrogen to helium releases massive energy. This makes the surface of the sun to

maintain high temperatures of approx. 5800 degrees kelvin, which is radiated uniformly to all directions.

The solar irradiations reaching the Solar PV panel are mainly direct radiation, diffused beam and the ground reflected beam which results from the reflection of the direct beam that is received on the surface of the earth as illustrated in Figure 2.6.

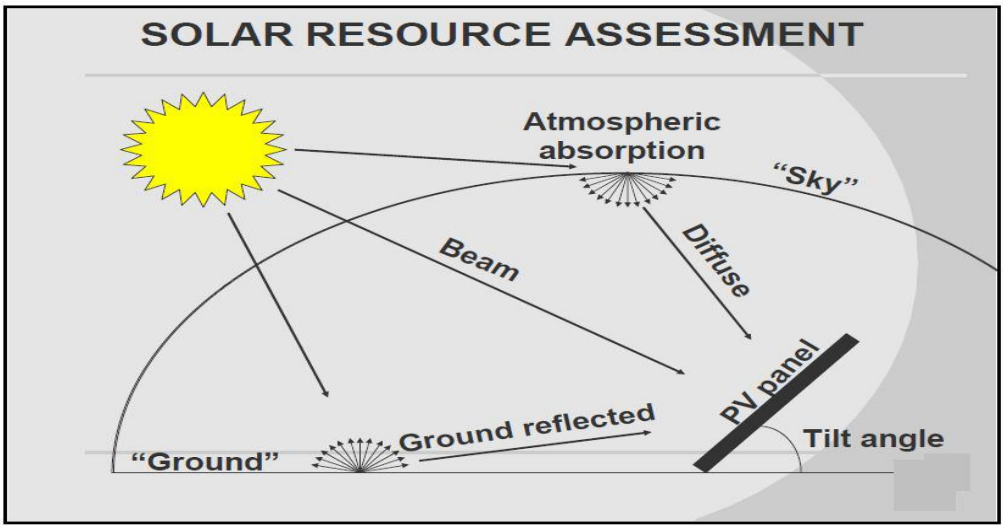

Figure 2.6: Picture illustrating solar resource radiation (Perez *et al.*, 2013)

Beam radiations refers to the global Irradiation's component that reaches the earth surface directly in a bright and clear day. Beam radiation represents about 85% of the insolation reaching the earth's surface. Diffuse radiation refers to the component of global irradiation indirectly reaches the surface of the earth. (See Figure 2.7). The sun's rays undergo scattering and absorption as it travels to the earth's surface. This component is approximately 8% of the total radiations reaching the surface of the earth (Khorasanizadeh *et al*., 2016).

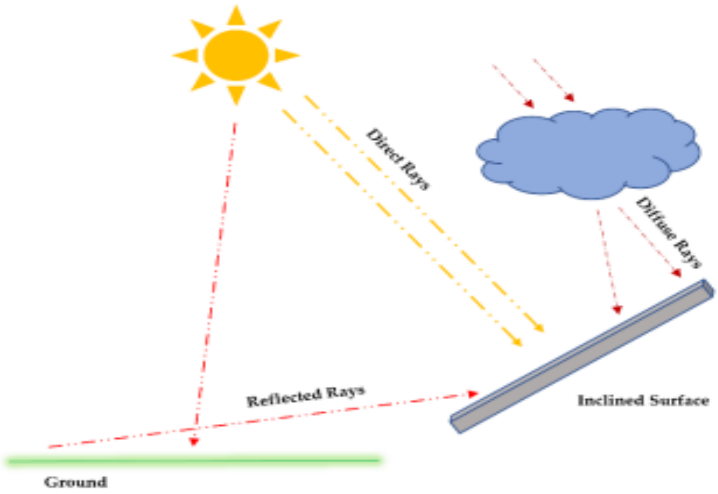

Figure 2.7: Schematic representation of types of solar radiation on tilted surface (Khorasanizadeh *et al.*, 2016)

2.2.6 Global Horizontal Irradiation

Global Horizontal Irradiation refers to the total sun's irradiations reaching the surface of the earth. The sun's rays touching the earth's surface include direct, ground reflected and diffuse irradiations (Perez *et al.*, 2013). The global irradiations reaching the horizontal surface is given by:

$$Hg = Hb + Hd \quad [2.1]$$

Where, Hg is the Global Horizontal Irradiation, Hb is the direct beam irradiations and Hd is the diffuse irradiations.

The global Horizontal Irradiation reaching the earth's surface is usually given as hourly and daily extraterrestrial radiation reaching the horizontal surface. The daily global horizontal irradiation on the horizontal surface is calculated by:

$$Ho = \frac{24*3600}{\pi} Gsc\left(1 + 0.033\cos\left(\frac{360n}{365}\right) * [\cos\emptyset\cos\delta\sin\omega + \left(\frac{\pi\omega}{180}\right)\sin\emptyset\sin\delta] \quad [2.2]$$

where, Gsc is the solar constant (1367w/m^2), n is the number of days in the year (n^{th} day in the year), ∅ is the latitude of the location, δ is the declination angle and ω is the sunset hour angle.

Solar irradiations reaching the horizontal plane of the solar PV modules influences the power being generated. The solar radiations through the atmosphere undergo various losses while others are absorbed by the clouds thus influencing the radiations reaching the horizontal surface. Equation 2.3 shows the relationship between the energy generated by the solar panels and solar irradiance.

$$E = A * G * PR * t * \eta \quad [2.3]$$

where, E is the energy that the solar panels produce in Watts-hour, A is the area of the solar modules exposed to sun radiations in square meters, G is the irradiance in Watts per Square Meter, PR is the performance ratio, η is the solar PV system efficiency and t time in hours during which energy is being supplied by the PV system.

2.2.7 Solar radiation on inclined surface

The solar energy reaching the solar array modules depends on both radiations' incident on the panel and the angle of incidence that is formed between the sun and the module. The solar panel surface receives maximum solar energy when the radiations are perpendicular to the module surface. The angle formed between the fixed horizontal surface and the sun varies throughout the year thus causing the incident solar energy to continuously change (Mousavi *et al*., 2017). The global solar radiation component reaching a tilted surface is given by:

$$Ht = (Hg - Hd)Rb + Hg\left(1 - \frac{\cos\beta}{2}\right) + Hd\left(1 - \frac{\cos\beta}{2}\right) \quad [2.4]$$

The function of atmospheric transmittance, Rb, is determined by the following expression for inclined surfaces sloping southwards in the northern hemisphere (Mousavi *et al*., 2017).

$$\mathrm{Rb} = \frac{\cos(\emptyset-\beta)\cos\delta\mathrm{Sin}\omega ss+\omega ss\mathrm{Sin}(\emptyset-\beta)\mathrm{Sin}\delta}{\cos\emptyset\cos\delta\sin\omega ss+\omega ss\mathrm{Sin}\emptyset\mathrm{Sin}\delta} \quad [2.5]$$

The numerator in Equation 2.5 is the extra-terrestrial radiations reaching the inclined surface whereas the denominator denotes the solar radiation on the horizontal surface.

$\emptyset$ is the latitude and ωss is the sunset hour angle for the inclined surfaces for a given month of the year. Sunset hour angle is expressed as:

$$\omega ss = \frac{\sin\emptyset\sin\delta}{\cos\emptyset\cos\delta} = \cos^{-1}(-\tan\emptyset\tan\delta) \quad [2.6]$$

$\boldsymbol{\delta}$ represents the declination angle which refers to the angular point of the solar noon with respect to the equator and is expressed as:

$$\delta = 23.45\sin[(\frac{360}{365})(284+\mathrm{n})] \quad [2.7]$$

Where n is any given day of the year.

2.2.8 Factors influencing the performance of Solar Photovoltaic modules

Tilt and Orientation of Solar PV Panel

The angle of tilt of a solar PV module refers to the angle at which the panel is inclined with the horizontal. When determining the optimum tilt angle, the mounting techniques, climatic conditions of the location, and topography are crucial aspects to consider. The solar PV module angle of tilt determines the levels of solar irradiation reaching the horizontal surface. It is globally accepted to set the solar PV panel at

inclination angle same as the altitude as concluded by Babatunde *et al*. (2018). Figure 2.8 illustrates the seasonal tilt angle of the solar panels.

Figure 2.8: Seasonal tilt angles for solar PV system (Babatunde *et al*., 2018)

Orientation refers to the direction and position of the solar panel relative to the sun's position and measures the direction of the solar panel relative to a reference point which is either north or south. Solar PV systems in the southern hemisphere and northern hemisphere should be oriented northwards and southwards, respectively for maximum power output. Figure 2.9 shows the solar panel orientation.

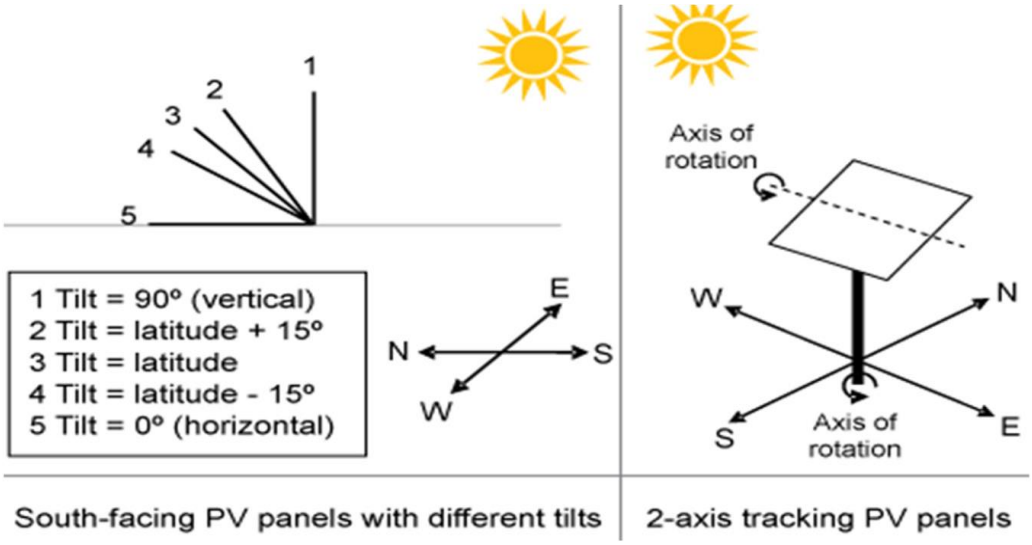

Figure 2.9: The orientation of a solar panel (Babatunde *et al*., 2018)

Soiling/Dust accumulation

Soiling refers to the accumulation of dust, snow, dirt, leaves, bird dropping and other foreign materials on the solar module surface. This has a direct impact on the solar PV performance. Dust and other materials accumulation on the PV panel surface decreases the glass transmittance. Soiling can be managed by cleaning the panels regularly. Mitigating the effects of soiling is essential for enhancing solar photovoltaic modules overall performance. This accumulation can lead a significant loss in the energy produced by the panels. Partial shading of the panels caused by some patches of soil in the surface also has a significant impact on the energy produced. Any material covering the PV panel surface contributes to general PV system performance. Many scholars have delved into studies to investigate soiling effect on the solar module performance (Kalogirou *et al*., 2013; Babatunde *et al*., 2018).

Temperature

Solar PV modules produce electricity through a process referred to as photovoltaic effect. This process ensures that the more sunlight rays on the solar PV module, the more power generated. However, overheating may occur on the solar PV modules that may negatively impact the solar PV conversion efficiency. The efficiency of conversion refers to the percentage of the sun rays that can be transformed to useful electricity by the panel. High temperatures are known to reduce the solar module efficiency (Lau *et al*., 2018).

The open circuit voltage decreases with increasing of the module's internal temperature whereas the short circuit currents increase considerably due to the absorption of light. This means that the maximum electric power generally decreases

with the temperature. The standard conditions chosen for the temperature equal to 25 °C. When the temperature increases above this standard condition of 25 °C, there is a considerable decrease in its efficiency due to the temperature coefficient. Temperature coefficient is the measure of the magnitude of the solar PV module power output loss due to an increase of a degree Celsius increase above the standard reference temperature (Chandra *et al*., 2018). By increasing the module temperature, the semiconductor material in PV cells becomes more conductive thus increasing the flow of charge consequently reducing the voltage considerably as shown in Figures 2.10 and 2.11.

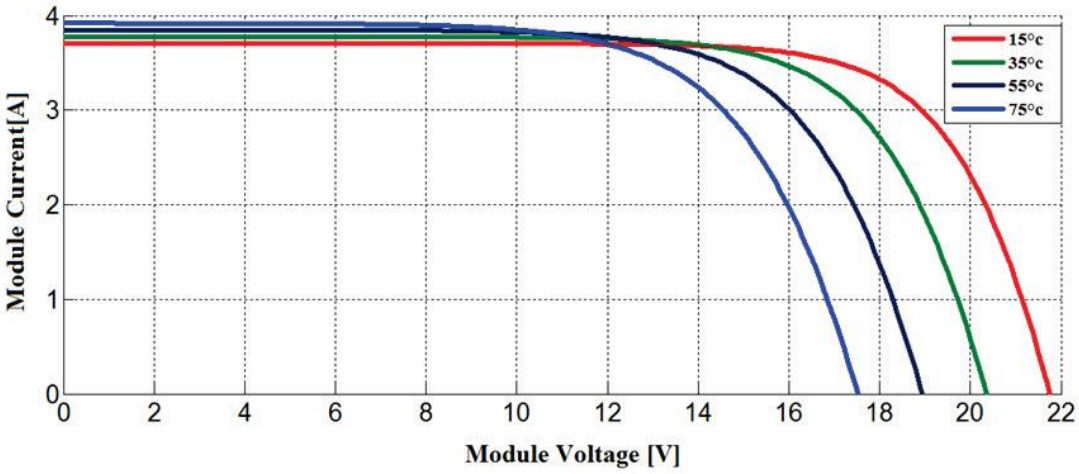

Figure 2.10: I-V characteristics of a solar PV module with varying ambient temperature

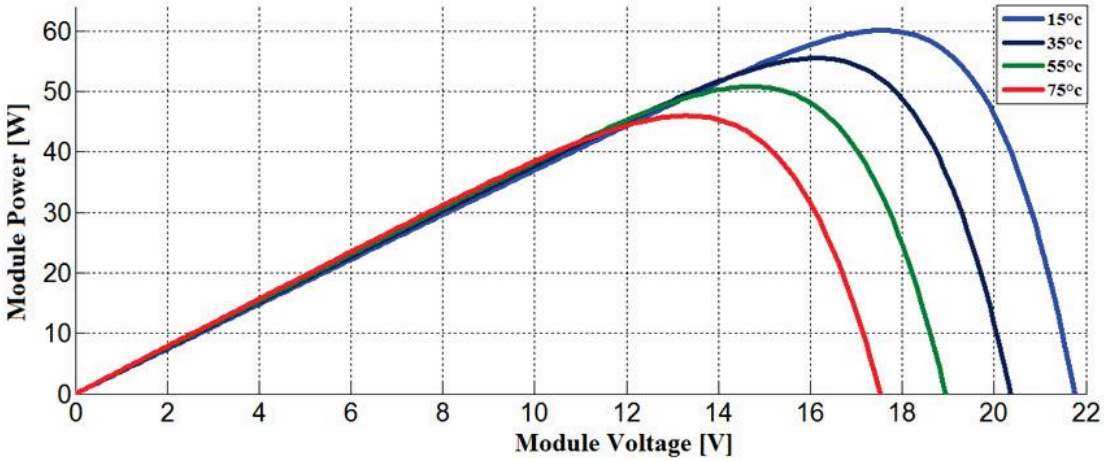

Figure 2.11: Power versus voltage (P-V) characteristics of a typical solar photovoltaic under changing ambient temperature

Solar Irradiation

The solar PV panels largely relies on the amount of solar irradiation reaching its surface. Solar irradiation is a very important factor in solar PV performance. High solar irradiance values lead to increased current output by the modules and hence the power increase as shown in Figures 2.12 and 2.13

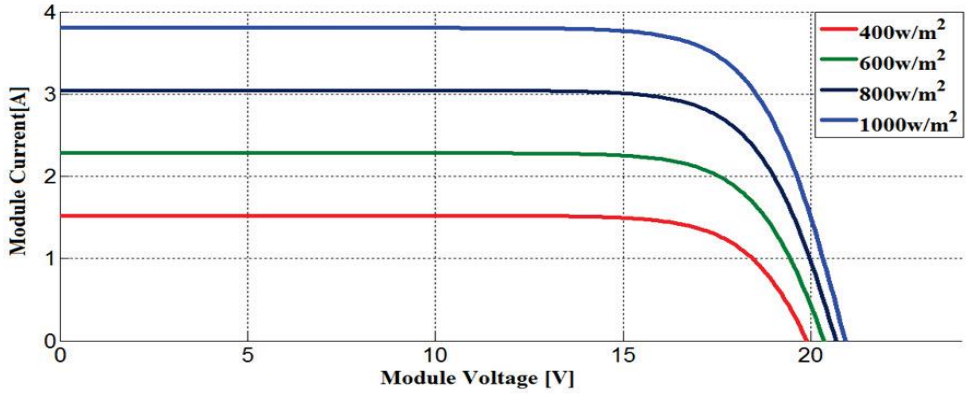

Figure 2.12: Current versus Voltage (I-V) characteristics of a typical solar PV cell under varied solar irradiation

Experiments done shows that by increasing the solar irradiation, more energy yields have been achieved (Buni *et al*., 2018).

The current I_{SC} increases with the irradiance and also the voltage V_{OC} slightly increases. This means that on high irradiance, the efficiency of the solar PV module is better.

The standard conditions of reference chosen are 1000 W/m^2 irradiance level.

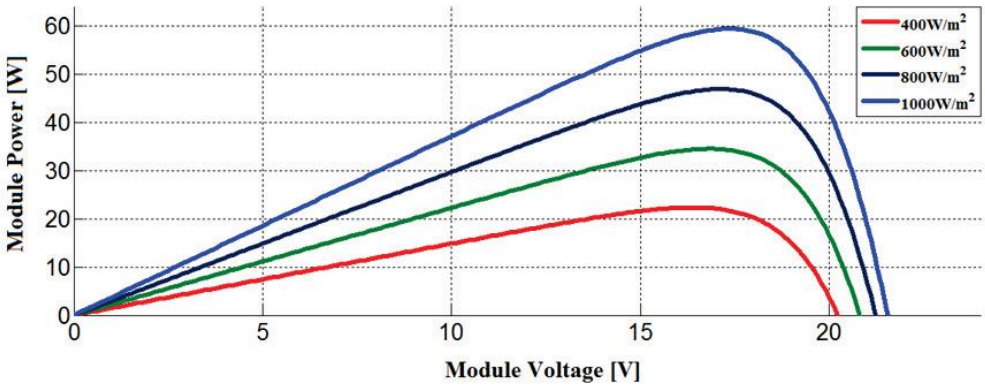

Figure 2.13: Power versus Voltage (P-V) characteristics of a typical solar Photovoltaic solar cell under varied solar irradiation

Wind

Wind speed greatly affects the operational efficiency of solar PV module. When the sun rays hit the PV module surface, electricity is generated and at the same time solar irradiation is transformed to heat energy. Due to the increase of in heat energy, this increases the operating temperature of the PV module considerably hence adversely affects power production. Therefore, air flow on the surface of the panels tends to lower the cell temperatures thus improving the conversion efficiency (Bhattacharya *et al*., 2014). Although wind loading may cause uplift when it flows between the roof and the PV module consequently damaging to the solar PV system, proper installation

prevents this possibility. Therefore, the wind factor in solar PV power performance plays a crucial role in improving conversion efficiencies

Shading

Shading causes a negative effect on the solar PV modules performance. The introduction of shades reduces the solar module efficiency directly thus impacting the power outputs. Shading in is normally caused by nearby trees, objects, passing clouds, leaves on the PV cells surface, or even buildings. Also, depending on the positioning of the panels, the panels may experience self-shading. This is normally a tradeoff between the row-to-row distance and the angle of tilt of the solar Photovoltaic modules. Higher angles of tilt and small row-row distance is known to cause more self-shading. Blocking the solar rays from reaching even a small section of the module cells leads to partial shading. Partial shading causes cumulative reduction of the electricity generation capacity. Therefore, it's important to consider the possibility of shading while installing solar Photovoltaic modules (Abdelaziz *et al*., 2021).

2.2.9 The Solar Photovoltaic grid tied Systems

The solar photovoltaic grid tied systems are connected to power distribution utility as a renewable dispersed generation or for metering purposes. Such systems don't have provision for autonomous supply thus does not require energy storage device like batteries. Grid tied solar system range from small kilowatts on the rooftop to very large ground mounted solar PV systems with their capacity in Megawatts (see Figure 2.14). Usually, solar PV produces DC electricity which is converted to AC power by use of inverters before being directly fed into the electric power grid. The conversion from DC to AC power enables supply to unlimited loads and necessitates annual

performance evaluation such like the typical grid supply systems (Ya'acob *et al*., 2014).

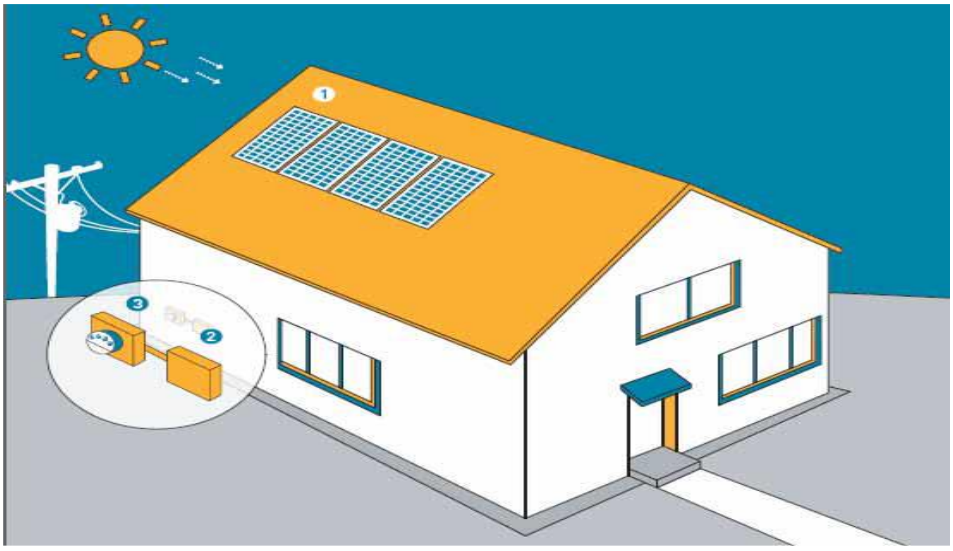

Figure 2.14: Picture illustrating grid tied solar PV system (Ya'acob *et al*., 2014)

Components of Solar photovoltaic grid tied systems

The main components of the solar photovoltaic grid tied systems includes solar Photovoltaic arrays, inverters, protective switchgear, combiner box and the MPPT (Mohammed *et al*., 2017). Depending on the type of electricity being injected into the grid, there may be more or less components. For the case of DC electricity, inverters are not needed. The following is the brief description:

Solar Photovoltaic array

Solar Photovoltaic array is the main active component converting solar irradiation to more useful DC electricity. As explained in the earlier sections, the irradiations directed to the surface of the cell ejects electrons which move freely creating electric current. The modules are normally connected in series to achieve the desired voltage in a string connection. To achieve desired current levels, parallel connection of

various strings is used. Normally, to curb adverse effects caused by shading, bypass diodes are used to protect the modules since shading introduces hot spots that are detrimental to overall energy production process as shown in Figure 2.15.

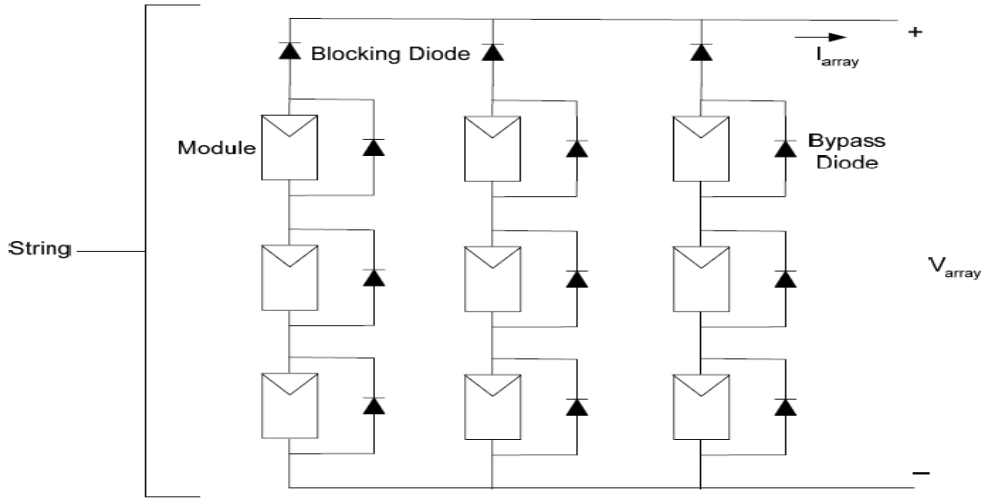

Figure 2.15: Solar PV Panels (Mohammed *et al*., 2017).

Inverters

The power from Solar PV panels is usually DC. This can only be applied directly to DC loads. However, most electrical loads require AC current which is achieved by using inverters. Most inverters have high efficiencies of up to 99%. The current inverter technologies ensure that minimal power is wasted during conversion. Inverters can be classified according to the waveform of the AC Voltage Output, functionality, topology and application.

Classification of Inverters based on waveform of the AC Voltage Output

Types of inverters include; pure sine wave, square wave and modified sine wave as shown in Figure 2.16. To produce pure sine wave , a modified sine wave is generated

and then a high quality, sensitive low pass filter is used for smoothing the waveform tom produce a pure sine wave.

Square wave inverters produce AC square wave at the output and hence the cheapest. Modified sine wave inverters use the PWM technology and uses a simple low pass filter to only allow required frequencies and blocking the harmonics generated. However, this filter is not able to smooth the output.

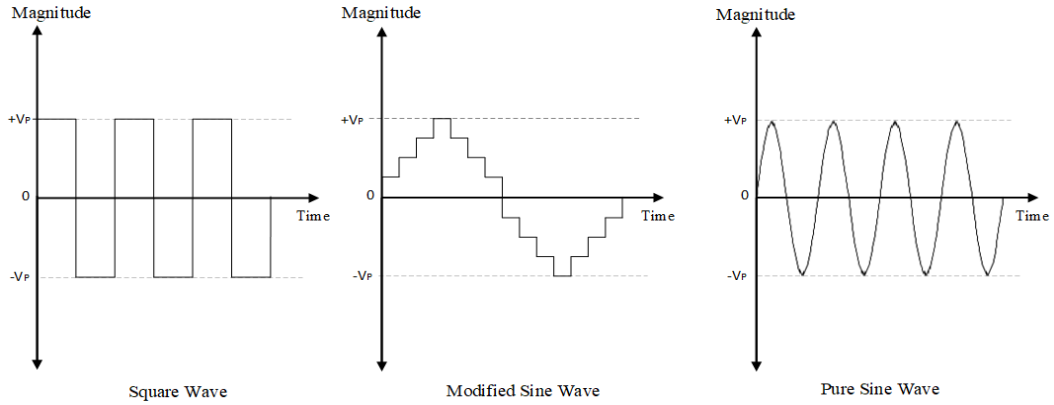

Figure 2.16: Output waveforms for square, modified sine wave and pure sine wave inverters (Mohammed *et al.*, 2017).

Classification of inverters based on functionality

String inverters: These kind of inverters are used in small commercial and residential solar PV installations. These inverters are usually connected to multiple solar panels connected in strings. Usually, the DC power from each solar panel is combined and converted into AC power.

Micro inverters: Micro inverters are usually installed on individual solar panel, converting DC power from the panel to AC power. These inverters are suitable for applications where shading issues are common. They ensure independent operation of each solar panel thus minimizing losses due to panel mismatch or shading.

Array Inverters: Also refereed to centralized inverters, these inverters convert DC Power to AC power from a multiple strings of solar panels. They are very crucial for converting DC power to AC power for consumption and feeding to the grid.

Classification of inverters based on topology

Single phase inverters: these are designed for converting DC to AC power for single phase electrical systems. These inverters are commonly used for residential homes and small commercial loads.

Three phase inverters: These inverters are commonly used for industrial applications and large commercial buildings where three phase electrical system is used. They are suitable for large solar PV systems and can handle high levels of power.

Grid-Tied Inverters: These type of inverters are usually connected to the utility grid where they synchronize the utility grid's voltage and frequency with its output. These inverters can feed excess power to the grid and can draw power from the grid.

Off-grid or standalone Inverters: these inverters are not connected to the grid and are usually used in remote areas for backup power systems incorporating battery storage.

Hybrid Inverters: These inverters are designed to work with both off grid and grid-tied systems and usually offers flexibility and resilience to the system, can manage energy production, battery storage and grid connection.

Combiner Box

In a solar PV system where only one centralized inverter is used, the output is channeled directly to the load or grid. In case several inverters are used, a combiner box is required to combine output from all the inverters before being injected to the

grid. This includes a bus system where the outputs are connected. Circuit breakers are used to isolate the individual inverters to prevent faulty situations.

Protective Switch gear

Solar Photovoltaics have advanced protection switchgear. The two most important equipment for electric power generation in a solar photovoltaic system are the photovoltaic panels and the inverter which need special protection attention. Currently, inverter technology has inherent safety controls. At the input to the inverter, over current and DC over voltage circuit breakers are installed to prevent damage to the inverter. The output side has the AC overcurrent protectors to protect the load side. String fuse and short circuit diodes are used to protect the equipment in case of reverse polarity situation. The ground fault and string failure detection are installed in some inverters for enhanced protection. Circuit breakers are used to isolate individual inverters in case a combiner box is used. The final three phase or single-phase connection to the grid or load, over voltage and over current protections are added to protect the entire system.

Types of Solar photovoltaic grid tied systems

AC loads and DC loads can be supplied from an off grid solar Photovoltaic systems or standalone system. However, solar photovoltaic grid tied systems supply AC electricity to the AC grids. In some countries where DC grids are available, the DC electricity is injected to those grids directly. Solar photovoltaic grid tied systems is divided into two; grid tied systems with back up storage battery system for supply at night in case of grid failure as shown in Figure 2.17.

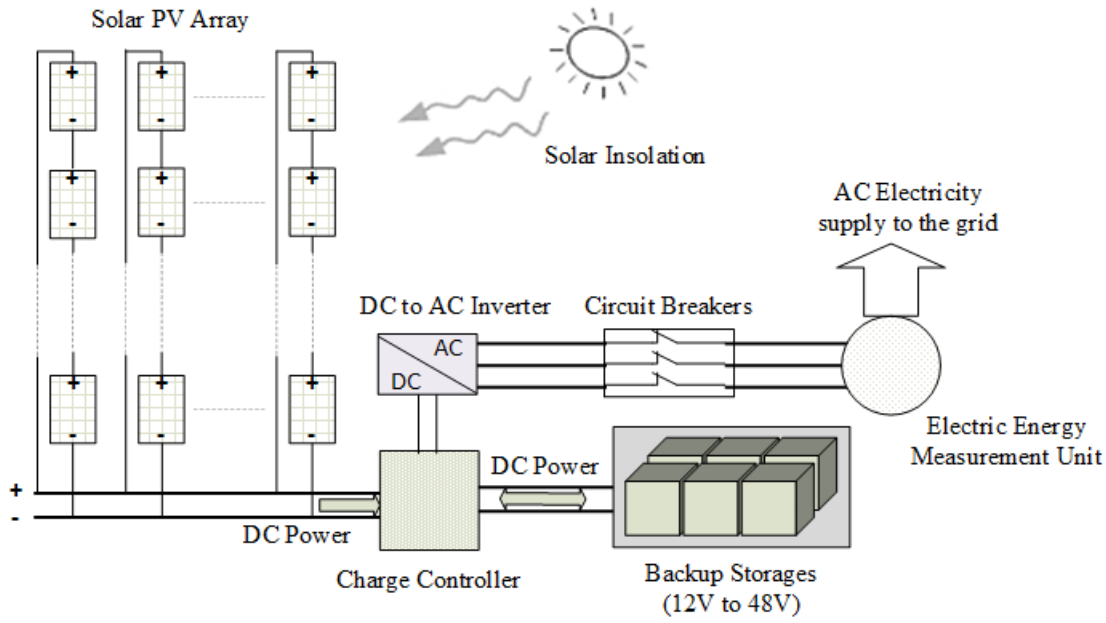

Figure 2.17: Solar photovoltaic grid tied systems with back up storage (Ya'acob *et al.*, 2014)

Grid tied solar PV systems without backup storages feeds the AC grids during the day time only (Mohammed *et al*., 2017). Such systems require less maintenance than those with battery storage systems hence economically efficient (see Figure 2.18).

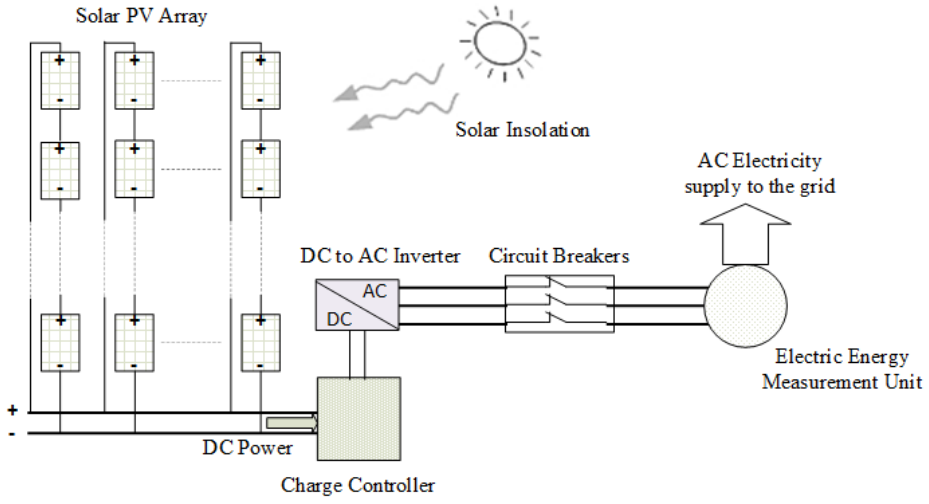

Figure 2.18: Grid tied solar PV system without back up storage (Xiao *et al.*, 2016)

Connection topologies

The grid connected solar photovoltaic systems have different connection topologies depending on how the PV panels and the inverters are connected (Xiao *et al*., 2016). The popular topologies include: master-slave, centralized inverter, team concept, string to inverter, modular and multi string. The Figure 2.19 illustrates the different topologies.

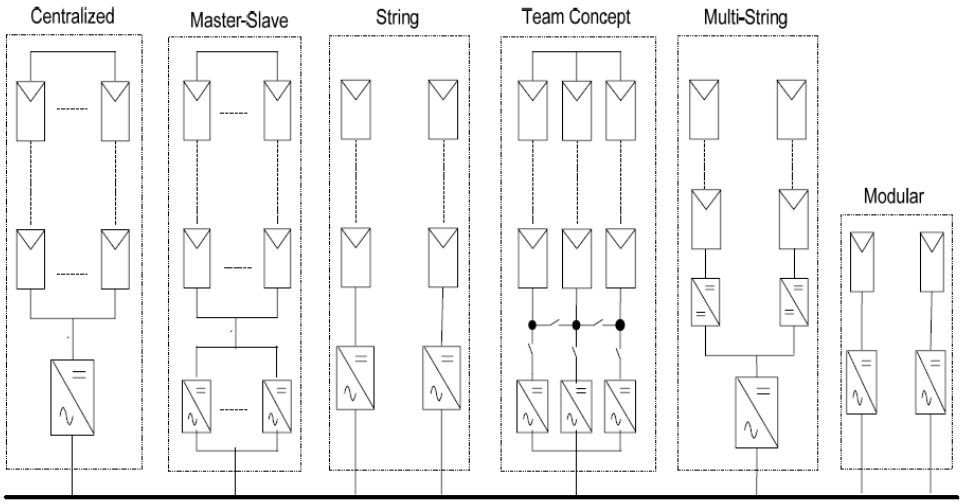

Figure 2.19: Grid tied solar PV systems connection topologies (Xiao *et al*., 2016)

Centralized topology

This is the most cost effective for very high-power outputs. This means that only one inverter is used for conversion. This further reduces the DC to AC losses. Because it has one inverter, then the system has one MPPT. This topology has the disadvantage in that if the inverter malfunctions, then the whole system will go down (Xiao *et al*., 2016). It also exhibits a challenge where in case of PV array mismatch, there are great power losses.

Master-Slave Topology

This topology is composed of a master inverter and a slave inverter for backup purposes. The power losses due to array mismatch is also evident here, though it's costlier and more reliable than the centralized one.

String to inverter topology

Here each inverter is connected to a string of photovoltaic panels. This is very reliable in case of PV panel failure. Every inverter tracks its maximum power point for every string with improved efficiencies. It is also easier to maintain the PV or inverter.

Team concept Topology

This topology borrows from both the master slave and string concept topologies. It's used for very large PV systems. It employs master slave topology for low irradiances but uses the string concept for high irradiances. String Connections are linked to individual inverters to ensure maximum power is tracked.

Multi-string topology

This topology taps the maximum power point and the voltage amplification by connecting each string to a DC-to-DC converter with all outputs to a centralized inverter and then to grid. Any inverter failure brings the entire system down, making this topology highly unreliable.

Modular topology

In this topology, the inverters are embedded onto the individual modules (Xiao *et al*., 2016). This is reliable in that there is no PV array mismatch because each of the modules are connected to individual inverters. It is easier to monitor the module

failure and reduces maintenance costs. The inverter life time is reduced in this case due to the thermal stress on the inverters.

2.2.10 Optimization of solar PV systems

Different scholars have done system performance optimization by factoring different system parameters. These factors include: The PV module system tilt angle, the solar panel air gap, Orientation, PV system optimal configuration and module spacing. These factors are crucial when designing roof top solar photovoltaic system as this affects its energy production. Several software tools have been used to carry out simulation. These are HOMER Pro, PVsyst, Helioscope, PV Watts Calculator, Plant Predic, system Advisor Model (SAM), TRNSYS, solar planner PVGIS, RETSCREEN, and PV sol. The PV Syst software has been widely been used to perform optimization simulation studies (Kumar, S. *et al*., 2019). This is due to the following reasons:

i. PV Syst is preloaded with Meteo database where users can use sources of meteorological data from Solargis, NASA, and Meteonorm
ii. PV Syst software has extensive libraries for inverters, solar batteries and solar PV modules
iii. PV Syt software is robust and quick to design PV system and give detailed hourly, daily, monthly and annual energy production
iv. PV Syst software is highly versatile and can handle grid tied systems, standalone systems and pumping systems functionalities and provide detailed project estimations.

Solar Panel Air Gap Optimization

Building integrated Solar Photovoltaics are affected by the air gap of the PV installation. The air gap between the roof and the panel affects flow of wind and general ventilation required to enhance cooling. Small air gaps have been known to increase the back sheet temperature and consequently the cell temperatures. Increase in cell temperatures introduce hot spots in the solar PV cells thus further decreasing the power output of the system. Several researchers have established that by choosing a suitable air gap during installations, optimal yields have been achieved.

Azimuth Optimization

Many design engineers install solar PV modules facing southwards due to the maximum production of energy. However, for most design engineers, they opt to align the panels as per the roof design. This is crucial in increasing the number of panels and hence higher array power as compared to positioning towards south. Therefore, this is a tradeoff between increasing the energy yield or maximizing on the number of modules and hence the array power. Aligning the panels according to the direction of the building is vital in ensuring the installation of bigger system despite slight reduction in the energy yield (Paul Gibbs, 2021).

PV module spacing and tilt: Optimization based on the Tradeoff between energy and power density

The row spacing and the tilt of the panel have an impact on photovoltaic module performance. These two aspects of PV system design are likely to introduce shading thus affected the module power performance. Therefore, designers face a critical tradeoff between maximizing the power yield per unit area (power density) and

maximum yield per module (energy density). The designer can increase the spacing and also can tilt the modules for maximum yield. However, by increasing the spacing, less modules can fit the area. Additionally, this mode of system arrangement tends to increase shading due to the bigger tilt angles. This is referred as maximizing energy density.

Alternatively, the PV designer can reduce the module tilt angle and reduce the spacing thus increasing the power density. The solar PV industry is shifting towards designs that embrace narrower spacing and lower tilt angles so as to accommodate more solar panels i.e., embracing improved power density and foregoing energy density. Paul Gibbs (2021) asserted that by reducing the tilt and row spacing, solar PV Module drops its power output by 2% but considerably improves the power density by 20% and more.

Maximum power point tracking optimization

Optimizing the performance of solar PV systems leveraging Maximum Power Point trackers is very crucial. Despite the changing solar insolation levels and varying ambient temperatures an MPPT is normally used to set the operating point close the maximum point as possible. The MPPT is basically DC to DC converter that is composed of capacitor, inductor, transformer and some power electronic components used to implement such operations. Figure 2.20 clearly illustrates the principle of operation of an MPPT.

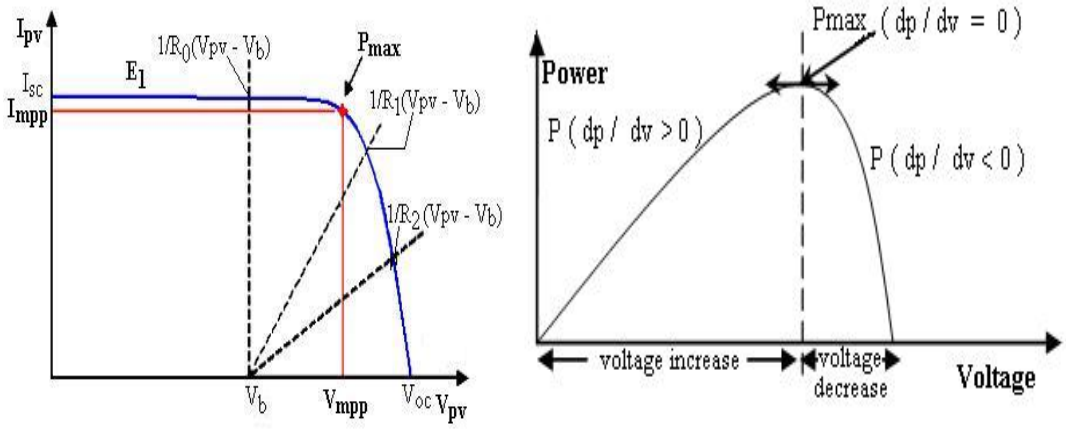

Figure 2.20: Illustration of Maximum power point tracking control for solar cell (Sreedhar *et al*., 2016)

When a connection is made between the source and the load, the electricity yield from the photovoltaic array is rarely maximum and also the operating point is never always optimal. This is due to the varying load characteristics and variation of the solar irradiation and the cell temperatures.

In order to deal with this problem, a switching device, mostly a chopper (converter) is used with the maximum power point tracker between the load and the source. In this case, the maximum power point tracking controller tracks the modified maximum power point in the curve when the temperatures and the solar irradiation variations occur.

There are several techniques used for MPPT optimization. The classification depends on the level of control it offers (Sreedhar *et al*., 2016). Despite the fact that the MPPTs are employed for the same objective, they differ largely in terms of complexity, accuracy, number of the required sensors, convergence speeds and robustness.

2.3 Previous works relevant to study

2.3.1 Studies on the effects of Tilt and Orientation on solar PV Performance

Salih *et al*. (2014) asserted that for grid tied solar PV system where they are attached to permanent structures, the PV modules should be installed at tilt angles equal to the location's latitude to optimize power being generated throughout the year. A study done by these researchers on the effect of the tilt angle and orientation on the photovoltaic module performance showed that the tilt angle and orientation have crucial impact on the output.

Khoo *et al*. (2014) did a study on the optimized tilt angle and orientation for maximizing the solar irradiation for Singapore solar PV systems applications and established that the solar PV modules performance is affected by the panel's angle of tilt and orientation since these factors influence the levels of solar irradiation received by the modules in a given region. The results showed that PV system tilted at an angle of 10° facing eastwards realized a high yield and performance ratio that is close to the other locations.

Dominic (2017) carried out tilt angle optimization using PV Syst for biannually adjusted Solar PV system based on the Perez transposition model. This model generates yearly global solar Irradiation incident with tilt angles varying from 0° to 46°. The optimized tilt angle for winter season was 25.46° whereas the optimized tilt angle for summer season was 0°. The results further indicated that the annual fixed optimal tilt angle was 7.16° with an annual transposition factor of 1.01 for the fixed system whereas 1.05 for the solar PV systems which are adjusted seasonally.

The latitude of a place also influences the solar energy that can be generated from the radiations. This is crucial because it determines the tilt angle and orientation at which

the solar PV panels shall be installed. Studies done depict that that the tilt angle at which maximum energy is generated is close to the latitude angle and therefore, most projects are installed at tilt angles that are close to the latitude of the area (Dominic Ekanem, 2017). However, there is a tradeoff between the solar module angle of tilt selected and self-cleaning aspect of solar panels. The solar PV orientation is also a crucial factor in installing the panels. Usually, solar PV cells in the northern poles are installed facing south whereas the PV cells in the south are installed facing the north i.e., they are oriented towards the north so as to tap maximum power.

2.3.2 Studies on the effect of soiling on Solar PV systems Performance

An investigation on the impact of soiling on grid tied solar PV systems was done in California, USA and found that the effect of soiling on the PV modules' power performance depends on the installation's location. It was discovered that soiling impact caused a reduction of between 1.5% and 6.2% depending on the location. A crucial finding of this study indicates that after a slight rainfall, certain panels performed better whereas some panels increased losses. The study concluded that at least rainfall of 20 mm is enough to clean the panels, otherwise the power performance degradation due to soiling will be highly severe (Maghami *et al*., 2016).

Kalogirou *et al*., (2013) investigated the effect of soiling on solar PV performance in Cyprus. The investigation showed that soiling contributed to 6-13% loss on the power loss. It was further concluded that a light rain makes the dust to form sticky patches of mud on the panels consequently reducing the performance. It was found that the heavy winter rainfall is crucial in cleaning the panels.

2.3.3 Studies on the impact of Temperature on Solar PV systems Performance

A study done by Chandra *et al*. (2018) on the impact of ambient temperature on polycrystalline solar module's performance ratio of revealed that by increasing temperature in the uncooled PV system, the power output decreased by 2.88% whereas the cooled PV module recorded a 2.85% increase in power output above the theoretical energy. Nabil and Mansour (2022) carried out an experiment whose results indicated improvement of PV system performance by decreasing its temperatures through cooling mechanisms. Establishing the optimal system configurations is essential for improving the solar photovoltaic system performance (Babatunde *et al*., 2018).

2.3.4 Impact of Solar Radiation on solar PV systems performance

Buni *et al*. (2018) investigated on the relationship between solar radiation and solar PV current generated and reached a conclusion that there is a direct proportionality between these two parameters consequently impacting on the solar PV modules efficiency. However, the study asserted that although the solar modules performance increases with increasing solar radiations, the increase beyond a certain level may lead to increasing internal cell temperature consequently decreasing the performance.

2.3.5 Effects of shading on Solar PV performance

Sathyanarayana *et al*. (2015) carried out experimental analysis on the shading effects on the solar panel's performance. The investigation concluded that during uniform shading, power output linearly decreased with the increasing shading. The research showed that non uniform shading impact on the solar PV performance was even more adverse. This was as a result of some cells experiencing reduced irradiance thus acting

as loads leading to considerable reduction in the current generated, power output and consequently the efficiency of solar PV module.

Simulation analysis carried by Abdelaziz *et al*. (2021) concluded that a reduction of the incident solar irradiation on a single Photovoltaic module cell causes a decrease of the power output from the system by 33.33%. The study concluded that bypass diodes are crucial in mitigating the impact of the partial shading.

2.3.6 Effect of Wind on Solar PV module Performance

Bhattacharya *et al*. (2014) investigated the impact of wind speed and ambient temperature on the monocrystalline PV module's performance in Tripula, India. The study showed a correlation coefficient of 68% and 96% for wind and ambient temperature on the conversion efficiency respectively. This study showed that there is high correlation between the speed of the wind and the solar module's conversion efficiency.

Leow *et al*. (2019) conducted a research study on the influence of wind on the performance of Solar Photovoltaic module performance. The research found out that the solar panel with wind flowing on its surface exhibited lower cell temperatures as compared to the PV panel on normal condition. This was due to the wind flowing on the surface thus lowering the operating temperatures. This further led to better power outputs for the PV panel with wind flow. Therefore, wind flow plays a very critical in improving the Solar PV systems performance.

2.3.7 Impact of Air Gap on Solar PV module Performance

Gan (2009) conducted research on the air gap impact on the electrical performance of the building integrated solar photovoltaics and established that the maximum photovoltaic temperature and the mean photovoltaic temperature and increases with

the reducing air gap. The researcher further found out that to reduce hot spots on the panel surface and overheating of Solar PV modules, an air gap of between 120 mm and 150mm for multiple panel installation and between 140 and 160mm for single module installation is required. The researcher further found out that the mean PV temperature decreases for air gaps equal or more than 80mm.

2.3.8 Studies on Tilt Angle Optimization

Several researchers have carried out solar PV system improvement by obtaining the optimal tilt angle. It is globally accepted that the latitude of the site is equal to optimal tilt angle for the Solar PV system. For maximum solar energy production from the solar photovoltaic panel, the panels must be tilted at the appropriate tilt angle.

Dogaheh & Puig (2019) carried out a study on tilt angle optimization of solar PV panels in Spain and researched on how to obtain the optimal tilt angle. The research established that the optimal angle varies according to seasons. The optimum tilt angle for autumn, summer, spring and winter obtained for the study was 56.4°, 29.11°, 13.76°, and 48.14° respectively. The annual optimal tilt angle obtained was 36.87° which realized a 10.54% increase in the energy generation.

Sugirianta *et al*. (2020) did research on tilt angle optimization on 300 Wp electric power grid tied model in Indonesia. The study entailed the use of PV Syst software to simulate the model with solar irradiation data from metronome 7.2. The tilt angle was found to have great impact on the energy yield. The results showed an annual output of 528 kWh with the optimal tilt angle ranging from 12-18 degree. The annual output corresponds to 100% of the system output.

Udoakah and Okpura (2015) carried out a study to determine the optimum tilt angle for solar photovoltaic systems located at Enugu in southern Nigeria. The study

established the optimum tilt angle for a fixed system was 6° with energy yield of 186.86 W/m^2. If the system is adjusted monthly, the optimal tilt angle for January, February, March, October, November and December are 30°, 24°, 6°, 18°, 30°, 36°respectively and 0°for April to September. The research further recorded an increase by 3% (192.7 W/m$^{2)}$ in the energy yield in a case where the system is adjusted monthly to its optimum tilt angle.

Kumar and Thakur (2011) carried out a study on solar PV system tilt angle optimization in Punjab, India with latitude 31.06°. The study showed that the optimum tilt angle was different across the seasons of the year. The research found out that during winter, the optimum tilt angle should be 57.48° while during spring, 18.16°. The optimal angle for summer and autumn is 2.83°and 30.61°, respectively. The average tilt angle was found to be 30.61° which is nearly similar to the latitude of the site.

Hailu and Fung (2019) carried out a study on orientation and optimum tilt angle of photovoltaic thermal system in Toronto area, Canada. The results showed that for maximum solar output the thermal system tilt angle should be varied in a year four times in order to yield maximum energy. The results further showed that the solar panels should be oriented east or west facing southwards with a flatter tilt angle.

Markam and Sudhakar (2016) studied optimum tilt angle estimation for solar photovoltaic systems in India's six different regions using RETSCREEN, PVsyst and NREL SAM software. The simulated results showed that the average solar irradiation lies between 5-6.5kWh/m^2 with yearly optimal angle varying by 2°to 3° from the latitude of the location.

Makenzi *et al*. (2020) conducted an algorithm necessary for optimizing the optimal tilt angle for various locations with a case study of Athi River location using 375Wp JKM375M-66H PV module. The optimum tilt angle was determined to be between 3.02° and 24.57° depending on the time of year.

Kumar and Thakur (2011) carried out tilt angle optimization for solar photovoltaic system in India and the annual optimized tilt angle was established to be 30.6° was nearly the same latitude angle location for Khatkar Kalan.

2.3.9 Review on Maximum Power Point Tracking Techniques

MPPTs can either be classified into intelligent and conventional ones. Conventional techniques are simple and easy to implement though they cannot be applied under partial shading conditions. They are only suitable for the uniform irradiation conditions. They include: hill climbing algorithm, ripple correlation approaches perturb and observe, incremental conductance, short circuit, and open circuit voltage. Sreedhar *et al*. (2016) concluded that these MPPT techniques are not suitable for solar photovoltaic modules under partial shading conditions. This review study asserted that the biologically and nature inspired MPPT algorithms such FLC based MPPT, Particle Swarm Optimization, Artificial Neural Network based MPPT, Firefly based MPPT, Ant colony based MPPT, and the genetic algorithm based MPPT could be crucial in maximum power production under partial shading conditions and under rapidly changing weather. This intelligent MPPT techniques does not need prior information on the photovoltaic panel and therefore this allows them be used under partial shading conditions.

2.3.10 Solar PV system power performance improvement through maintenance practices at Strathmore University 600 kWp solar PV system

For optimal power performance, the Strathmore University 600 kWp solar PV systems undergo regular maintenance practices. The maintenance department embraces both corrective and planned maintenance practices. The corrective maintenance practices done on this system includes: replacement of components such as cracked solar PV modules, failed solar edge power optimizers attached to the PV modules, and inverters. Planned maintenance operations are also undertaken. This includes, regular cleaning, system inspection and monitoring. Usually, the solar PV system is cleaned twice a month to ensure optimum operations. Cleaning by water sprinkling has resulted into considerable increase in the energy output from the system. The solar Photovoltaic system's strategic location attracts swarms of birds flying over and perch on top of the panels. The bird droppings on the panels cause partial shading which contributes to hot spots. According to report by Kumar *et al*. (2014), they concluded that bird droppings cause more power losses as compared to soiling. The solar panels at Strathmore University are manually cleaned by sprinkling water on the panels. However, to increase the panel efficiencies, Hammoud *et al*. (2019) investigated the effect of wet cleaning of solar Photovoltaic modules using robots regularly and established that this procedure resulted in increased power output by 32.27% during the period under study. For increased power production, more regular intervals of cleaning should be done on this solar PV system i.e., once a week.

2.3.11 Performance investigation of grid tied solar Photovoltaic systems

Solar PV system performances analysis has been done in various locations across the world. The grid-connected solar photovoltaic system performance analysis has been

widely done using the International Electrotechnical Commission's 61724 standard of 1998 (IEC, 1998). The performance indices entrenched in this standard are essential in assessing the Solar PV systems performance and establishing the losses exhibited by the systems (Sathiracheewin *et al*., 2020). The performance indices evaluated are performance ratio, energy output, collection/system losses, reference yield, capacity utilization factor and final yield. These indices provide a basis for comparing worldwide grid-connected systems operating under different conditions. The system design configurations determine the solar PV system optimal performance and hence very essential. Some scholars have conducted performance evaluation with the aim of establishing the optimal configurations. Many researchers across the world have done performance analysis on Solar PV systems, as referenced by Dahmoun *et al*. (2021), Milosavljević *et al*.(2015) and Sharma and Goel (2017) among others.

Querikiol and Taboada (2018) conducted a performance evaluation of a 1.5 kW off-grid solar PV system in Camotes islands, Philippines where they used the HOMER simulation software to determine the optimized configuration based on actual load. The simulation results depicted that the all-PV system sizing of 2.63 kW was the most optimized. Sensitivity analysis done to assess the impact of increasing the load and variations of the fuel costs realized an optimal value US $ 0.202 and US $ 8,405 for COE and NPC respectively.

Haji (2019) investigated the performance of the installed PV system in two regions in Tanzania using Homer software. The simulation results showed that there is high sensitivity of system's technical performance to the load growth. In this study, optimal values for the Total Net Present Cost were $ 474,744 and $ 29,168, the

levelized cost of energy (LCOE) was $1.05/ kWh and $ 0.0117/ kWh and whereas a renewable fraction of 14% and 21% for institutions in Zanzibar and Arusha respectively.

Laith (2017) carried out performance analysis of hybrid systems in Sabah, Malaysia. Homer modelling software was used to model and analyze the system. The results showed that the load demand was satisfied with minimum total NPC and LCOE. The software performed sensitivity evaluation on the effect of varying the fuel cost, PV, Load demand, and battery prices on system performance.

Yadav and Bajpai (2018) conducted a study on the effect of temperature on the performance of 5 kW solar Photovoltaic plant. The annual reference yield, array yield and final yield were established to be 5.23 kWh/kWp/day, 4.51 kWh/kWp/day and 3.99 kWh/kWp/day, respectively. The annual capacity utilization factor and performance ratio were 16.39% and 76.97% respectively. The annual average daily solar array, system and inverter efficiency were 11.34%, 10.02% and 88.38% respectively. The solar PV project yielded 7175.4 kWh for the whole year under observation.

Kumar *et al*. (2014) investigated the performance of 20 kW grid tied solar Photovoltaic system installed in India's Tiruchirappali region. From the data monitored, the annual energy generated was 30,140kWh. The solar PV system efficiency varied between 10.13 and 12.5% while the efficiency of the inverter varied between 88.91% and 96.50%. The annual capacity utilization factor and performance ratio were established as 17.2% and 82% respectively.

Omkar *et al*. (2015) carried out the analysis of the performance of 50 kWp solar PV plant installed in India's Andhra Pradesh region for the year 2014. The results

indicated the average daily energy output, capacity utilization factor and performance ratio for October 2014 to be 175.183 kWh, 5.822% and 69.3% respectively.

Sharma & Goel (2017) conducted a performance investigation of 11.2 kW grid tied solar Photovoltaic system in Eastern India between September 2014 and August 2015. The total energy yield during the period under study was 14.96 MWh and the performance ratio, inverter efficiency, PV module efficiency was 0.78, 89.83% and 13.42 % respectively.

De Lima *et al*. (2017) carried out performance evaluation of 2.2 kWp grid tied solar Photovoltaic system in North Eastern Brazil. The PV system performance was monitored between March 2013 and May 2014. The annual yield for duration under observation was 1685.5 kWh/kWp. The average array, final and reference yield were 4.9 kWh/ kWp, 4.6 kWh/ kWp and 5.6 kWh/ kWp respectively. The inverter efficiencies, PV system efficiency, annual average array and average daily system losses reported were 94.6%, 12.6%, 13.3%, and 1.05 kWh/kWp respectively. The performance ratio and capacity utilization factor registered were 82.9% and 19.2% respectively.

Ayompe *et al*. (2011) conducted a performance evaluation of a 1.72 kW grid tied solar PV system in Ireland. The total energy yield was 884.1 kWh/kWp whereas the annual array, reference and annual average daily final yield was 2.61 kWh/kWp/day, 2.84 kWh/kWp/day and 2.40 kWh/kWp/day respectively. The inverter, system and annual average daily PV module efficiency was 89.2%, 12.6% and 14.9% respectively. The average daily performance ratio and annual capacity utilization factor and were 81.5% and 10.1%, respectively.

2.3.12 Thermographic analysis

Thermographic analysis entails use of infra-red thermal cameras to check the temperature distribution of the solar panel (Herraiz *et al*., 2020). The distribution of temperature on a solar panel cell can accurately depict the solar panel's condition. Since the temperature coefficient of the power peak for solar modules is negative, it is crucial to monitor the temperature distribution to assess the power performance of the panels. Although visual inspection is sometimes deployed, there are some faults that can only be detected using thermal cameras. Thermal imaging allows the detection of anomalies such as delamination due to external damage, cracked cells, glass cracks, dirt or moisture penetration, short circuits, loose contacts, damaged substrings, and defective individual cells, and hot spots (Acciani *et al*., 2010).

2.4 Research Gap

The exploration of alternative and sustainable energy sources in Kenya, driven by concerns over global warming and rising petroleum prices, underscores the urgency to tap into the abundant solar irradiation resources available throughout the country. Despite significant investments in solar photovoltaic (PV) systems, particularly in institutions like Strathmore University, there remains a critical gap in understanding the long-term performance and optimization of these systems. While the Kenyan government and institutions are increasingly embracing solar energy to supplement the national grid, the lack of comprehensive studies evaluating optimal configurations and performance improvement strategies hinders the efficiency and reliability of these systems. Specifically, the omission of factors such as tilt angle, air gap, and environmental considerations during installation compromises the overall

performance of solar PV systems, highlighting the need for tailored research to address these gaps and enhance their contribution to the national energy grid.

The investigation into the performance and optimization of the 600 kWp grid-tied solar PV plant at Strathmore University holds significant potential to address these gaps and drive tangible benefits for both the institution and the broader community. However, such studies are scarce in Kenya, making the monitoring and optimization of these systems imperative for informed decision-making and effective utilization of solar resources. By evaluating the performance of the Strathmore University system and developing optimal operational parameters, this research aims to establish a benchmark for PV systems across the country. Insights gained from this study will inform strategies to enhance system efficiency, reduce electricity bills, and alleviate strain on the national grid, thereby contributing to Kenya's clean energy transition and sustainable development goals.

Moreover, the findings of this research have practical implications for other institutions and off-grid areas within Kenya, as well as broader implications for promoting sustainable energy adoption nationwide. By showcasing the successful operation and positive outcomes of the Strathmore University system, this research paves the way for the replication and adoption of similar solar energy systems, driving broader access to clean and reliable electricity. Furthermore, the economic, thermographic, and environmental performance analyses conducted as part of this study will provide valuable insights into the feasibility and benefits of solar PV systems, facilitating a more environmentally friendly and economically viable approach to power generation across the country.

CHAPTER THREE

METHODOLOGY

3.1 Introduction

This chapter highlights the procedures undertaken for effective study of the stated main and specific objectives. All the materials and methods used to do this research are detailed in this chapter. The description of the system under study and the geographical location is presented. The description of the data collection for this study are discussed. The methodology for performance analysis of the Strathmore 600 kWp rooftop grid tied solar PV system using the IEC 61724 standards is presented. In addition, the steps for carrying out thermographic and economic analysis of the system are detailed. The greenhouse gas carbon savings for this system are detailed. The procedure for conducting tilt angle optimization simulation analysis for the Strathmore University's Solar PV System is presented. Lastly, an experimental validation, effect of air gap and irradiation on solar PV performance methodology is presented.

3.2 Grid tied PV Performance Analysis Parameters

The solar photovoltaic grid tied system performance was analyzed using the International Electrotechnical Commission standard of 1998 (IEC, 1998). The performance indices entrenched in this standard are essential in assessing the performance of photovoltaic systems and establishing the losses by the systems (Sathiracheewin *et al*., 2020). The parameters evaluated are performance ratio, energy yield, collection losses, reference yield, capacity utilization factor and final yield. Many researchers have used these performance parameters worldwide (Agbetuyi *et*

al., 2018; Adebiyi *et al*., 2020; de Lima *et al*., 2017; Mensah *et al*., 2019; Ayompe *et al*., 2011; Haji *et al*., 2019).

3.2.1 Capacity Utilization Factor

The capacity utilization factor refers to the ratio of the actual energy produced by the photovoltaic system to the energy generated if the photovoltaic system were operated at its full capacity for 24 hours a day for a defined period (Hioki *et al*., 2019). This study considered CUF indices for one year. This is expressed mathematically as in equation [3.1]

$$\mathrm{CUF} = \mathrm{E_{AC}}/[\mathrm{P_{PV,rated}} \times 8760\ ] \qquad [3.1]$$

where E_{AC} is the actual energy produced by the System and P_{PV} is the system's rated full capacity. Also referred to as nameplate capacity.

3.2.2 Total Energy Output

This refers to the total electric AC power produced by the power plant over a defined period of time (Yadav & Bajpai, 2018). This can be total hourly, daily, monthly or even yearly energy yield. Usually, it is evaluated monthly for the grid-connected systems and measured in kWh. This is given as shown in equation [3.2];

$$\mathrm{E_{ac,m=\sum_{d=1}^{n} Eac,d}} \qquad [3.2]$$

where $E_{ac,\,m-}$ monthly AC output

n- Number of days a month.

3.2.3 Reference yield

Reference yield (Y_r) is the ratio of total solar radiation (kWh/m^2) reaching the panel to the reference solar irradiance (1 kW/m^2) under standard test conditions

(Chokmaviroj *et al*., 2006). It is established by dividing the in-plane solar irradiation by 1 kW/m^2. Reference yield shows the in-plane solar irradiation or an equivalent to the hours at the reference irradiance, as shown in equation [3.3].

$$Yr = \left(\frac{H_t}{G_{STC}}\right) \quad (kWh.kWp^{-1}) \qquad [3.3]$$

where H_t is the total in-plane solar radiation and G_{STC} is the reference/source irradiance at Standard Test Conditions.

3.2.4 Array yield

Array yield (Y_A) is the ratio of DC energy produced by the PV arrays divided by the rated kW of the PV array (P_o). This parameter calculates the day's energy yield per rated installed PV array power output (kW) and can be used to calculate the monthly average values(Agbetuyi *et al*., 2018). Array yield is given by equation [3.4].

$$Y_A = \left(\frac{E_{DC}}{P_O}\right) (kWh.kWp\text{-}1) \qquad [3.4]$$

where E_{DC}- DC energy output from the photovoltaic arrays (kWh)

P_O is the rated installed photovoltaic array power output (kW).

3.2.5 Final Yield

Final yield (Y_F) refers to the ratio of the useful daily electrical energy or the inverter output to the rated electrical power of the installed photovoltaic array. It is the power output from the Inverter after conversion. The final yield is typically expressed in kWh/kWp/day (Agbetuyi *et al*., 2018). This relationship is given by equation [3.5].

$$Y_F = \left(\frac{E_{AC}}{P_O}\right) (kWh.kWp\text{-}1) \qquad [3.5]$$

where E_{AC} -AC power output/yield from the Inverter

P_o is the rated Photovoltaic array Power output

3.2.6 Total System Collection Losses

According to IEC 61724 standard, the collection losses occurring in the entire PV system are calculated (IEC, 1998). The total collection losses, L_T, refers to PV array losses due to the solar PV conversion, wiring, thermal, module quality, shading, solar PV module mismatch, dirt, MPPT, and other environmental factors. Numerically, it represents the difference between the final and reference yields. This is expressed mathematically as in equation [3.6].

$$L_T = Y_R - Y_F \ \text{(kWh.kWp-1)} \qquad [3.6]$$

The total system collection losses comprise the array capture and system losses.

Conversion losses/system losses

Conversion losses occur during DC-AC conversion by the system inverters. These losses, also referred to system losses depend on inverter temperature, voltage fluctuations input power and voltage, and the grid voltage (Yadav and Bajpai, 2018). The IEC standard provides the system losses as in equation [3.7]. The system losses (L_S) are caused by equipment effect such as wires, panels and inverters.

$$L_S = Y_A - Y_F \ \text{(kWh.kWp-1)} \qquad [3.7]$$

Array capture losses

Array capture losses is the loss occurring from the PV array. The array capture losses are categorized into two (thermal and miscellaneous). The thermal capture losses result from high temperatures, usually above 25 $^{\circ}$C. The miscellaneous capture losses are caused by low irradiance, wiring, maximum power tracking errors, snow

covering, spectral losses string diodes, dirt accumulation, and mismatch (Miguel *et al*., 2002). Array capture losses refers to the difference between the reference yield and the array yield and is calculated as depicted in equation [3.8]

$$L_C = Y_R - Y_A \ (\text{kWh.kWp-1}) \quad [3.8]$$

3.2.7 Performance Ratio

Performance ratio refers to the ratio of the electrical energy supplied to the grid (final yield) and the ideal electrical energy that the system could generate at its rated DC power for a specific peak sun-hours (Reference Yield) (Agbetuyi *et al*., 2018). This parameter is crucial in establishing details on the photovoltaic system, such as inverter losses, losses due to shading, DC cable losses, AC cable losses, and dust accumulation losses on the rated output of the solar photovoltaic system (Aravindan *et al*., 2019). This performance index is crucial for determining the system efficiency from solar conversion to the final power fed to the grid. This parameter is affected by system efficiency and other environmental factors. This relationship is shown in equation [3.9], provided by the IEC standards (IEC, 1998).

Also given as the ratio of final yield to reference yield

$$\text{Performance Ratio} = \frac{Y_f}{Y_r} * 100\% \quad [3.9]$$

where Y_F and Y_R Final Yield and Reference Yield, respectively

Also, Performance ratio is calculated as in equation [3.10]

$$\text{Performance Ratio} = \frac{\text{Actual Energy Generated}}{\text{Calculated Energy Generated}} \times 100\% \quad [3.10]$$

where,

$$\text{Calculated Energy Generated} = \text{Annual Global Horizontal Irradiation (GHI)}$$

$$\times \text{Area of the PV modules surface} \times \text{PV module efficiency}$$

The PV plant at Strathmore main campus covers an area of 3920.4 m^2 and has an annual GHI of 2182.7 kWh/m^2. The solar module efficiency is 15.27%. Using this information, the PV performance ratio was calculated.

3.3 Data Acquisition and Monitoring for Performance Analysis

The ambient temperature and solar irradiation required for this performance analysis were obtained from the NASA-SSE database. The site location coordinates (latitude and longitude of S01°18.621' and E036°48.918', respectively) of Strathmore University served as the input to the NASA tool to ensure retrieval of accurate ambient temperature and solar irradiation data. The Strathmore University's Solar photovoltaic system power output data was monitored for one year (January 2019 to December of 2019) and retrieved from the solar edge monitoring system installed at the institution. This Solar PV system has solar edge optimizers, each attached to two PV modules, which relay real-time voltage, current, and power output to the solar edge inverters. The solar edge inverters are configured with Local Area Network (LAN) that relay the data to the gateway, which transmits the data to the solar edge monitoring system servers. This real-time data is accessed remotely through the online solar edge portal. The power performance data is available daily, monthly, or yearly from the solar edge monitoring portal. The solar edge monitoring unit provides real-time solar PV plant power performance data. The data acquisition and monitoring system are crucial in detecting faults within the system for quick resolution.

3.4 Thermographic analysis

Thermographic analysis entails use of infra-red thermal cameras to check the temperature distribution of the solar panel. The distribution of temperature on a solar panel cell can accurately depict the solar panel's condition.

To perform thermographic analysis for the Strathmore University roof top 600 kW grid tied system, a FLIR E5xt Wifi thermal camera was used as shown in Figures 3.1 and 3.2. This thermal camera works between -20.0 °C and 250.0 °C. The captured thermal images have been analyzed using the FLIR Thermal studio. During the thermal camera set up, specific parameters were set to ensure accurate results since these influences the results greatly. The thermal camera conditions were set as shown in Table 3.1.

Table 3.1: FLIR thermal camera parameter settings

Parameters	
Emissivity	0.95
Distance	1.00 m
Reflected temp.	20.0 °C
Atmospheric temp.	20.0 °C
Relative humidity	50.0%
Ext. optics temp.	20.0 °C

Figure 3.1: Thermal Images collection

Figure 3.2: FLIR E5xt Wifi Thermal camera

3.5 Economic analysis

The 600 kWp Strathmore University solar photovoltaic plant was installed at a cost of US$1,300,000.00. The exchange rate during commissioning was US $1=Ksh 90 as provided by the publication of Central Bank of Kenya (Central Bank of Kenya, 2014). Therefore, the investment cost of this project was Ksh.117, 000, 000.00. The University entered a 20-year power purchase agreement with Kenya power utility and reached a deal of US$ 0.12/kWh of solar electricity delivered to the national grid as per the agreement under Feed-in Tariff regulations of 2012. The maintenance cost for Strathmore University 600 kWp solar PV systems is estimated at US$ 15 per MWh (1US$ = Ksh.140) of energy generated as provided by the publication of Central Bank of Kenya (Central Bank of Kenya, 2024). For economic analysis, a simple payback period and Levelized cost of energy (LCOE) was used to determine the economic performance for the project's estimated life time of 25 years. The LCOE is used to

compares electric power generation technologies despite the differences in project size, location, system specifications, and even lifetimes. The LCOE is calculated by dividing the total investment costs (Life cycle costs) associated with project by the energy generated during its lifetime (Kerboua *et al*., 2022). LCOE basically refers to the lowest price of selling energy to break even. The Levelized cost of energy is given as:

$$\mathrm{LCOE} = \frac{\mathrm{CRF}*\mathrm{C}_1 + \mathrm{C}_{\mathrm{O\,\&M}}}{\mathrm{E}_a}\ \mathrm{cost/kWh} \qquad [3.11]$$

Where C_1 is the investment capital, $\mathrm{C}_{\mathrm{O\,\&M}}$ is the yearly operational and maintenance costs, E_a is the total yearly electricity produced and CRF is the ratio of a constant annuity to the present value of receiving that annuity for a specified period of time. This is given by:

$$\mathrm{CRF(i,n)} = \frac{\mathrm{i}(1+\mathrm{i})^{\mathrm{n}}}{(1+\mathrm{i})^{\mathrm{n}}-1} \qquad [3.12]$$

Where i- discount rate (fraction)

n- Installation life (years).

The following assumptions were made in calculating LCOE:

a) The installations annual energy output of 734,707.73 kWh is assumed to be same throughout the 25-year cycle
b) The economic lifetime (n) of the solar photovoltaic project is taken as 25 years
c) Considering the current inflation rate and interest rate of 8.0% and 13.1% respectively, using Fisher's expression, the discounted rate is estimated at 5.1%. The Fisher's expression is given by equation 3.13
d) $\mathrm{i} = \mathrm{r} + \pi$ [3.13]

e) Where i- nominal interest rate, r is the real interest rate, π is the inflation rate

f) The annual operations and maintenance costs of Ksh.1, 102,061.60 is assumed to be constant for the system's lifetime.

g) The captive energy consumption for the Institution Solar photovoltaic system is assumed to be 595,520.53 kWh per year and assumed to be constant for the 25 years life time. The cost per kWh according to Kenya Power was Ksh.20.58 (EPRA, 2014). This is also assumed to be constant throughout the project life time.

The simple payback period economic indicator refers to the length of time taken for a projects cash flows to cover the investment capital costs (Qadourah, 2022). The simple payback period is given as:

$$\text{SPP} = \frac{\text{IC}_0}{\text{CF}_1} \qquad [3.14]$$

Where IC_0 is the invested capital and CF_1 is the annual cashflow for project.

The annual cash flow, CF_1, is estimated by summing the annual savings by offsetting grid electricity (captive consumption) and Income from energy sold to the Kenya Power Utility and subtracting the annual expenses on Operations and Maintenance of the PV system.

3.6 Greenhouse gas savings (GHG emissions reductions)

Solar PV systems have the advantage of not releasing Greenhouse Gases (GHG) during its life time (Peyvandi *et al*., 2023). The average grid emission factor for solar PV systems in Kenya for the period between 2019 and 2020 was 0.4087 tCO_2 /MWh (Standardized baseline Grid Emission Factor for the Republic of Kenya, 2020). The grid emission factor normally calculates the quantity of CO_2 that could be avoided

by generating power using solar photovoltaic systems. Using this grid emission factor, the carbon savings was calculated by the formulae:

$$(CO_2)_a = 0.4087 * E_a \text{ Metric tonnes} \quad [3.15]$$

where, E_a is the energy generated in the specified period, a.

3.7 Strathmore University Grid-tied solar PV system simulation studies

3.7.1 Strathmore University solar PV system geographical site

Strathmore University is located approximately 5.5 km away from the Nairobi City Centre. The solar PV system is located at latitude and longitude of S01°18.621' and E036°48.918', respectively, and an altitude of 1794 m above sea level. Figure 3.3 depicts a picture of the grid-tied Solar PV system on the Strathmore energy research center building roof top.

Figure 3.3: Grid connected solar Photovoltaic system at Strathmore Energy Research Centre building

The location latitude and longitude were used for establishing the ambient temperature and solar radiation data from the PV Syst NASA-SSE database. The meteorological data extracted from the NASA-SSE is as shown in Table 3.2.

Table 3.2: Geographical site meteo data

	Global horizontal irradiation	Horizontal diffuse irradiation	Temperature
	kWh/m²/day	kWh/m²/day	°C
January	6.66	1.76	21.6
February	7.09	1.76	23.6
March	7.27	1.95	25.2
April	6.49	1.98	24.4
May	5.44	1.83	21.3
June	4.36	1.75	19.9
July	5.25	1.77	20.6
August	5.59	1.91	21.6
September	6.11	1.91	22.9
October	5.83	2.03	21.5
November	5.94	2.05	20.8
December	5.79	1.82	19.9
Year	**5.98**	**1.88**	**21.9**
	Paste	Paste	Paste

Global horizontal irradiation year-to-year variability 4%

3.7.2 PV system specification

To carry out optimization simulation, the solar PV module type was selected as a standard module type, polycrystalline cell technology, tilted roof-mounting disposition and free air circulation ventilation property as shown in Figure 3.4.

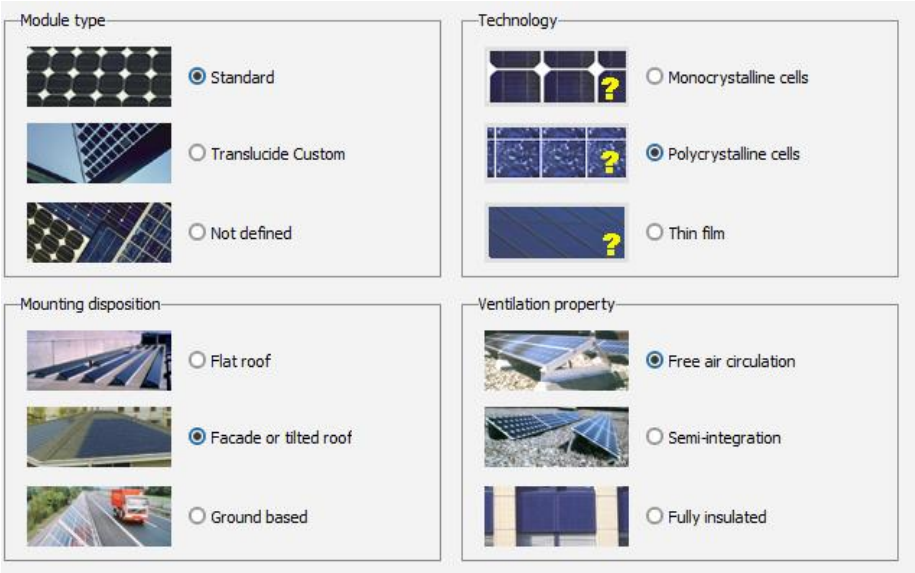

Figure 3.4: Module type specification

The system array specification simulation parameters were entered in the PV Syst simulation software as shown in Figures 3.5 and 3.6.

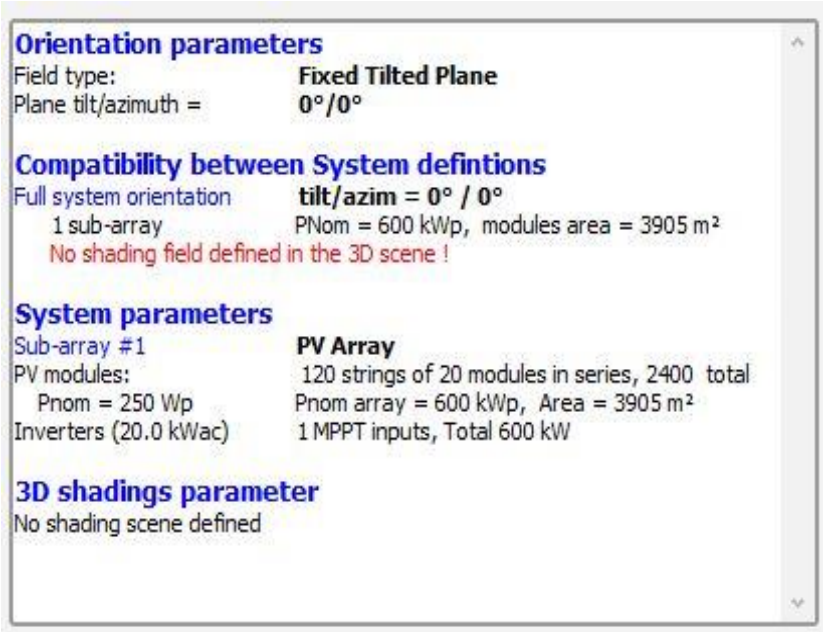

Figure 3.5: solar PV system specification parameters

Figure 3.6: Simulation parameters

3.7.3 Optimization simulation procedure

In the PV Syst software, the location coordinates were entered which aided in the extraction of the meteorological data for Strathmore University from the NASA-SSE database. The module type specification was selected and system array specification parameters were entered in the PV Syst software as shown in Figures 3.4 and 3.5. The orientation parameters i.e., Azimuth and tilt angle and main simulation parameters were set as shown in Figures 3.5 and 3.6, respectively. The Azimuth was fixed at 0˚while the tilt angles were changed from 0° to 15° at intervals of 1°. In each step, the annual energy output value (MWh/Yr) and Global Horizontal Irradiation (kWh/m^2) was captured. To determine the optimal tilt angle, an optimization tool within the PV syst software was used where 15 steps of optimization simulations were done. Figure 3.7 shows the optimization tool used for obtaining optimized tilt angle.

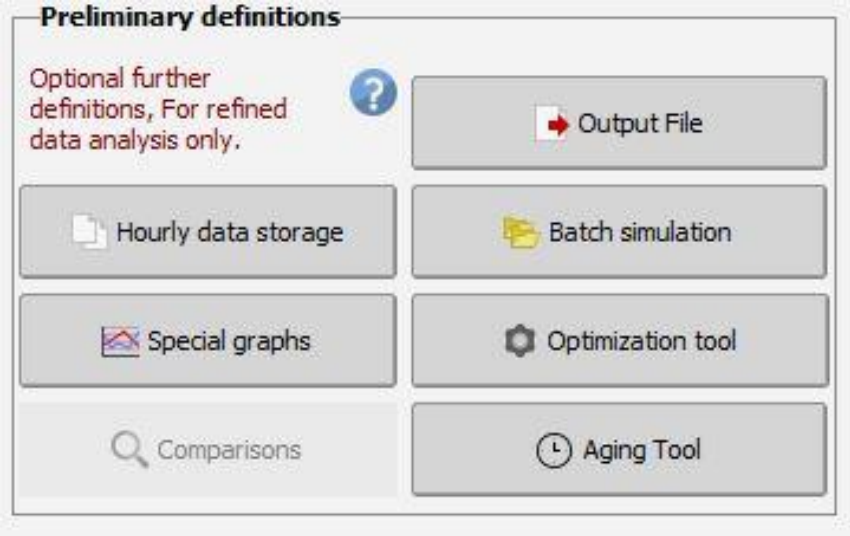

Figure 3.7: Tilt angle optimization tool

3.8 Experimental validation of tilt angle optimization simulations, impact of air gap on module back surface temperature and effect of irradiation on module power performance

3.8.1 Kenyatta University Experimental Site

An experiment was set up at Kenyatta University Energy Laboratory rooftop to further validate the optimization simulation results for Strathmore University Solar photovoltaic system as shown in Figure 3.8. The location for this setup was S01°10.758'E036°55.543' and 5,164 feet above the sea level. The solar panels were set facing True North to match the orientation for the one of the installations in Strathmore University. Since the experimental site location was different from the Strathmore university simulation setting location, a simulation for Kenyatta University site location was done. The simulation at the energy technology building roof top of Kenyatta University used weather data input as sourced from NASA-SSE meteo database. The simulation was done as detailed for the Strathmore University

site with the location's coordinates used to retrieve meteo data from the NASA-SSE data base.

The experimental set up consisted of six polycrystalline panels installed on the rooftop. Table 3.3 shows the PV module specifications:

Table 3.3: Solar Module specifications

System Parameters	PV specifications
Solar Module type	Polycrystalline
Maximum Power (P_{max})	20 W
Open circuit voltage (V_{oc})	21.56 V
Short Circuit Current (I_{sc})	1.23 A
Voltage at Pmax (I_{mp})	17.55 V
Current at Pmax (Imp)	1.14 A

3.8.2 Experimental Setup and procedure

Figure 3.8 shows the experimental setup that was carried out for a period of 3 weeks i.e., from 23/03/2022 to 14/04/2022. The data was collected from 09:00 AM to 4:00 PM daily. The six panels were positioned into 3 pairs with each pair set at 4°, 11° and 15° as shown in Appendix M. The choice of these tilt angles for experimental analysis was because of the following rationale:

4° tilt angles: This angle was chosen since it was within the optimal range i.e., between 1° and 5° from the simulations done as shown in Figure 4.12.

11° tilt angles: Chosen to mimic the installation tilt angle for the solar PV panels in one of the roof top buildings at Strathmore University.

15° tilt angles: This tilt angle was chosen for analysis since it is considered as the industry best practice installation angle by most companies in Kenya to allow self-cleaning. To study the effect of air gap on the performance solar photovoltaic system, one panel of each pair was set with an air gap of 100 mm while the second panel was positioned with an air gap of 150 mm for each of the three pairs of the solar panels (see appendix M).

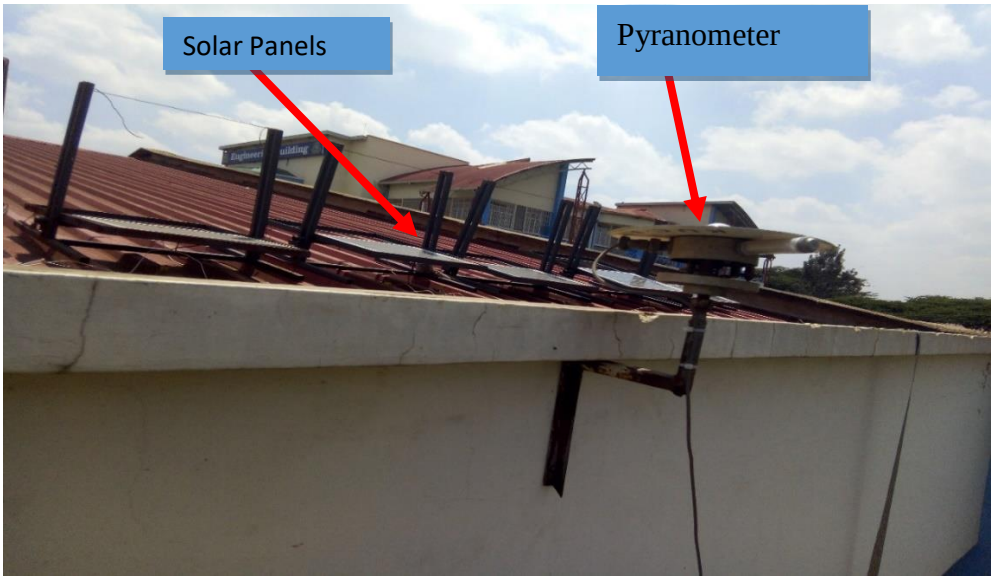

Figure 3.8: Experimental set up at Kenyatta University Energy Laboratory Rooftop

Data logging was done using the Rigol M300 data logger and the Arduino Microcontroller based data logger at 5 seconds intervals. The Arduino Microcontroller based data logger was designed and programmed to collect short circuit current and open circuit voltage. The data collected by this data logger was displayed on LCD display in real time and stored on the embedded SD card. The microcontroller-based data logger was designed with voltage and current sensors thus measuring data.

The Rigol M300 data logger was configured to collect and store solar irradiation data, ambient temperature and the temperature of the back surface of the panel. The K type thermocouple temperature sensors attached at the back surface of the solar panel measured the temperature. The data logger recorded irradiation data measured by a pyranometer attached at the rooftop. The readings were recorded at intervals of 5 seconds, which gave an accurate account of the environmental behaviour and their impact on the power performance characteristics of the panels.

A Laptop computer was used to retrieve the data logged on the Rigol and microcontroller-based data logger. Figure 3.9 shows the complete data logging setup.

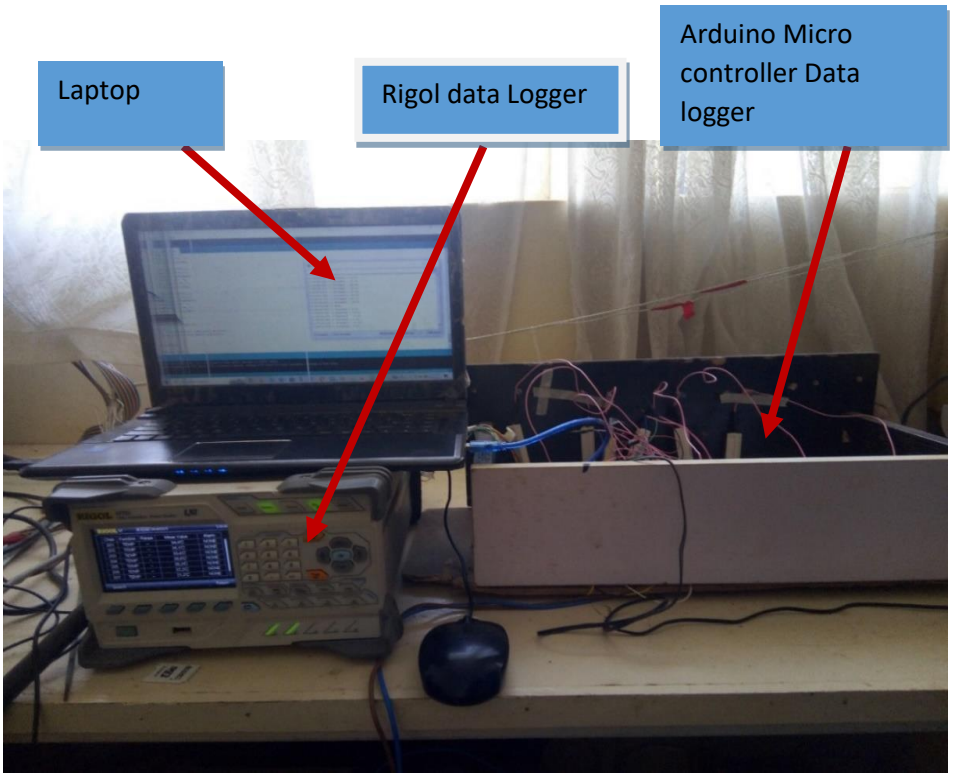

Figure 3.9: Data logger equipment set up

3.8.3 Statistical Correlation tools

In this study, Root Mean Square Error (RMSE) and Mean Absolute Error statistical tools were used to make comparison between the simulated and experimental results.

Root Mean Square Error (RMSE) statistical tool was used to establish the relationship between the simulated and experimental results. RMSE is given by:

$$\mathrm{RMSE} = \sqrt{\frac{1}{n}\sum_{i=1}^{n}(ci - mi)^2} \qquad [3.16]$$

where n is the number of simulations, ci is the expected simulation and mi is measured or the observed experimental results. Usually, RMSE values of between zero and 0.3 are considered acceptable i.e., $0 < \mathrm{RMSE} \leq 0.3$

Further, Mean Absolute Error was used to validate the simulated and experimental findings. Mean absolute error is a metric used to evaluate the mean average magnitude between the measured and predicted value of a given set of quantity. The Mean Absolute Error is given by the formulae:

$$\mathrm{MAE} = \frac{1}{n}\sum_{i=1}^{n}|yi - y| \qquad [3.17]$$

Where n is the number of simulations, yi is the expected simulation and y is measured or the observed experimental results. The acceptable range for MAE is $0 < \mathrm{MAE} \leq 0.1$.

3.9 Research assumptions and limitations

3.9.1 Assumptions

i. Environmental Conditions: The assumption is made that the environmental conditions at the simulation and experimental locations were sufficiently similar or accounted for during the analysis.

ii. Data Accuracy: It is assumed that the data collected during both the simulation and experimental phases are accurate and free from systematic errors or biases.

iii. Representative Sample: The assumption is made that the sample used for the experimental analysis is representative of the population or system being studied.

3.9.2 Limitations

i. Location-Specific Effects: The experimental analysis conducted at a different location may be subject to site-specific factors, such as local topography or other environmental variations, which might not be fully accounted for in the simulation.

ii. Unforeseen Variables: There could be unknown or uncontrolled variables such as wind and equipment variability at the experimental location that were not considered in the simulation, leading to discrepancies between the two sets of results.

CHAPTER FOUR

RESULTS AND DISCUSSION

4.1 Strathmore University Grid-Tied Solar PV System

4.1.1 Strathmore University grid-tied solar PV system description

The 600 kWp grid-tied solar Photovoltaic system is composed of two systems, 260 kW and 340 kW, connected to two transformers. The PV system comprises 2400 solar panels; each rated 250 Wp, spread across six buildings in the University with an area coverage of 3,920.4 m^2.

Figure 4.1: Solar PV system spread on Strathmore University building rooftops (Google Earth, 2022)

The six buildings have their rooftops installed solar PV modules with varied orientations. Building one as indicated in Figure 4.1 has a total of 720 solar PV modules with a totaling to 180,000 Wp. Building six has 600 solar PV modules installed with total capacity of 100,000 Wp. Both building one and six rooftop's solar Panels are oriented towards the west. Buildings two and three have equal solar PV

system capacities of 80,000 Wp each; and consisting of 320 solar PV modules in each building.

Building 2 and 3 rooftop's solar PV modules are oriented towards south. Building 4 and 5 have solar PV system's capacities of 40,000 Wp and 120,000 Wp respectively. Building 4 and 5 are both oriented towards the North. Since the solar modules orientation affects its power performance, the varied orientations exhibited in the case of Strathmore University's solar PV system influences energy generated greatly.

For optimal power performance, panels in the southern hemisphere should be oriented towards the North. Since only two sets of solar PV systems are aligned towards the North, most of the Strathmore University buildings' rooftops are not optimized and affects the performance parameters such as capacity utilization factors, Performance Ratio, and energy yields as discussed in the following sections.

In addition, there are 30 solar edge inverters, each rated 20 kW. Each Inverter is interconnected to 30 strings of 80 solar modules. The solar edge inverters capture the voltage, power output, and current from the panels by use of solar edge optimizers attached to the solar modules.

The Strathmore solar PV system is connected to two transformers at 415 V in two locations, i.e., at Mvule and Keri house. Figure 4.2 represents the diagram for the Solar Photovoltaic system.

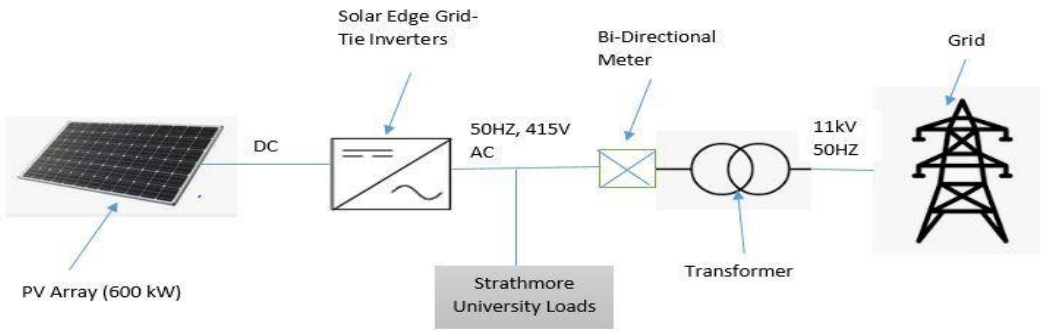

Figure 4.2: Solar Plant System at Strathmore University schematic diagram

4.1.2 Technical specifications

The rating of solar modules is established to ensure that they perform according to the specifications under the laboratory setting to allow measurements and comparisons. The Strathmore university solar Photovoltaic cells are the Jinko solar 250 Wp polycrystalline type. The specifications are illustrated in Tables 4.1 and 4.2 (See datasheet in appendix B).

Table 4.1: Technical details for existing system

Designation	Strathmore University rooftop PV system
Rated Power output	600 kWp
Total Area	3,920.4 m^2
Tracking system (Single/Dual axis)	No tracking system
Tilt	Varied
Installation type	Rooftop
No. of inverters	30
No. of modules	2,400

Table 4.2: PV Module specifications

Parameter	STC Value
Maximum power rating	250 Wp
Open circuit voltage	37.7 V
Short circuit current	8.85 A
Rated voltage at maximum power	30.5 V
Rated current at maximum power	8.20 A
Module efficiency	15.27%
Weight	19 kgs
Dimensions	1650*992*40 (mm)
Maximum system voltage	600(UL)/1000 V(IEC)
Operating Temperature (°C)	-40 °C to 85 °C
Maximum series fuse rating	15 A
Power tolerance	± 3%
Temperature coefficients of Pmax	-0.45%/ °C
Temperature coefficients of V_{OC}	-0.27%/ °C
Temperature coefficients of Isc	0.05%/ °C
Nominal operating cell temperature (NOCT)	$45^0 \pm 2$°C
Cell Type	Polycrystalline
No of cells	60
Module type	JKM250PP-60
Company	Jinko Solar

4.2 Ambient temperature and solar radiation

The solar radiation and ambient temperature data for Strathmore University site were obtained from NASA (see appendix K). Several researchers have used data obtained from NASA to conduct performance analysis. For instance, Querikiol and Taboada (2018) conducted a performance study on an off-grid PV system for agricultural farms in Camote, Philippines. The annual average ambient temperature and annual average solar irradiation in this location are 21.9 ^{0}C and 5.98 kWh/m^2, respectively. Figure 4.3 depicts the region's ambient temperatures and solar irradiation for 2019 as obtained from NASA.

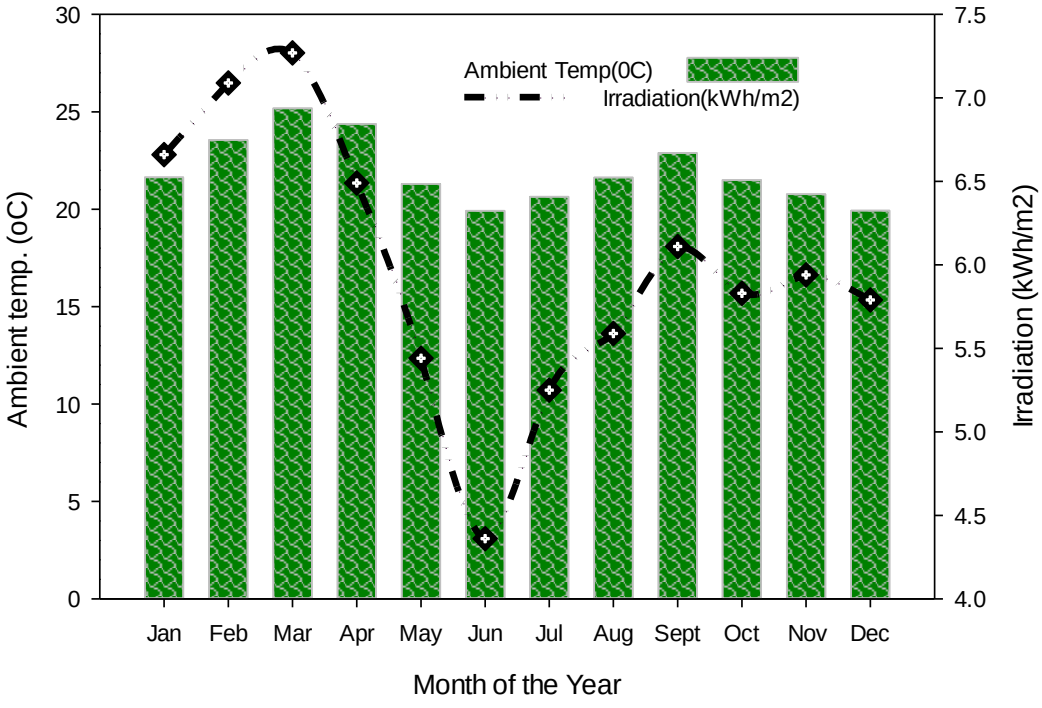

Figure 4.3: Monthly average ambient temperature and Solar Radiation at Strathmore Solar Plant in 2019

In 2019, the highest recorded monthly average temperature was 25.2 ^{0}C in March, and the lowest recorded monthly average ambient temperature was 19.9 ^{0}C in June.

March reported highest average solar irradiation of 7.27 kWh/m^2, while the lowest solar irradiation was observed in June with a reading of 4.4 kWh/m^2, as depicted in Figure 4.3. It was observed that periods of high solar irradiation recorded high ambient temperature levels.

Daut *et al*. (2012) conducted a study that examined the connection between ambient temperature and solar irradiation in Perlis. They discovered a strong correlation between these two variables, as indicated by a linear correlation coefficient value of 0.7473. The findings suggests that changes in solar irradiation have a significant impact on ambient temperature which aligns with the observed relationship between solar irradiation and ambient temperature in the Strathmore University area.

4.3 Performance analysis of the grid tied solar PV system

4.3.1 Energy generated and solar irradiation

Figure 4.4 shows the energy generated by the 600 kWp plant at Strathmore University for the year 2019. The highest energy generation occurred in March, and the lowest occurred in June, as shown in Figure 4.4. Further, the energy generated in March and June was 83 MWh and 41 MWh, respectively. The total annual energy yield in 2019 was 735 MWh, with a specific yield of 1,225 kWh/kWp. Notably, the energy yield was relatively high in January, February, and March.

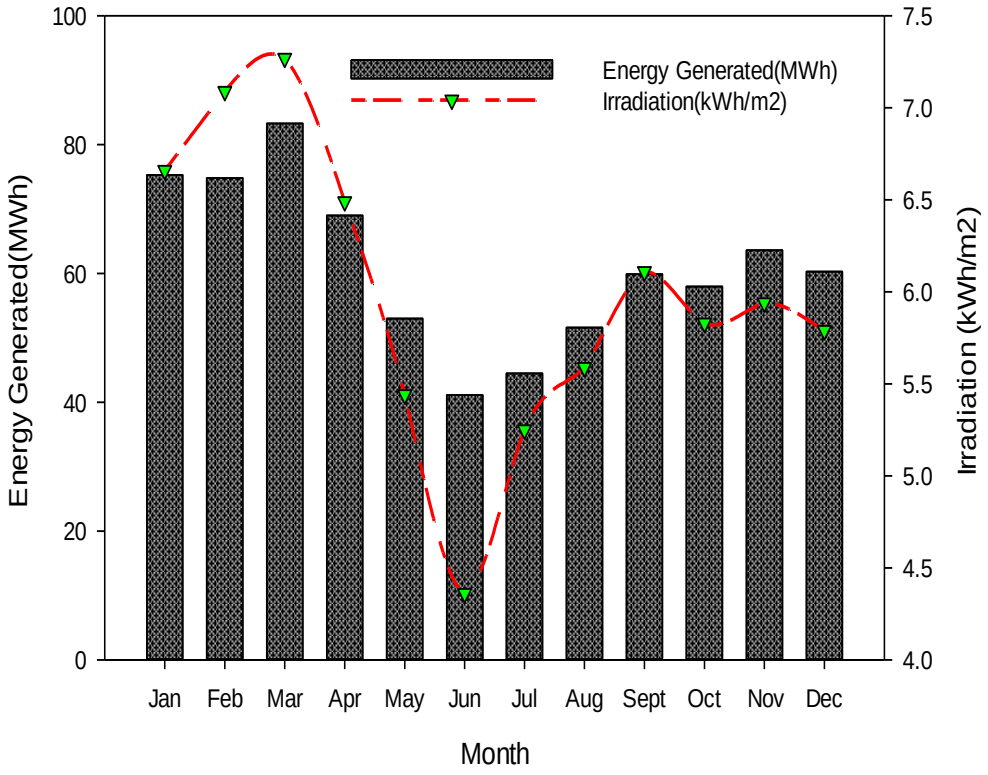

Figure 4.4: Monthly Energy generation for Strathmore University Plant for 2019

On the other hand, low energy generation occurred between June and August. Higher energy yield in January, February, and March was attributed to the relatively high solar insolation, averaging at of 6.95 kWh/m^2 monthly. The average energy yield for the first three months is 77.3 MWh.

On the other hand, June, July, and August generated an average energy yield of 45.3 MWh. This can be attributed to the relatively lower solar irradiation averaging at 5.65 kWh/m^2. The average monthly yield for 2019 was 61 MWh. March exhibited highest power generation occasioned by the high solar radiation levels. Nasrin *et al*. (2018) conducted an investigation on the impact of high solar irradiation on power and energy. They found that as solar irradiation increases, the efficiency of solar panels

improves significantly, resulting in higher energy outputs as depicted by equation 2.1. This effect occurs because higher solar irradiance leads to a considerable increase in current levels in the solar panels, which in turn increases power generation. This further explains the high energy generated during January, February, March, and April.

Figure 4.5 shows the energy exported to the grid, captive energy consumption and the system's energy generated for the year under review. The system exported 139 MWh to the grid and supplied 596 MWh to the institution for captive consumption. The energy supplied to grid accounted for 19% of the total generation.

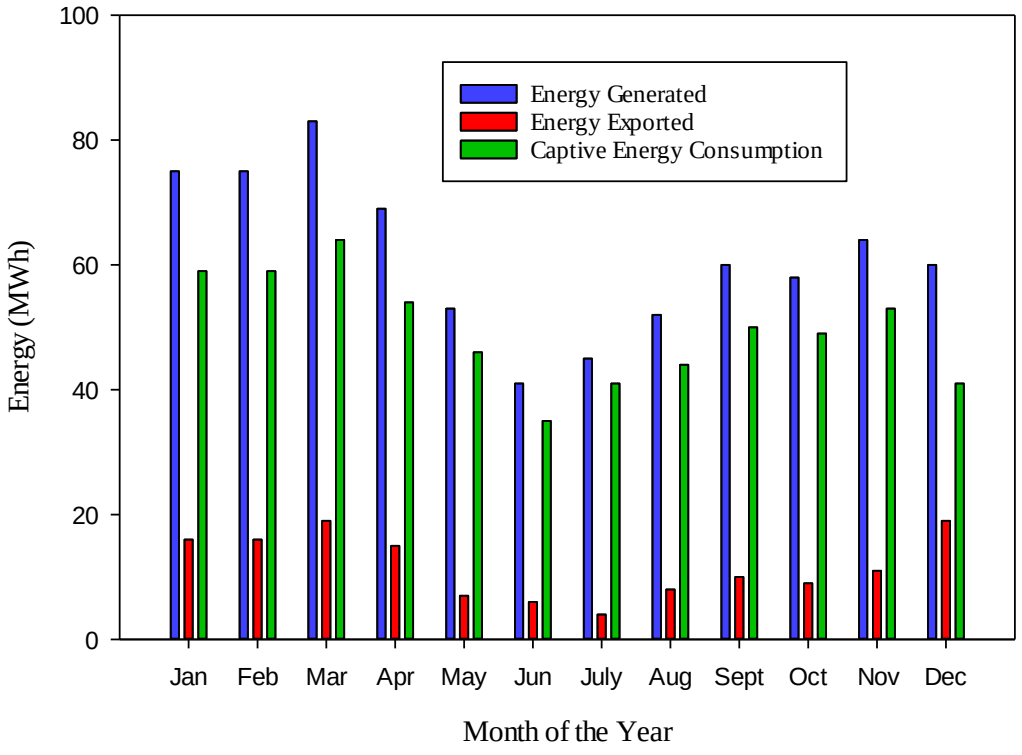

Figure 4.5: Energy generated, Exported and Captive consumption

The energy yielded by this solar Photovoltaic system varied linearly with solar irradiation with a strong correlation R^2=0.9326, as shown in Figure 4.6. Mensah *et*

al. (2019) established a very close relationship between electricity generated and solar irradiation with a strong correlation R^2=0.8683. This is because higher solar irradiation levels cause higher energy production, as exhibited in Figure 4.2.

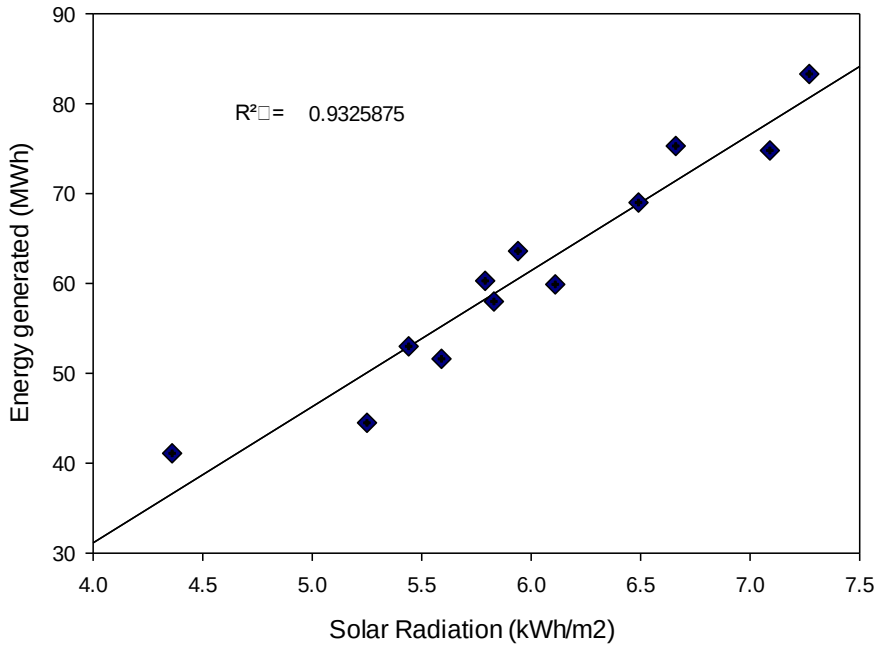

Figure 4.6: Effect of Solar Radiation on Energy Generated

4.3.2 Performance Ratio

The performance ratio (PR) was calculated from data collected in the solar PV system monitoring unit at the University using equation 3.10. The monthly average performance ratio reported had a minimum of 45.8% in July and a high of 62.9% in February 2019.The annual PR and average monthly PR was 56.4% and 55.9% respectively. This indicates that the system was performing slightly above average. This performance was attributed to the failing solar module optimizers and the low solar irradiation levels experienced in the last quarter of the year. The average

monthly PR for the solar Photovoltaic system for 2019 was relatively high during the first three months of the year and the last quarter of the year. This was attributed to high solar irradiation experienced during these seasons, as seen in Figure 4.3. Although the performance Ratio for Strathmore University 600 kWp Solar PV system compares with other installations across the world, the relatively lower performance is attributed by the non-optimized rooftops at the site. Omkar *et al*. (2015) conducted a performance evaluation of 50 kW rooftop solar Photovoltaic plant installed in India's Andhra Pradesh, region in 2014. The results indicated that the performance ratio for October 2014 was 69.3%, whereas the Strathmore PV system depicted a PR of 55% during the same month, as exhibited in Figure 4.7. The low average annual performance ratio for Strathmore University location was mainly attributed to non-optimal orientations exhibited by the solar PV modules spread across the six buildings.

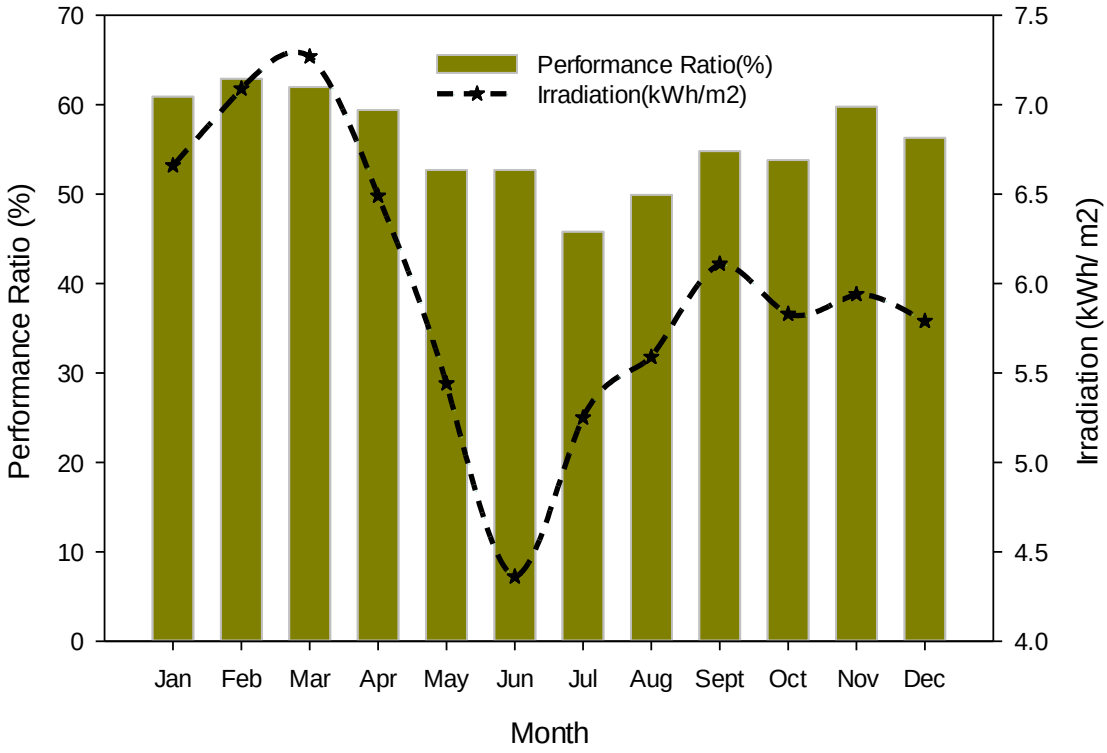

Figure 4.7: Performance Ratio for 2019

This shows that the Strathmore University Solar PV system performs similarly to other systems worldwide, although lower. The difference in performance could be attributed to the varying climatic conditions for these regions. In addition, the technical PV system parameters for these PV projects are different, causing a variance in performance. Other scholars conducted performance ratio evaluation for solar photovoltaic systems, whose results are comparable to those for Strathmore University PV systems (Kumar *et al*., 2014; Yadav & Bajpai,2018).

4.3.3 Array Yield, Final Yield and Reference Yield

The array, final and reference yield were calculated using equations [3.3-3.5] from the data obtained in 2019. The array, final and reference yield parameters were vital

in establishing the system's total losses. Figure 4.8 depicts the monthly trends of these parameters.

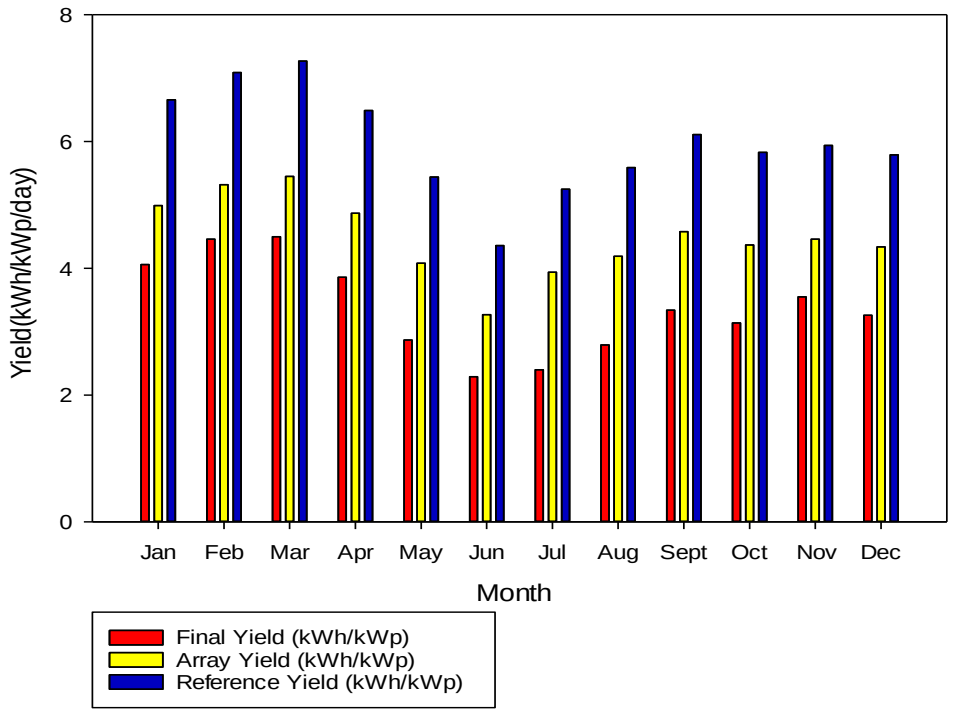

Figure 4.8: Array, Final, and Reference yield

As observed in Figure 4.8, the reference yield reported in June and March was 4.36 kWh/kWp and 7.27 kWh/kWp, respectively. The final yield reported in June and March was 2.29 kWh/kWp and 4.46 kWh/kWp, respectively. The average monthly array yield was lowest at 3.27 kWh/kWp in June and highest at 5.45 kWh/kWp in March. The high array, reference and final yield during March are attributed to high solar radiation levels. Notably, the increase in the incoming solar radiation increased the power output of the solar panels which consequently influenced these performance indices. For instance, the solar radiation for June was 5.25 kWh/m^2 whereas, in March, the area registered average solar radiation of 6.49 kWh/$m^{2.}$ The annual average monthly reference, final and array yield for the year 2019 was 5.9

kWh/kWp, 3.37 kWh/kWp and 4.49 kWh/kWp, respectively. This study revealed that the array, reference and final yields for the year's first three months were relatively higher than the year's second quarter. This was attributed to the higher solar irradiations experienced in January, February, and March, as depicted in Figure 4.3.Yadav & Bajpai (2018) performed a performance analysis on a solar Photovoltaic power plant in India's Northern region and established that the average annual reference, final, and array yield were 5.23 kWh/kWp, 3.99 kWh/kWp and 4.51 kWh/kWp, respectively. These results are comparable to the Strathmore solar PV plant and found to be almost similar, as discussed above.Other scholars have investigated the performance of grid-tied solar Photovoltaic systems and reported similar results to this study (Omkar *et al*.,2015; Attari *et al*.,2016).

4.3.4 PV System Total Losses

The Strathmore University grid-tied solar PV system exhibited high losses in July, which recorded total system collection losses of 2.85 kWh/kWp. In contrast, the lowest total system collection losses were recorded in June, with 2.07 kWh/kWp, as shown in Figure 4.9.

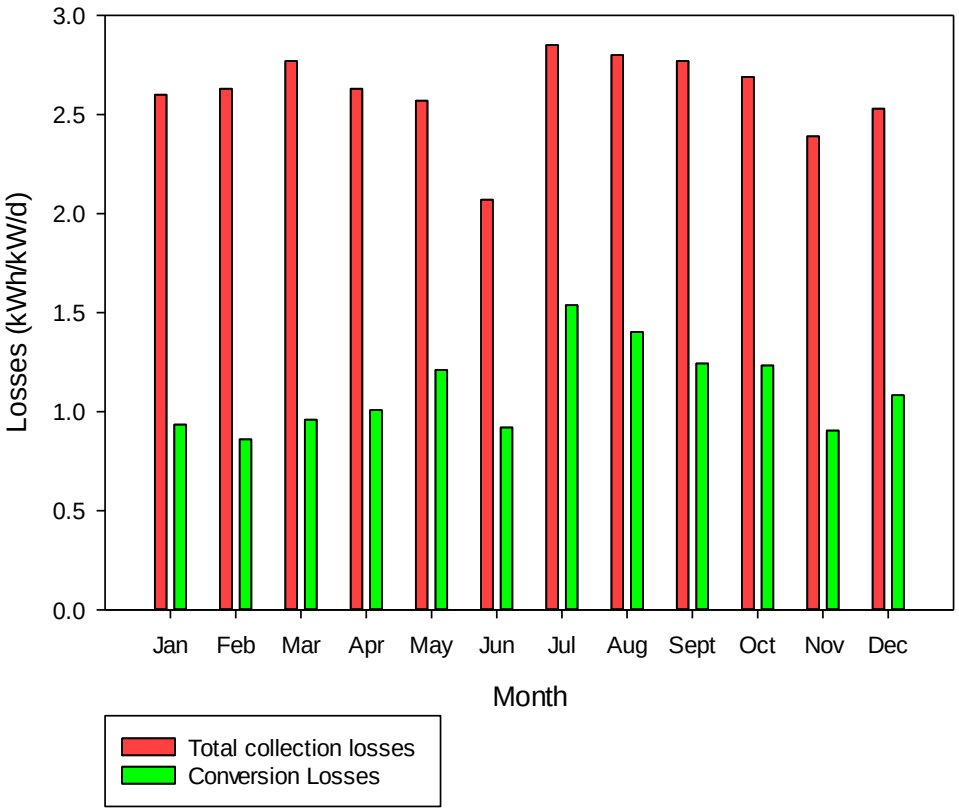

Figure 4.9: PV losses

The monthly average total system collection loss and conversion losses were 2.53 kWh/kWp and 1.11 kWh/kWp, respectively. High total collection losses and conversion losses in July could be attributed to failure of solar edge optimizers, cable and inverter losses. In addition, bird droppings, dirt and dust accumulation could also account for the high losses in July. The lower losses depicted in June could be due to the lower ambient temperature recorded (20.64 °C) and solar module self-cleaning, as there were isolated days of rainfall. Usually, higher temperatures cause the relative increase of the cell temperatures, consequently leading to thermal losses. Thermal capture losses are usually due to the decreasing PV voltage caused by the increasing PV cell operating temperature. Elhadj Sidi *et al*. (2016) reported high thermal capture

losses during summer and autumn due to the high temperatures exhibited during that period.

4.3.5 Capacity Utilization Factor

The capacity utilization factor (CUF) for the 600 kWp plant at Strathmore University varied monthly caused by the changing local environmental factors and the system losses as depicted in Figure 4.10.

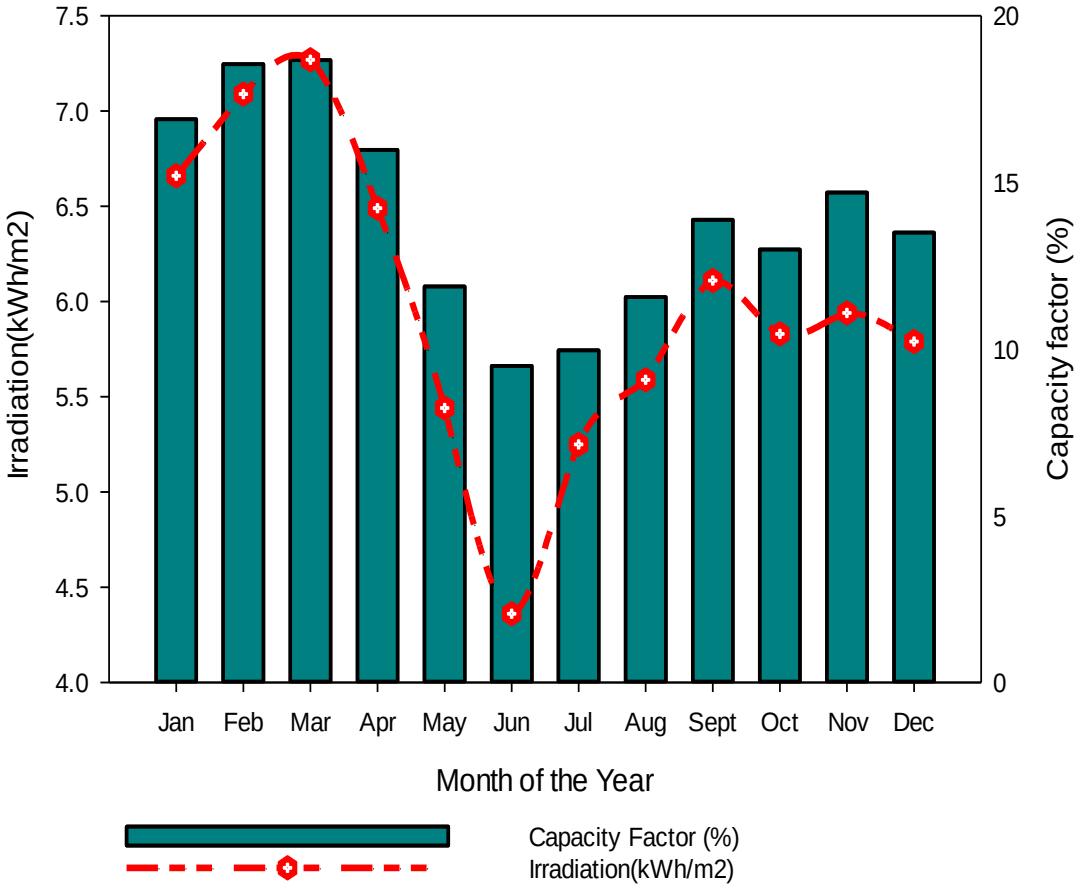

Figure 4.10: Capacity Utilization factor

The system capacity factor ranged from 9.5% in June to 18.7% in March. The annual average monthly capacity utilization factor was 14%, whereas the annual CUF was 13.9%. The seemingly low capacity factors exhibited at Strathmore University Solar

PV plant could be attributed by the fact that the solar PV system is not optimized in terms of orientation. The capacity utilization factor was highest in March when the energy generated was high. On the other hand, the CUF was lowest in June when the solar plant's yield was lowest. The high CUF in March could be attributed to high solar radiation levels during this month and hence the increase in solar PV system's energy yield. The month of June experienced low solar radiation levels, causing a dip in the CUF value. The results from similar studies in various places show how the CUF changes throughout the year, majorly attributed to the changing climatic factors. For instance, Ayompe *et al*. (2011) studied grid-tied PV system performance and concluded that seasonal climatic conditions affected the system's performance. The CUF recorded for winter, spring, summer, and autumn was 5.5%, 13%, 13.1%, and 8.6%, respectively. The researchers concluded that the performance variations were due to the seasonal changes in the wind speed, daily in-plane solar radiation, module temperature, and ambient temperature. Nabil and Mansour (2022) concluded that the solar PV panel efficiency decreases with increasing solar module temperature. In addition, a study by Ayompe *et al*. (2011) found that high wind speeds and low ambient temperatures are important in improving the PV system performance. Sharma and Goel (2017) evaluated the performance of 11.2 kW grid-tied rooftop solar system in India's Eastern region and established that the system had average monthly capacity factor of 15.3%. The highest CUF was in March, with 19.4%, whereas the lowest CUF was 11.5% in December.

Other similar performance analysis studies have shown that the capacity factor ranges from 5% to 20.1%, as referenced by Attari *et al*. (2016), Ayompe *et al*. (2011) , Adebiyi *et al*. (2020), and Mensah *et al*. (2019) among other scholars (see table on

Appendix II). This shows that the PV system at Strathmore is stable and operates within the expected performance levels.

4.4 Thermographic analysis results

The module in Figure 4.11 (a) depicts that a wider area of the PV module had a crack and therefore has a superior temperature of about 3.85 °C with respect to the average one. The solar module has several hot spots with the highest at 40.5 °C. The interrupted cells contribute to reduction in electricity production. Of the 150 samples of solar panels investigated, three panels had major cracks whereas two panels had minor cracks. Cracks are critical in influencing the energy production.

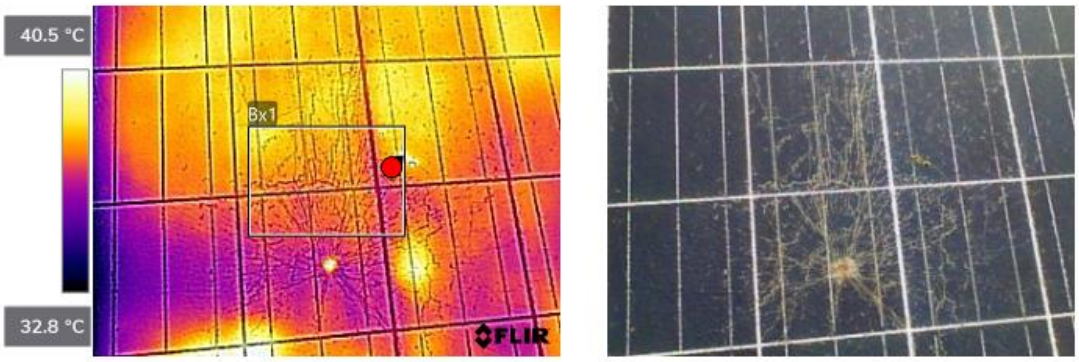

Figure 4.11 (a): Hotspots due to cracked cells

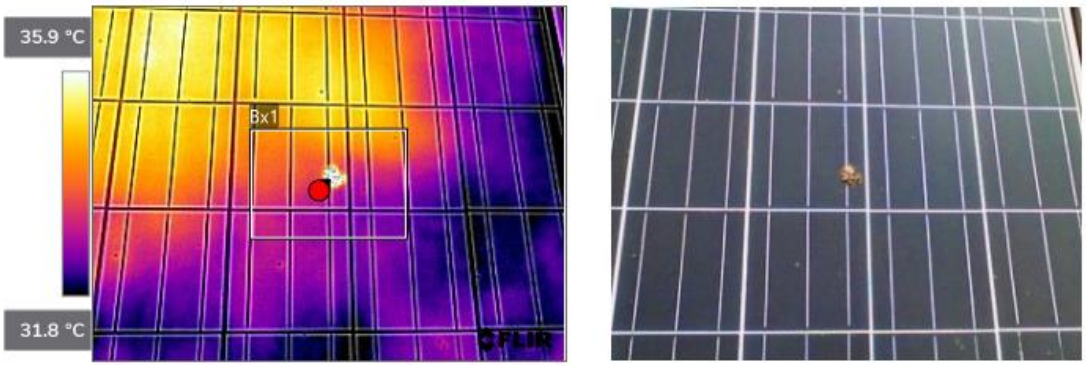

Figure 4.11 (b): Solar Panel hot spot due to dirt

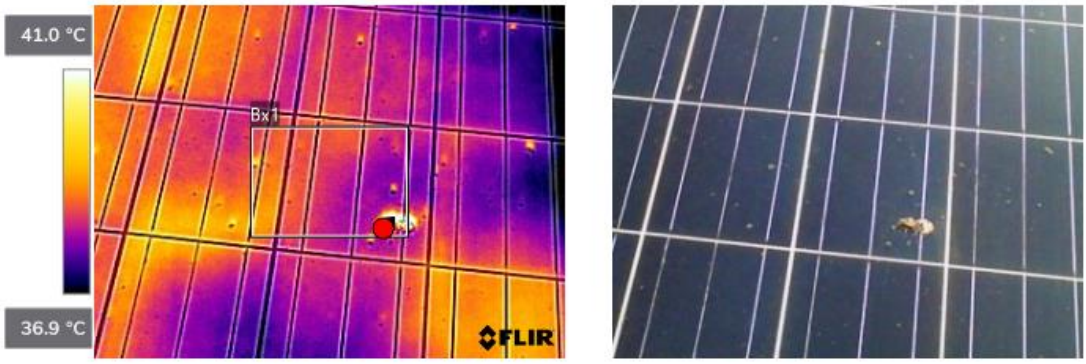

Figure 4.11 (c): Non uniform distribution of temperature due to dirt and bird droppings accumulation

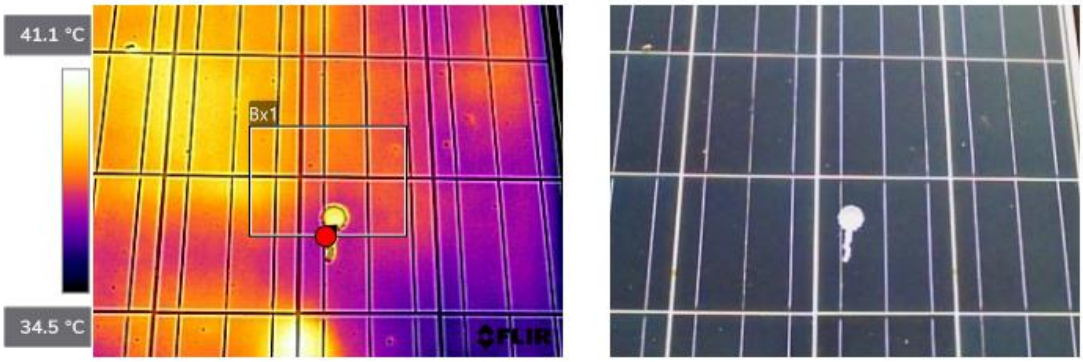

Figure 4.11 (d): Hot spot due to dirt on the solar panel surface

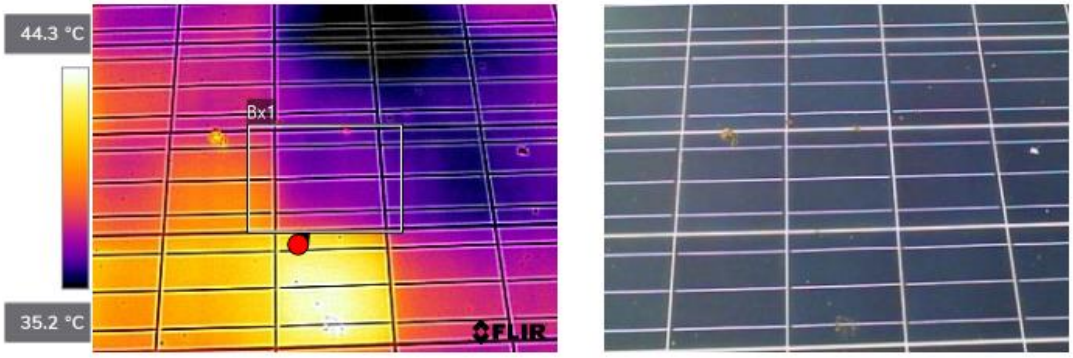

Figure 4.11 (e): Module with overheating single cells

Figure 4.11 (f): Solar module depicting widespread warming

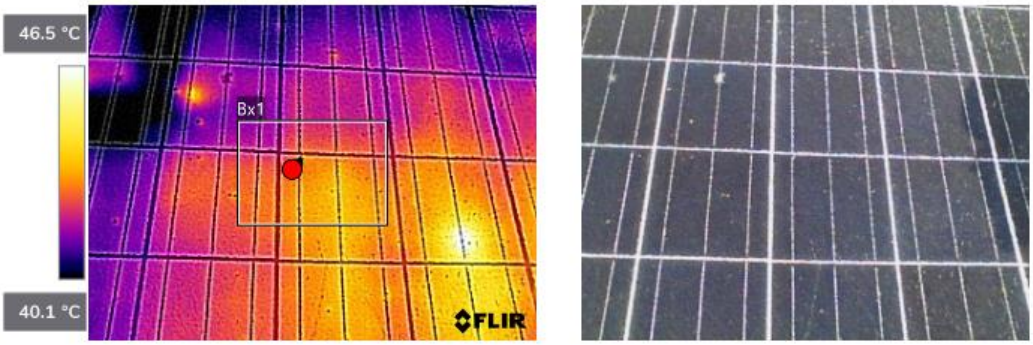

Figure 4.11 (g): Solar module depicting widespread warming with some few patches of hotspots

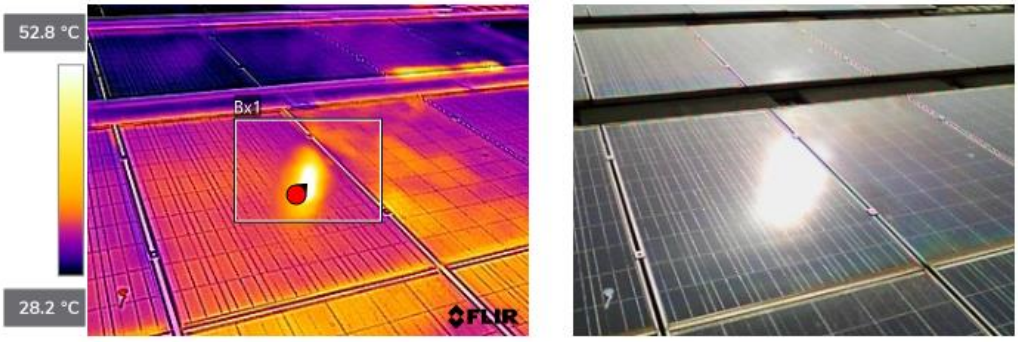

Figure 4.11 (h): Hot spot due to Reflections and glares

As shown in Figure 4.11 (b), the presence of dirt has caused partial shading that is critical in causing hot spots as shown. The hotspot in Figure 4.11 (c) has a superior temperature of 2.05 °C with respect to the average one. The non-uniform distribution of temperature in the panel in Figure 4.11 (c) is due to accumulation of dirt on the

panel's surface. Dust and dirt accumulation covered a wide area of the panel. Figure 4.11 (d) shows solar panel cell hot spot due to foreign material on the surface. The partial shading caused by these materials has resulted in superior temperature of 3.3 °C with respect to the average temperature. Figure 4.11 (e) shows a single cell experiencing abnormal overheating of about 4.55 °C with respect to the average temperature experienced in the other module cells. Probably, this cell is damaged or defective. This can cause considerable power production losses. Figure 4.11 (f) and 4.11 (g) shows PV module depicting widespread overheating with an average temperature of 36.25 °C and 43.3 °C, respectively. This was caused by a widespread accumulation of dust covering the solar module surface, hence shadowing. This could be occasioned by the low rainfalls experienced in the region which could help to potentially self-clean the PV modules.

Figure 4.11 (h) depicts hot spots due to reflections on the surface of the solar Photovoltaic modules. This could cause decrease in power generated. The hot spot created is at 52.8 °C with a temperature difference of 24.6 °C. This large temperature difference is critical in accelerating thermal losses hence decreasing the power production. These reflections are likely to accelerate system degradation and cause severe failures. The thermographic analysis done on the 150 sample thermal images picked during this study indicates that 99% of the samples depicted an average of 5.48 °C temperature difference between the highest and the lowest point for each reading. According to Jahn *et al*. (2018), temperature differences of 30 °C depicts a serious failure, while temperature range between 10 °C to 30 °C indicates moderate or medium failure. All gradients lower than 10 °C are considered unproblematic. Although the report showed that the solar panels exhibited less severity, regular

thermal inspections should be done in the subsequent schedules as the severity could increase due to continued operations. Temperature variations above 20 °C may cause the system to degrade over time and eventually result into a more serious failure. Therefore, from the thermographic analysis done, the Strathmore University 600 kW Solar PV system exhibits normal properties, although more frequent cleaning of the solar panels will improve the systems performance.

Acciani *et al*. (2010) carried out thermographic analysis of 20 kW grid tied system and concluded that the solar photovoltaic system's efficiency largely influenced by the cell temperatures and that over-heating can cause cell break downs, hot spots and other problems resulting in loss of power production.

4.5 Economic Indicators

From the available data, Strathmore University grid tied system achieved annual savings in the electricity bill equivalent to 31%. The levelized cost of energy (LCOE) was established using equation 3.11. The LCOE of this system was estimated at US$0.143/kWh. Kumar *et al*. (2014) carried out economic analysis on 20 kW grid connected solar PV installation in India and found an LCOE of US$ 0.13. This shows that the Strathmore system performs similar to other solar photovoltaic systems worldwide. Following the assumptions that the installation will generate 734,707.73 kWh yearly for the entire lifetime and with the guaranteed FiT, the annual income (Annual savings by offsetting grid electricity (captive consumption) + Income from energy sold to the Kenya Power Utility) generated is Ksh. 13,976,166.3. The estimated annual cash flow (Income - Expenses (O & M costs)) is Ksh.12, 874,104.70. Using equation 3.13, the simple payback period for this installation is estimated as 9.1 years. Mensah *et al*. (2019) carried out economic evaluation on 2.5

MW grid tied solar PV system and found the simple payback period and LCOE to be 8.34 years and US $ 0.2411/kWh, respectively. Plants (2015) concluded that for a grid tied Solar Photovoltaic system to be considered economically viable, the simple payback period is recommended to range from 8 to 18 years. Therefore, Strathmore University grid tied Solar PV system is considered to be economically viable.

4.6 Greenhouse Gas (GHG) emissions reductions

As earlier mentioned, this solar Photovoltaic system reported energy yield of 735 MWh in 2019. By applying equation 3.15, this generation corresponds to a carbon savings of 300.4 metric tons per year of carbon dioxide. For hypothetical car emitting Carbon dioxide of 150 g/km and covers estimated distance of 10,000 km per year, the total emissions saved are 1.5 metric tons per year of carbon dioxide. This savings is equivalent to removing 200 fossil fuel powered cars from Kenyan roads.

4.7 Tilt Angle optimization

4.7.1 Simulated optimal tilt angle for Strathmore University Grid tied roof top PV system

Figure 4.12 shows a graph of simulations results for 0° to 15° tilt angles for the Strathmore University's 600 kWp plant throughout the year.

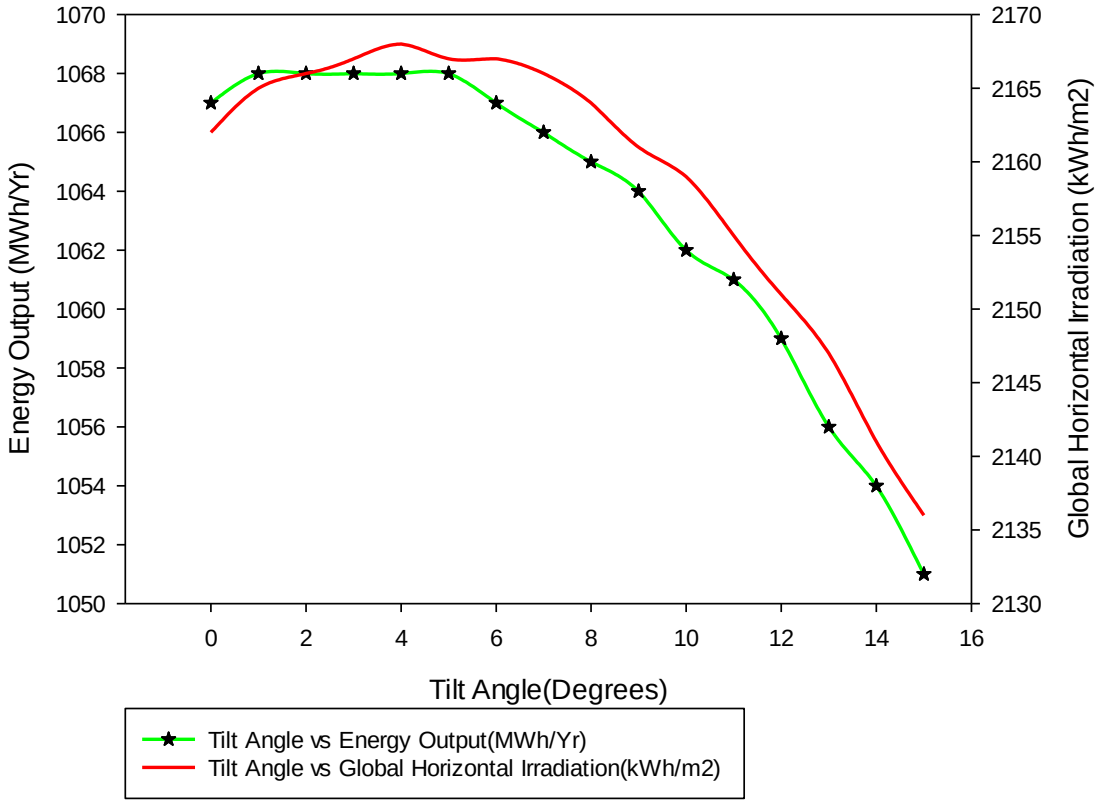

Figure 4.12: Simulations results for 0° to 15° tilt angles

As seen in Figure 4.12, the energy yield values for this system at azimuth 0° with tilt angles ranging between 0° and 15° varies from 1051 MWh/Yr to 1068 MWh/Yr. The annual global horizontal irradiation ranged between 2136 kWh/m^2 to 2168 kWh/m^2. The simulated annual optimized tilt angle for this Solar PV system was estimated at 3.2° as shown in Figure 4.13. At this optimum angle, the annual energy tied is 1068.4 MWh/year.

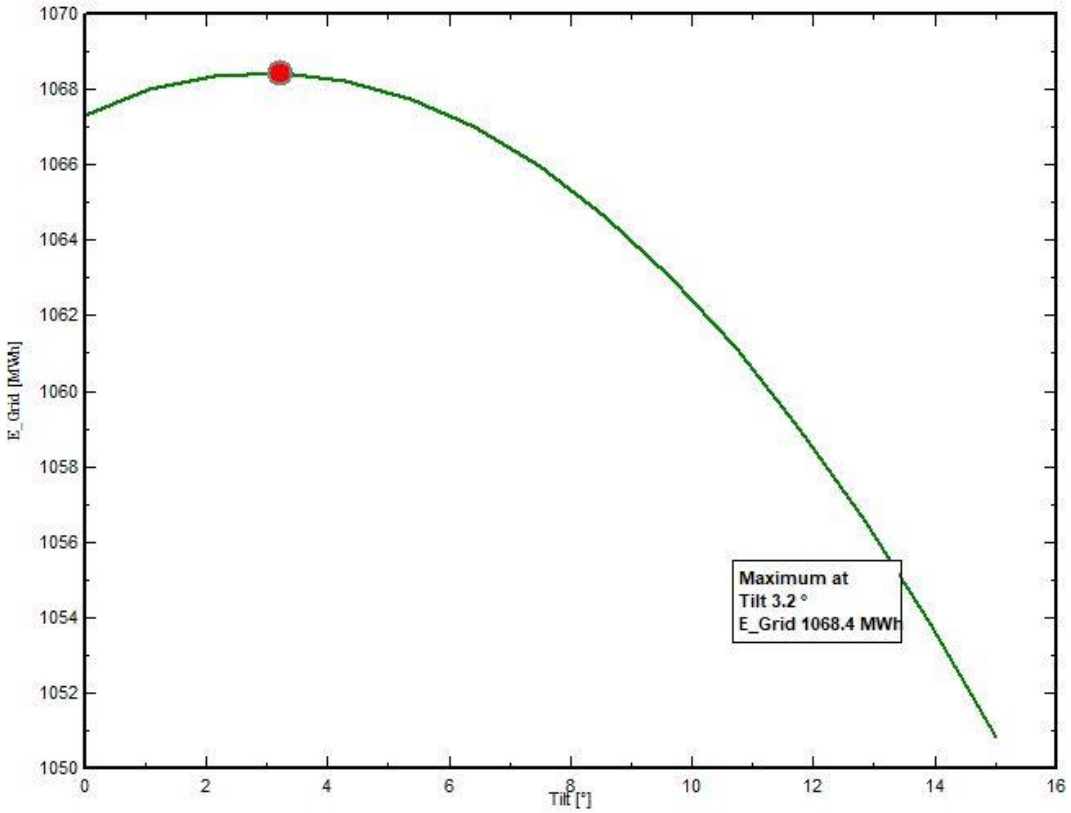

Figure 4.13: Simulated Strathmore University Solar PV system annual optimized tilt angle

These results agree with findings from other studies. The variance is due to the different latitude locations. For instance, Sugirianta *et al*. (2020) carried out research on tilt angle optimization of 300 Wp solar panel at Bukit Jimbaran area of Bali with a latitude of -8.805' and found out that the tilt angle with highest energy value for the fixed solar photovoltaic systems was 12° to 18°. Numerous studies done on optimizing the tilt angle for solar photovoltaic systems installed in a given region shows that optimized tilt angles are close to the location's latitude (Dominic, 2017; Hailu and Fung, 2019; Kumar, 2011). Therefore, the optimization simulation findings for Strathmore University system agree with other scholars.

Table 4.3 exhibits a summary comparison of energy yield and global horizontal irradiation as simulated for the various tilt angles at azimuth 0° for Strathmore University site.

Table 4.3: Comparison of the simulated energy outputs and global horizontal irradiation for Strathmore University Site

Tilt Angle (Degrees)	Energy Output (MWh/yr)	Global Horizontal Irradiation (kWh/m^2)
0	1067	2162
1	1068	2165
2	1068	2166
3	1068	2167
4	1068	2168
5	1068	2167
6	1067	2167
7	1066	2166
8	1065	2164
9	1064	2161
10	1062	2159
11	1061	2155
12	1059	2151
13	1056	2147
14	1054	2141
15	1051	2136

4.7.2. Simulation results for 4°,11° and 15° tilted Strathmore University 600 kW Solar PV system

The solar PV panel at 4° tilt angle simulations reported a Global Horizontal Irradiation yield of 2168 kWh/m^2 with a transposition factor of 1 at Azimuth 0° as shown Figure 4.14 (a).

The solar PV panel at 11° tilt angle simulations indicates a yield of 2155 kWh/m^2 with a transposition factor of 1 at Azimuth 0° shown in figure 4.14 (b). The solar PV panel at 15° tilt angle simulations indicates a yield of 2136 kWh/m^2 with a transposition factor of 0.99 at Azimuth 0° shown in Figure 4.14(c).

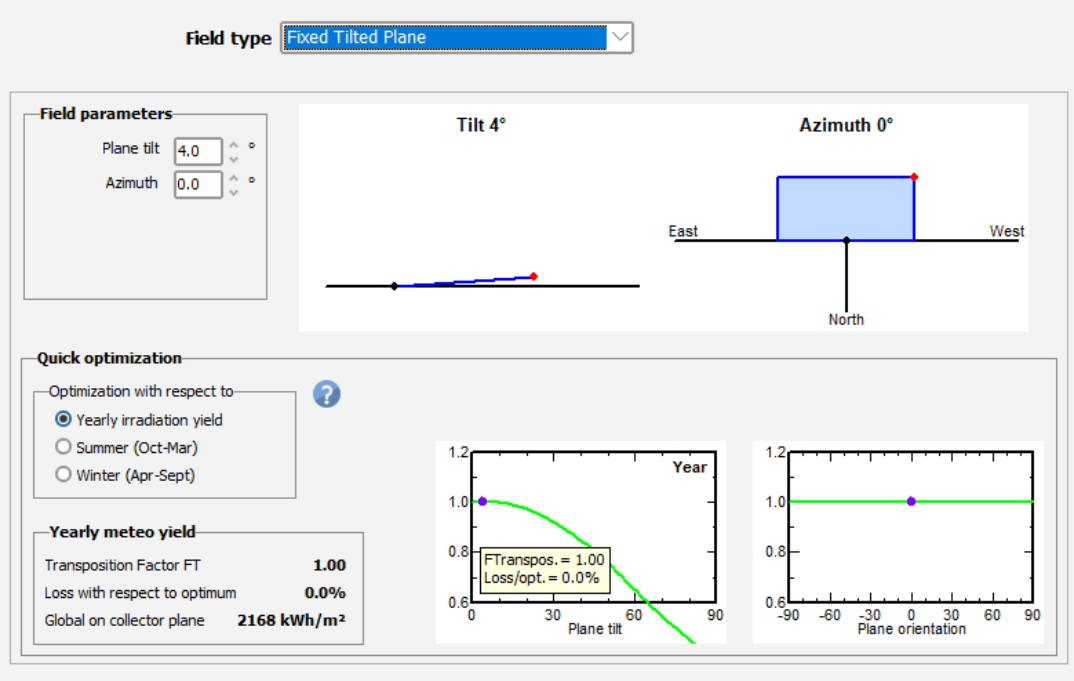

Figure 4.14(a): Global Horizontal Irradiation yield

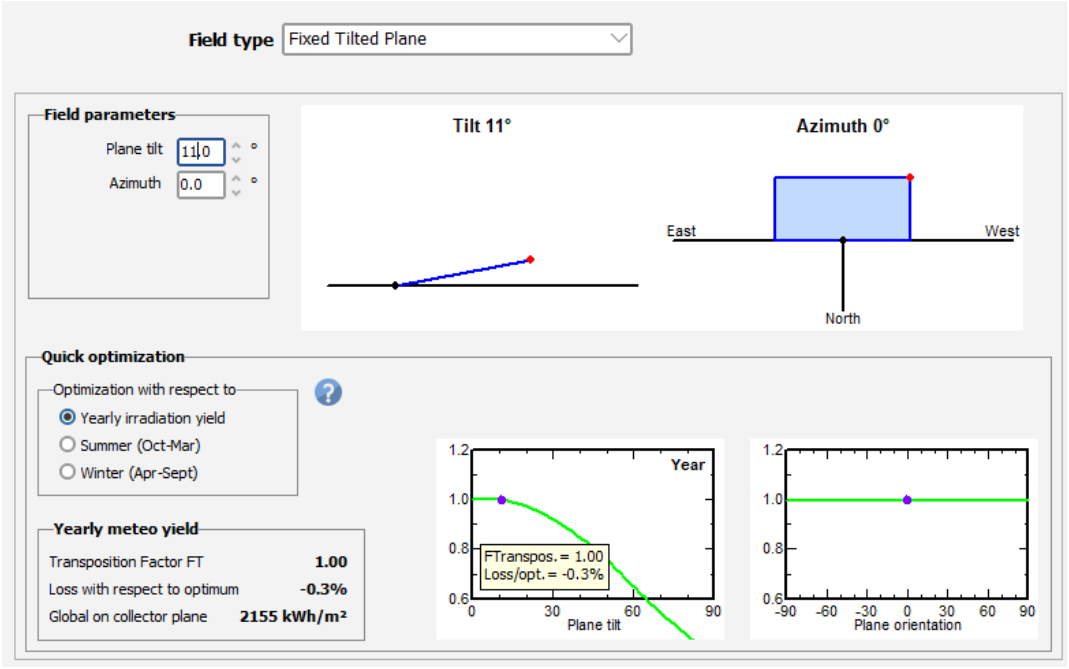

Figure 4.14(b): Global Horizontal Irradiation yield

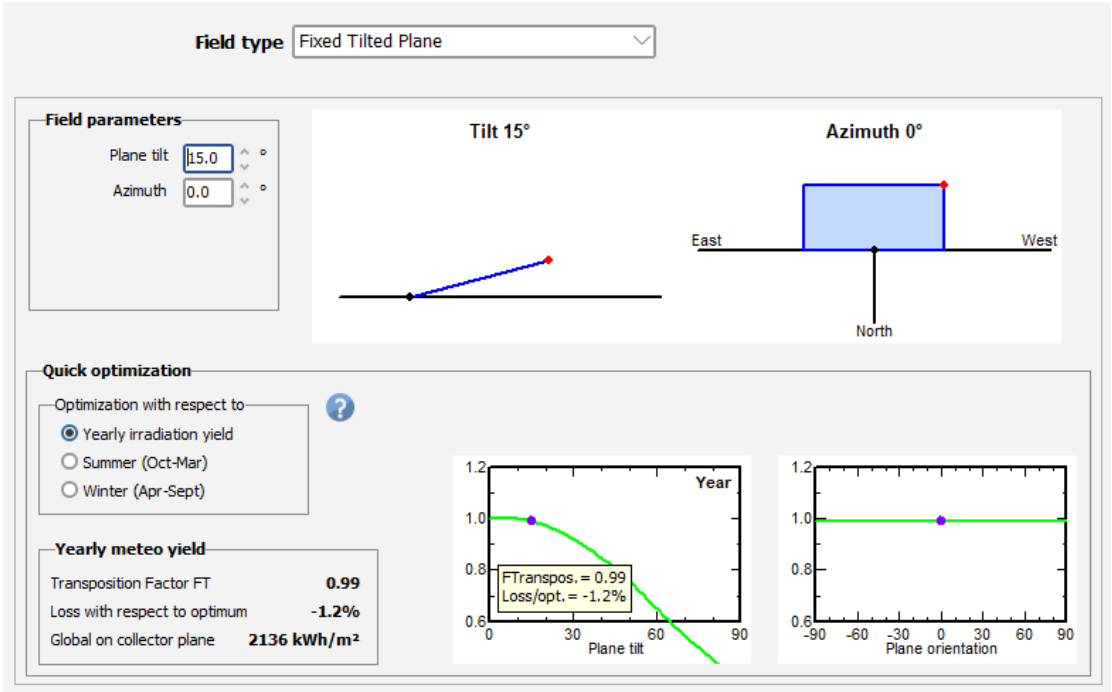

Figure 4.14(c): Global Horizontal Irradiation yield

The simulated PV system tilted at 4°,11° and 15° exhibits a transposition factor of 1.00,1.00 and 0.99 respectively. Transposition factor is the ration of the incident radiation to horizontal global irradiation and usually measures how much radiations

are lost or gained when the collector plane is tilted. The global on tilted plane and global horizontal plane for 4° is 5.9 kWh/m^2 as depicted in the Figure 4.15.

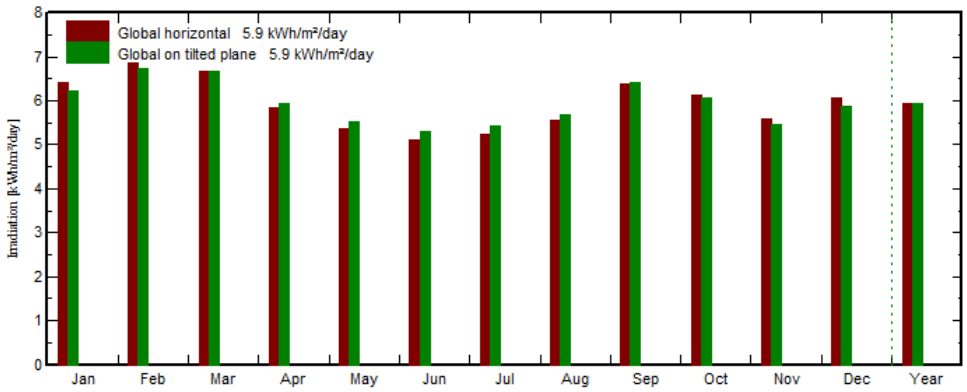

Figure 4.15: Global on tilted plane and global horizontal irradiation

The electrical performance simulation for the Strathmore PV system indicates a yield of 1068 MWh/Yr, 1061 MWh/Yr and 1051 MWh/Yr for the 4°,11° and 15° tilted solar PV system respectively. The 4°, 11° and 15° tilted solar PV system simulations exhibited a specific production of 1781 kWh/ kWp/year, 1768 kWh/KWp/year and 1751 kWh/KWp/year respectively. The performance ratio, system losses and array losses for the 4° are 82.3%, 0.1 kWh/kWp/day and 0.94 kWh/kWp/day, respectively as shown in Figure 4.16(a). The performance ratio, system losses and array losses for 11° are 0.824 kWh/kWp/day, 0.1 kWh/kWp/day and 0.93 kWh/kWp/day respectively as shown in Figure 4.16(b). Figure 4.16 (c) depicts a performance ratio, system and array losses of 0.825 kWh/kWp/day, 0.1 kWh/kWp/day and 0.92 kWh/kWp/day respectively.

Khasawneh *et al*. (2015) carried out tilt angle optimization studies in northern Jordan and established a simulated Performance ratio and specific yield of 82.7% and 1934 kWh/kWp/year, respectively; which is comparable with the studies for Strathmore University system.

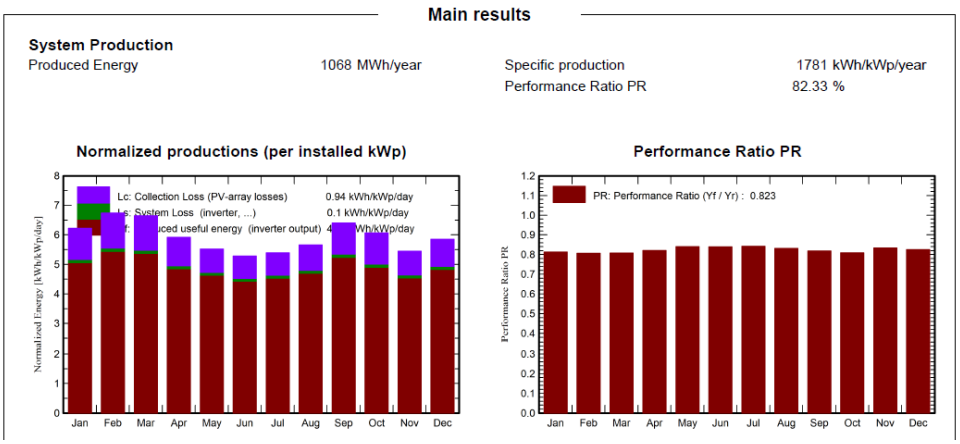

Figure 4.16(a): Main simulation results for Performance Ratio and normalized productions for 4°

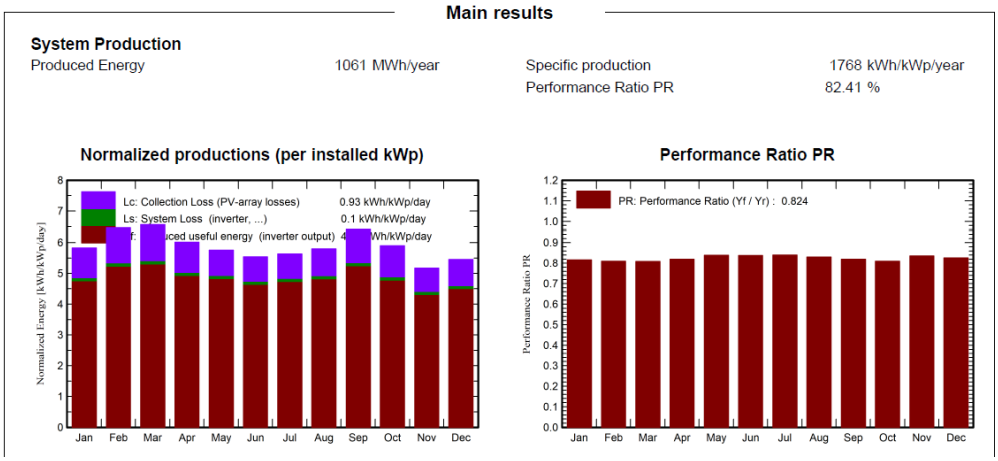

Figure 4.16(b): Main simulation results for Performance Ratio and Normalized productions for 11°

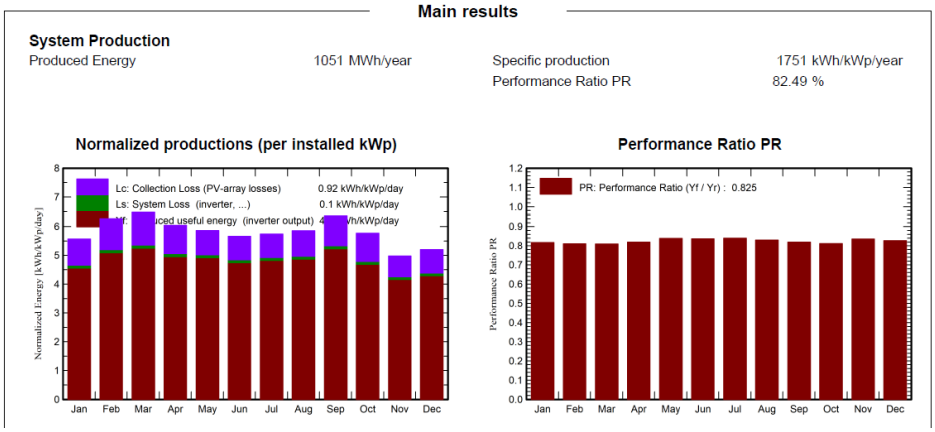

Figure 4.16(c): Main simulation results for Performance Ratio and Normalized productions for 15°

The loss diagram shown in Figures 4.17 (a) 4.17 (b) and 4.17 (c) depicts the energy input and energy output as well as the step-by-step collection system losses for the 4°, 11° and 15° tilted solar panels respectively.

Loss diagrams are crucial for determining the system efficiencies (Prasad *et al.*, 2020). As shown, the total energy injected to the grid is 1051 MWh,_1061 MWh and 1068 MWh for 15°,11° and 4° tilted solar PV panels respectively. The system exhibits an array nominal energy of 1243 MWh, 1256 MWh and_1268 MWh for the 4°, 11° and 15° tilted solar panels respectively.

The total collection losses are derived from the difference between the total energy injected to the grid and the array nominal energy. Therefore, the total system losses are 200 MWh, 195 MWh and 192 MWh for 4°, 11° and 15° tilted solar panels respectively.

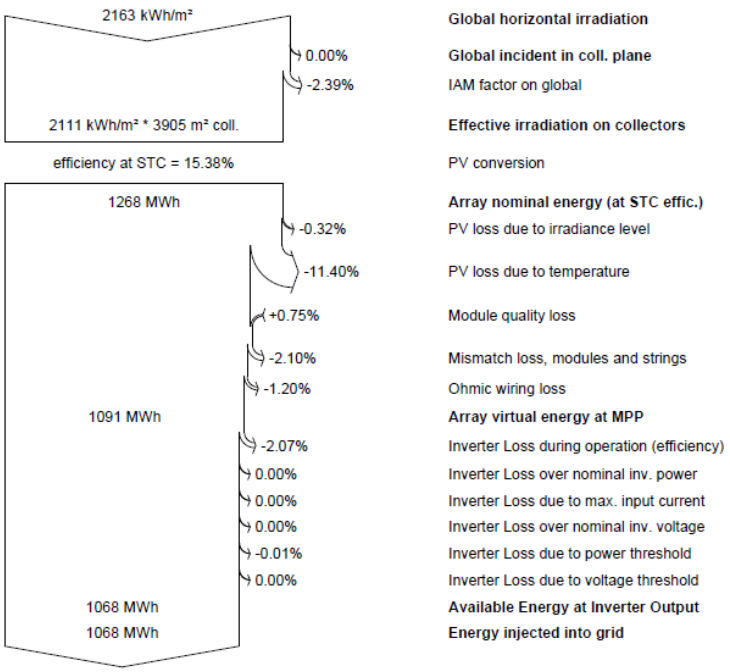

Figure 4.17(a): Loss diagram for 4 degrees tilted

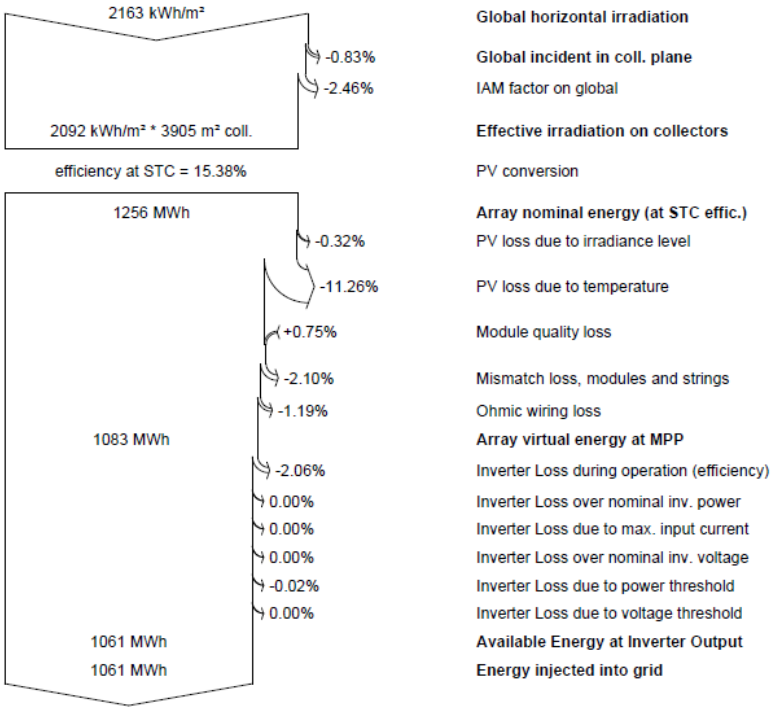

Figure 4.17(b): Loss diagram for 11 degrees tilted PV system simulation

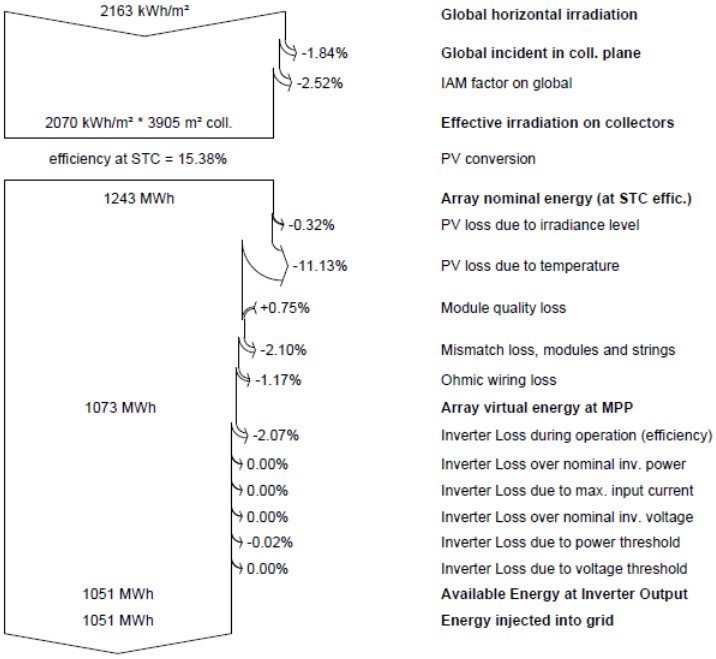

Figure 4.17 (c): Loss diagram for 15 degrees tilted PV system simulation

4.7.3 Simulation results for Kenyatta University Experiment site

The tilt angle optimization simulations done for the Kenyatta University site location showed a close similarity with the Strathmore university site location. The simulated optimal tilt angle obtained from the Kenyatta University simulation was 3.2° with a maximum yield of 1049.6 MWh/Yr as shown in Figure 4.18.

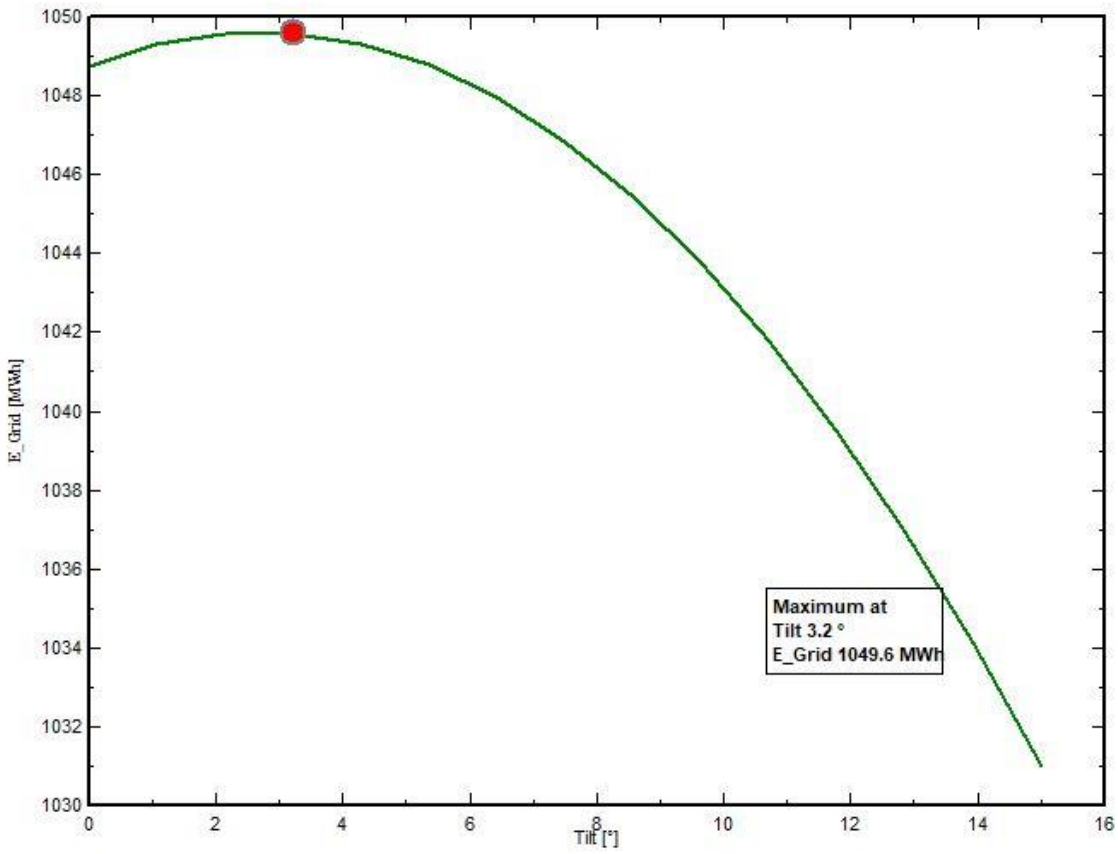

Figure 4.18: simulated optimized tilt angle at Kenyatta University site

This simulated optimized tilt angle was similar to that the Strathmore University site location, although the maximum yield difference for the two sites depicted a percentage variation of 1.8%. These results show that the climatic conditions for the two sites were similar, thus, confirming the suitability of conducting experimental

validation at Kenyatta University. See appendix C to H for the main simulation results and loss diagrams for Kenyatta University site.

Table 4.4: Comparison of the simulated energy outputs and global horizontal irradiation for Kenyatta University site

Tilt Angle (Degrees)	Energy Output (MWh/yr)	Global Horizontal Irradiation (kWh/m^2)
0	1049	2163
1	1049	2165
2	1050	2166
3	1050	2167
4	1049	2167
5	1049	2167
6	1048	2166
7	1047	2165
8	1046	2163
9	1045	2160
10	1043	2157
11	1041	2154
12	1039	2150
13	1037	2145
14	1034	2140
15	1031	2134

Table 4.4 exhibits a summary of comparison of energy yield and global horizontal irradiation as simulated for the various tilt angles at azimuth 0° for Kenyatta University site.

4.8 Experimental Results

4.8.1 Experimental Validation

The experimental analysis was done to validate the 600 kWp grid tied solar PV system optimal tilt angle simulation analysis. The experiment explored the impact of solar irradiation and different air gaps on the solar panels' back sheet temperature on power outputs across different tilt angles. The simulation depicted an optimal tilt angle of 3.2°. The simulated results for 600 kWp solar PV system were scaled down to match the experimental model of 20 Wp solar PV module under investigation between 0900hrs and 1600hrs. The estimated simulated total energy output for 20 W solar PV system for 4°, 11° and 15° tilt angles were 97.5 Wh, 96.89 Wh and 95.98 Wh, respectively. The experimental energy yielded by the 20 W panel at a tilt angle of 4°, 11° and 15° was 108.26 Wh, 110.91 Wh and 103.18 Wh, respectively. Although the simulation yielded maximum energy output at 3.2° tilt angle, the variation between 3.2° tilted solar Panel and 11° tilted solar PV panel under the simulation depicted a percentage variation of 0.695%. This percentage variation is very small and therefore justifies the experimental findings of 11° tilted solar PV panel as the optimal tilt angle. These experimental results are comparable to the simulation results with the small variation justified by the varying environmental conditions in the outdoor settings.

The RMSE values for the measured and simulated values for 4°, 11° and 15° tilted panels was 0.01076, 0.01402 and 0.0072, respectively. These values are very close to zero i.e., within acceptable range of $0 < \text{RMSE} \leq 0.3$ and thus shows high correlation

and accuracy between the experimental and simulated results. This variation was caused by the impact of the fluctuating external environmental factors as compared to the standard conditions in the simulation setting. In addition, the Mean Absolute Error for the observations obtained for 4°, 11° and 15° tilted panels was 0.01076, 0.01402 and 0.0072, respectively. These values are within the acceptable range of $0 < MAE \leq 0.1$.

Table 4.5: Validation results

	4 Degrees	11 degrees	15 Degrees
Annual Energy yield (MWh/Yr)	1068	1061	1051
Global on collector Plane (kWh/m2)	2168	2155	2136
Simulated Energy Yield (kWh)	0.0975	0.0969	0.0960
Experimental Energy yield (kWh)	0.1083	0.1109	0.1032
Mean Absolute Error	0.01076	0.01402	0.0072
RMSE	0.01076	0.01402	0.0072

From the experimental validation done, solar panel at 11° tilt angle was the most optimal with highest energy yield of 110.91 Wh for the specified duration (0900hrs-1600hrs). The small variation from the simulated energy output values was attributed to other external environmental factors in the experimental location.

4.8.2 Irradiation and Ambient temperature distribution

Figure 4.19 presents solar irradiation and ambient temperature versus daytime. The average ambient temperature and solar irradiation was recorded from 23/03/2022 to 14/04/2022 and the average data plotted against the daytime.

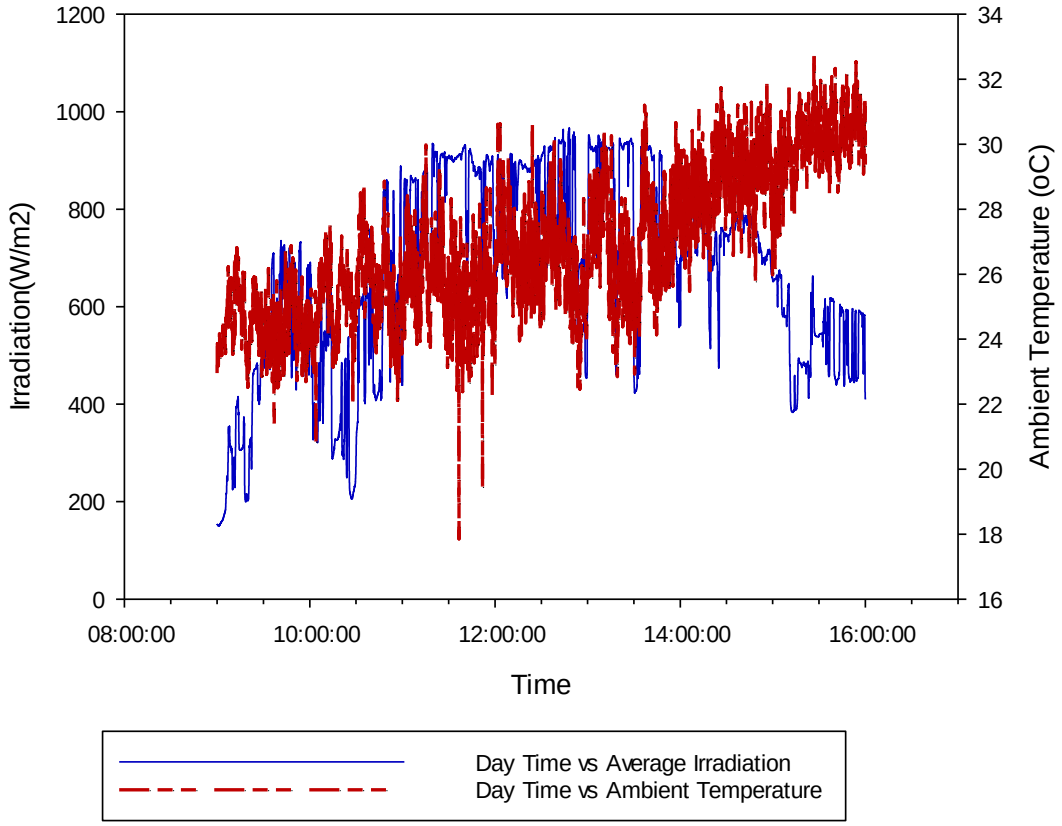

Figure 4.19: Average Daily Irradiation and Ambient temperature

Ambient temperature and solar irradiation have an impact on the solar module performance. The solar Photovoltaic module electrical performance is influenced by the prevailing weather conditions at the site. These parameters fluctuate considerably on the outdoor settings due to the changing environmental phenomena. The ambient temperature is observed to rise gradually to a peak of 31.2 °C at 3:45pm. This was caused by the decreasing solar irradiation levels which directly influenced the ambient temperature. The ambient temperature was lowest at 9:00 am with a recording of 22.9 °C. At this time, the solar irradiation levels are low. On the other hand, Solar Irradiation recorded lowest with 165.8 W/m^2 at 9:03 am and fluctuates gradually increasing to a peak of 984.6 W/m^2 at 1307hrs. The ambient temperature

increases gradually from 9:00 am with the increasing levels of solar irradiation. This observation concurs with the findings obtained by Mamun *et al*. (2021). This is because as the solar irradiation increases, the atmospheric air is heated further causing the increase in ambient temperature. Diffuse and direct sun rays ae responsible for the increasing ambient temperatures. The atmosphere is heated also from below i.e., the reflected rays from the earth surface contribute significantly to the increasing ambient temperatures.

4.8.3 Back Sheet Temperature distribution on solar panels at different tilt angles

Figure 4.20 presents the back sheet temperature versus varying tilt angle.

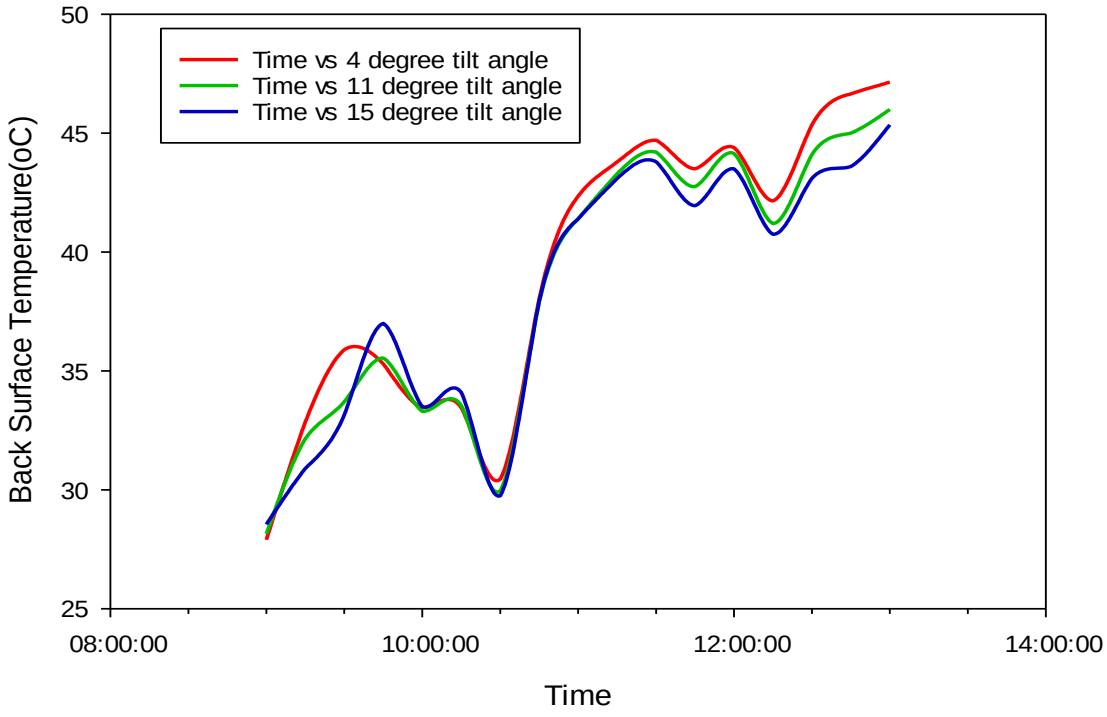

Figure 4.20: Back surface Temperature of the panels at different tilt angles

The back sheet temperatures for all the panels steeply increase from 9:00 am and start dipping at 09:45 am. The temperatures rise again from 10:30 am to attain peak from between 12 noon and 1 pm. During this period, the solar irradiance was highest and this accounts for the high back surface temperature. Panel at 4°tilt angle record significantly higher temperatures as compared to the panels at 15° and 11° tilt angles. The general trend shows that the back sheet temperatures of the panels decrease with increasing tilt angle. This is because as the angle of tilt is increased, heat is lost due to natural convection hence causing the reduction of temperature .Furthermore, increasing the tilt angle results in the panels being unable to intercept the solar irradiance perpendicularly, leading to a further drop in temperatures.

The panel at 4° tilt experience highest back surface temperature with a high of 46.4 °C. Mamun *et al*. (2021) performed an experiment on tilt angle's effect on cell temperature and established that increasing tilt angle by 5° resulted in a reduction of cell temperature by 2.70 ˚C.

4.8.4 Effect of Tilt Angle on Electrical Power output

The tilt angle of a PV module influences how solar radiations are intercepted at the surface of the panel consequently affecting the energy yield by the solar panel. The optimal performance of a solar module is greatly affected by the angle of tilt in a particular location. In this experiment, power output was monitored between 0900hrs and 1600hrs as depicted in Figure 4.21.

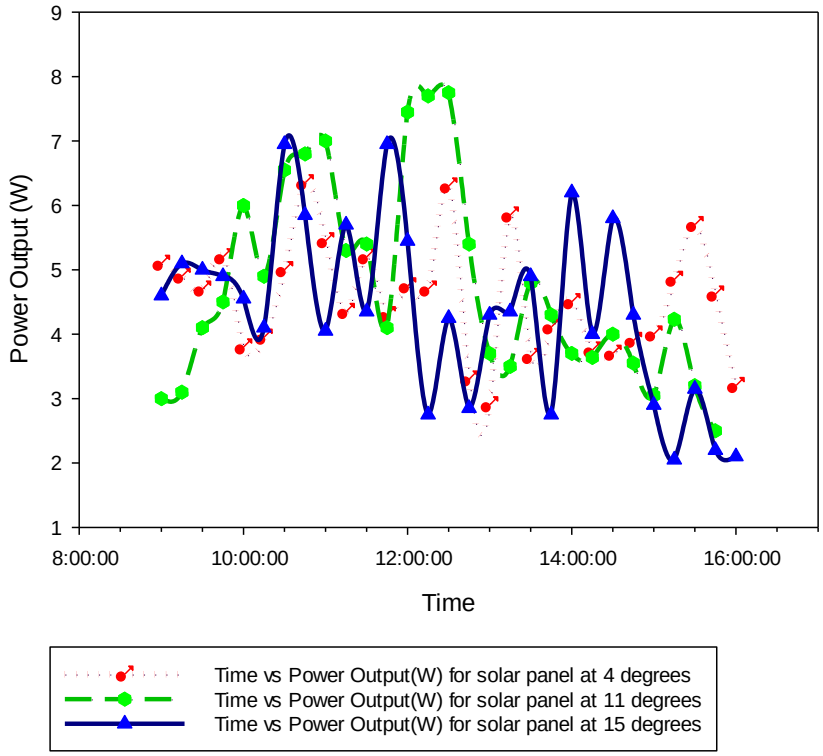

Figure 4.21: Solar Panel Power Output at different tilt angles

The solar panel tilted at 11 degrees recorded highest energy yield while the panel at 15 degrees tilt angle lowest energy yield. The total energy generated by the panels tilted at angles 4 degrees, 11 degrees and 15 degrees were 108.26, 110.91 and 103.18 Wh respectively from 0900hrs to 1600hrs. Therefore, the panel at 11 degrees exhibited highest energy yield as compared to the other Solar Panels. This means that the solar PV panel tilted at 11° produced optimal energy yield results. Although the simulation yielded maximum energy output at 3.2° tilt angle, the variation between 3.2° tilted solar Panel and 11° tilted solar PV panel under the simulation depicted a percentage variation of 0.695%. This percentage variation is very small and therefore justifies the experimental findings of 11° tilted solar PV panel as the optimal tilt angle. This study revealed that the power output increased with increasing tilt angle and achieves optimum output at 11° tilt angles. Further increasing tilt angle by 4° to

15° reduces the power output by 6.97%. These results agree with George *et al*. (2012) who concluded that for every slight increase of tilt angle by 5°, there is a 2% power loss or even more. Mamun *et al*.2021 concluded that by increasing tilt angle by 5°causes a drop in power by 3.45 W for the outdoor environments. A study done by Lau *et al*. (2017) on the effect of tilt angle on hybrid PV and diesel systems shows that the total electricity generated by the solar photovoltaic system decreased with increasing tilt angles but exhibited minimal changes when the modules were positioned at angles close to the latitude of the locations. Therefore, this study concurs with the outcomes from other researchers.

4.8.5 Effect of Irradiation on PV Power Output

The experiment reveals that by increasing solar irradiation intensity causes an increase of the power output. As depicted in Figures 4.22(a), 4.22(b) and 4.22(c), increasing irradiation intensities caused an increase on the instantaneous power output from the solar panel. This is because when more solar irradiation intercepts the panel surface; more electrons are ejected hence increasing the current flow.

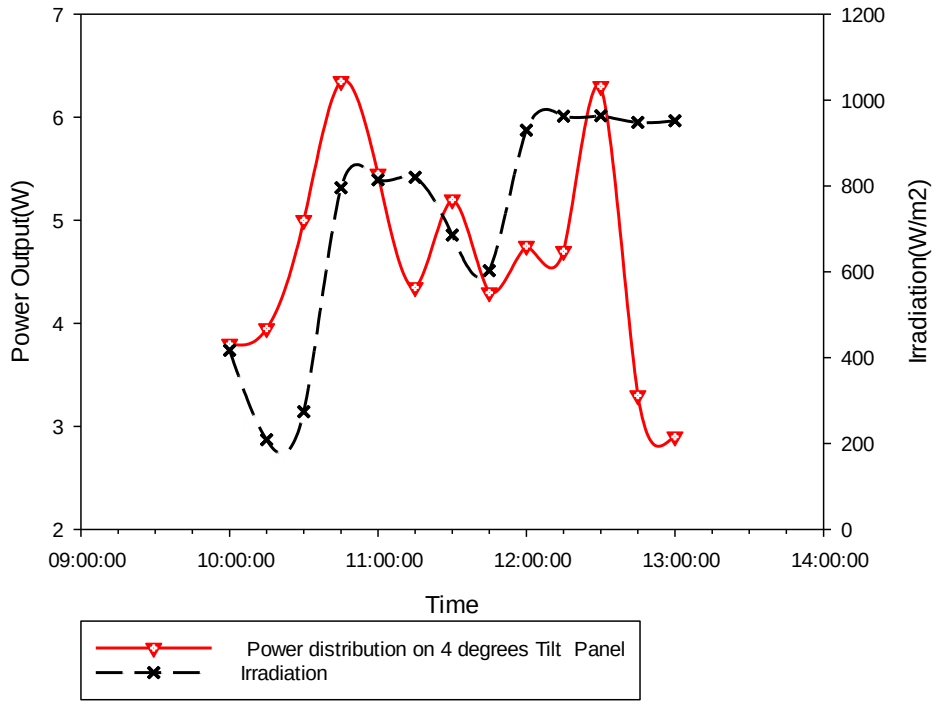

Figure 4.22(a): Power Output for 4° tilted panel

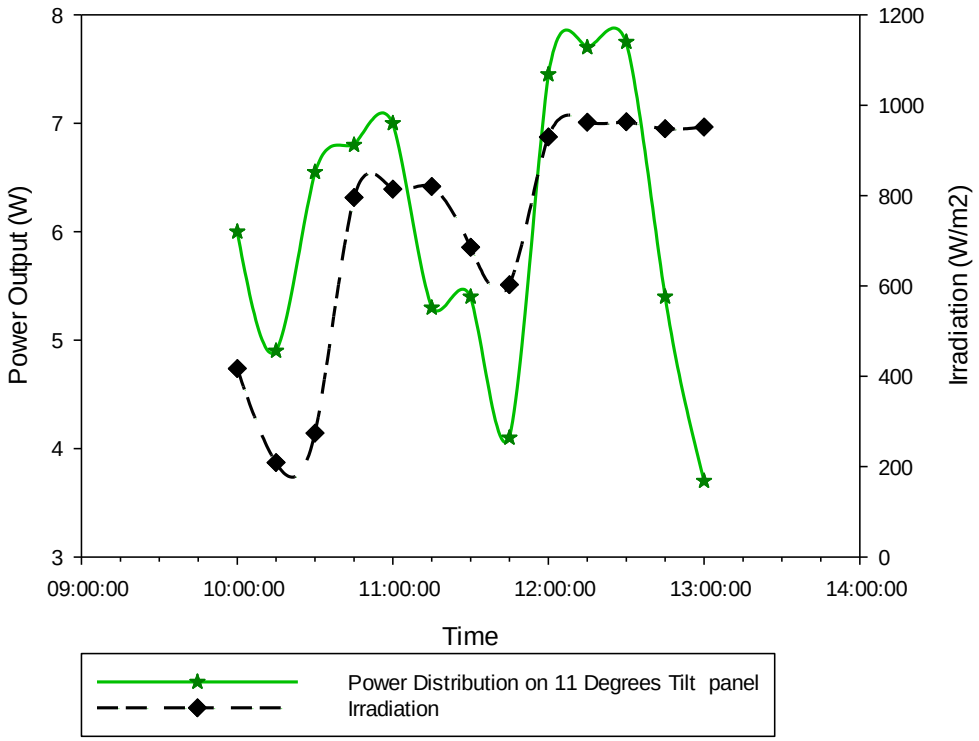

Figure 4.22(b): Power Output for 11° tilted panel

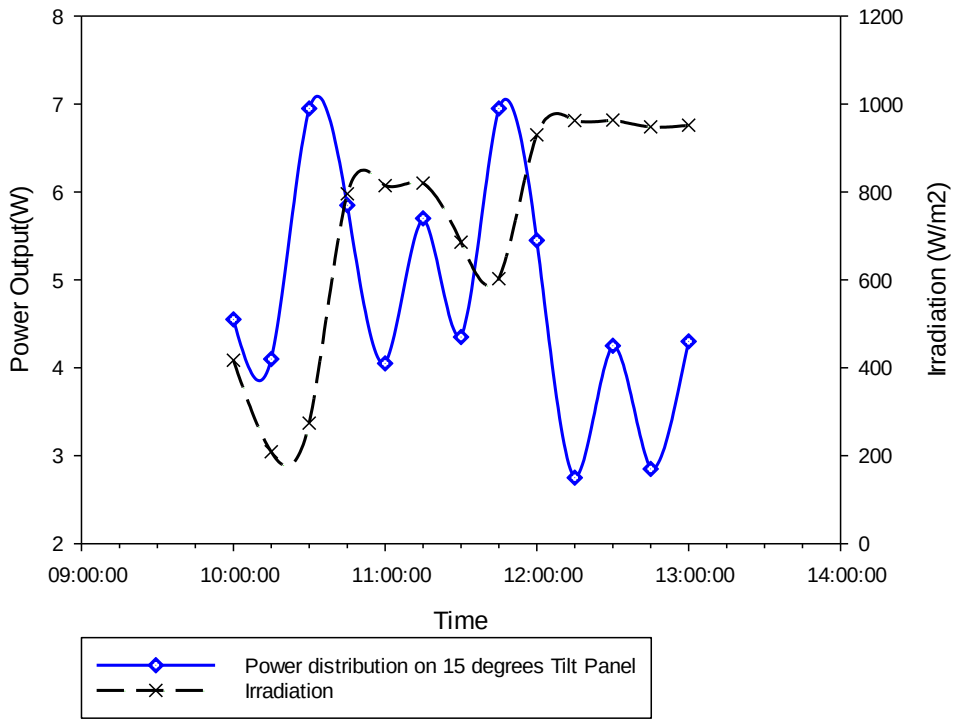

Figure 4.22(c): Power output for 15°tilted panel

This study revealed that increasing solar radiation intensities caused an increase in the short circuit currents and open circuit voltage. This increases the power output. As illustrated by Figures 4.22(a), 4.22(b) and 4.22(c), a decrease in the solar radiation intensities between 11 am and 12 noon resulted in a drop in power output. The study revealed that the power output from the panels was highest around 12 noon when the solar irradiation intensity was highest. This study concluded that by increasing the solar irradiation by 100 W/m^2, the output power from the solar panels increased by 8.3%. Mamun *et al*. (2021) concluded that for every 100 W/m^2 increase in the solar radiation levels, the V_{OC}, I_{SC}, V_{MPP} and I_{MPP} increases consequently increasing the power output.

4.8.6 Effect of Air gap on Back Sheet Temperature

In this experimental analysis, back sheet temperature of the solar panels with air gap of 100 mm was found to be relatively higher than the PV modules with air gap of 150 mm. This revealed that by increasing the air gap of the solar panel from 100 mm to 150 mm, back sheet temperature of the module decreased by 7.5 % due to the increased flow of cooling convection air currents. Panel 3 (blue graph) with an air gap of 150 mm experienced the lowest back sheet temperatures whereas the panel 4 (green graph) with 100 mm air gap experienced highest back sheet temperatures as shown in Figure 4.23.

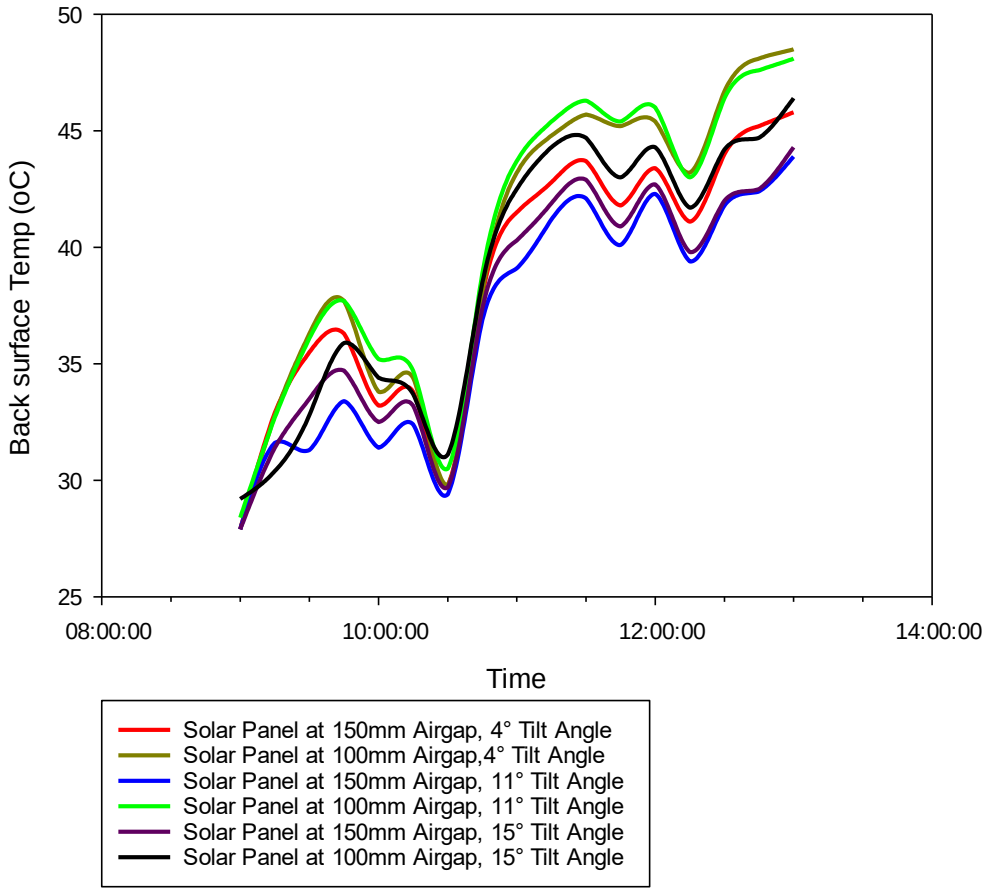

Figure 4.23: Effect of Air gap on back surface Temperature of the Solar Panels

Notably, the solar PV module air gap affects the airflow rate underneath the solar PV module and consequently the back sheet temperature and has a great effect on the solar photovoltaic module electrical performance. The airflow rate is a product of air gap and air velocity; therefore, this has an impact on natural convection cooling of the solar modules. Bigger air gap allows sufficient flow of natural air thus lowering the cell temperatures. Therefore, the air gap is a very crucial factor in influencing the back sheet temperature and ultimately the open circuit voltage of the solar photovoltaic module.

Gan (2009) conducted research on the air gap impact on the electrical performance of the building integrated solar PV and established that the maximum PV temperature and mean solar PV temperature increases with the decreasing air gap. The researcher concluded that the overheating of Solar PV modules and hot spots on the panel surface can be significantly reduced by installing panels with an air gap of between 120 mm and 150 mm for multiple panel installation and between 140 mm and 160 mm for single module installation is required. The researcher further found out that the mean PV temperature decreases for air gaps equal or more than 80 mm.

Figures 4.24(a), 4.24(b) and 4.24(c) shows the back sheet temperature variations for air gaps of 100 mm and 150 mm and positioned at 4°, 11° and 15°, respectively.

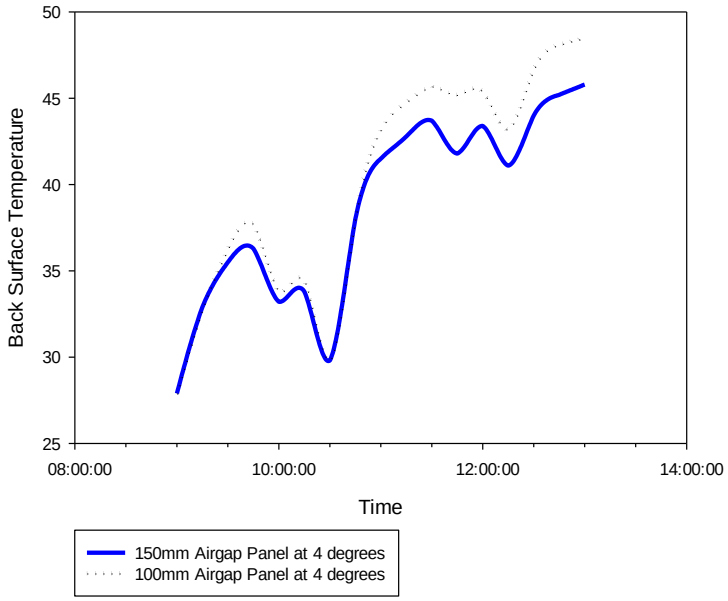

Figure 4.24(a): Effect of Air gap on Back Surface Temperature for panels tilted at 4°

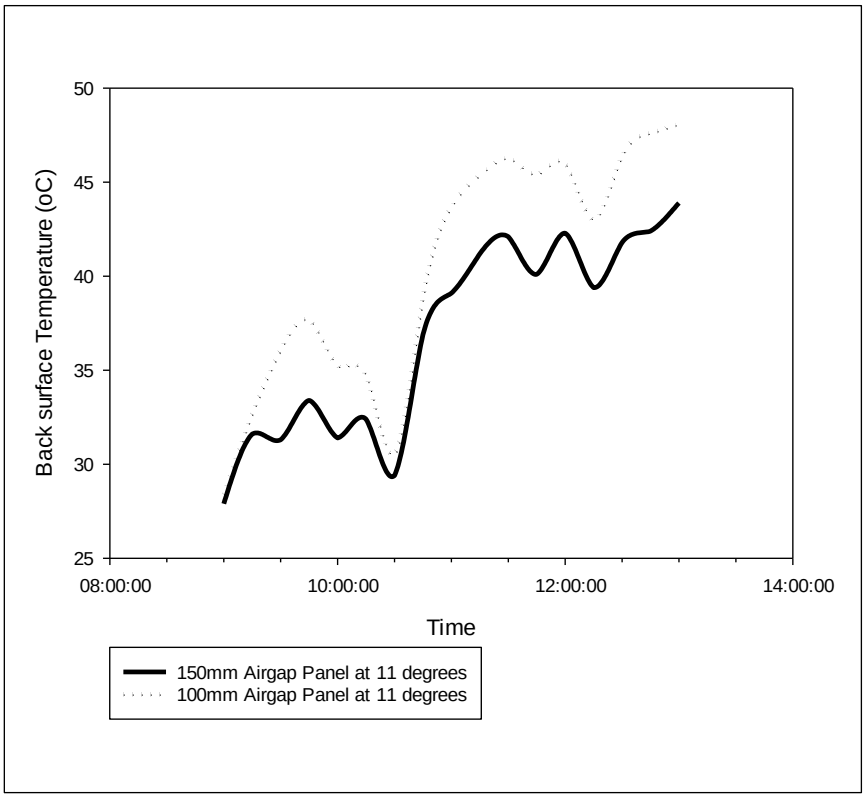

Figure 4.24(b): Effect of Air gap on Back Surface Temperature for panels tilted at 11°

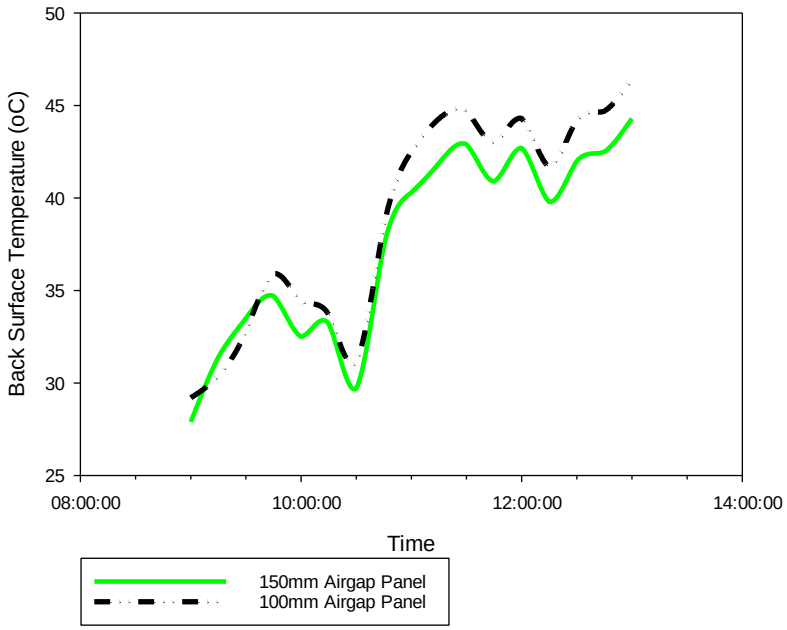

Figure 4.24(c): Effect of Air gap on Back Surface Temperature at 15°

This clearly demonstrated that the 150 mm air gap offered least resistance to the airflow thus allowing more space for natural flow of air hence cooling the solar PV module.

CHAPTER FIVE

CONCLUSIONS AND RECOMMENDATIONS

5.1 Conclusions

The performance evaluation of the Strathmore University's 600 kWp grid-connected solar photovoltaic system in 2019 revealed several key findings. The system generated 735 MWh of energy during the year, with an annual capacity utilization factor of 13.9% and a performance ratio of 56.4%. The Strathmore University solar plant system depicted a final yield of between 2.29 kWh/kWp and 4.46 kWh/kWp. The annual average monthly final, reference, array, and total system collection losses were 3.37 kWh/kWp, 5.9 kWh/kWp, 4.49 kWh/kWp and 2.53 kWh/kWp, respectively. The thermographic analysis done showed that the system exhibited normal temperature distribution. Economic analysis estimated a levelized cost of energy (LCOE) of US$ 0.143/kWh and a simple payback period of 9.1 years. Experimental validation determined that solar modules tilted at 11° exhibited optimal performance, yielding 110.91 Wh of energy, which is extrapolated to correspond to 1,215 MWh/yr for Strathmore University’s 600 kW Grid-tied Solar PV system. It was concluded that by increasing tilt angle by 4° i.e. from 11 to 15 degrees, the energy yield drops by 6.97%. The variance between the simulated and experimental analysis was due to other environmental variations which were not fully accounted for in the simulations. It was concluded that by increasing the tilt angle, the back sheet temperature of the modules decreases. The study also found that increasing the air gap between panels from 100 mm to 150 mm decreased back sheet temperatures by 7.5%, due to enhanced cooling convection air currents.

The study revealed a direct correlation between solar irradiation levels and power output from solar panels. Consequently, it is imperative to optimize the interception of solar irradiation by the panels to enhance performance. This underscores the importance of implementing suitable strategies to maximize solar energy capture and improve overall system efficiency. The performance analysis research findings for Strathmore University's grid-tied Solar PV system were comparable to other solar plants across the world, showing great similarity, and provide valuable insights for improving power generation in other institutions and off-grid areas.

5.2 Recommendations

This study reveals that following recommendations are crucial in achieving optimized performance for roof top grid tied solar PV system.

1. For future studies, orientation and wind speed effect on the solar PV performance should be studied.
2. Future studies should be done to comprehensively understand the impact of soiling on solar PV performance.
3. For a comprehensive study on thermographic analysis of the solar photovoltaic system, it is recommended to inspect the entire PV system and investigate the effect of solar module reflections on solar module power output.

REFERENCES

Abdelaziz, G., Hichem, H., Chiheb, B. R., & Rached, G. (2021, December). Shading effect on the performance of a photovoltaic panel. In 2021 IEEE 2nd International Conference on Signal, Control and Communication (SCC) (pp. 208-213). IEEE.

Acciani, G., Simione, G. B., & Vergura, S. (2010, March). Thermographic analysis of photovoltaic panels. In International Conference on Renewable Energies and Power Quality (ICREPQ'10) (pp. 23-25).

Adebiyi, A. A., Ojo, E. E., & Davidson, I. E. (2020). Performance Evaluation of a Grid-tied PV System in the East Coast of South Africa. 2020 IEEE PES/IAS PowerAfrica, 1–5. https://doi.org/10.1109/PowerAfrica49420.2020.9219905

Agbetuyi, A. F., Udeme, E. O., Obiakor, E., Kayode, O. O., & Owolabi, B. (2018). Performance and Yield Assessment for Renewable Dispersed Generation in Nigeria: Case Study on Grid-Tied Solar PV Systems. IOP Conference Series: Materials Science and Engineering, 413, 012013. https://doi.org/10.1088/1757-899X/413/1/012013

Akpolat, Dursun, Kuzucuoğlu, Yang, Blaabjerg, & Baba. (2019). Performance Analysis of a Grid-Connected Rooftop Solar Photovoltaic System. Electronics, 8(8), 905. https://doi.org/10.3390/electronics8080905

Aravindan, M., Balaji, V., Saravanan, V., & Arumugam, M. (2019). Performance evaluation of rooftop solar photovoltaic systems in Tamilnadu. International Journal of Applied Power Engineering (IJAPE), 8(3), 265. https://doi.org/10.11591/ijape.v8.i3.pp265-276

Attari, K., Elyaakoubi, A., & Asselman, A. (2016). Performance analysis and investigation of a grid-connected photovoltaic installation in Morocco. Energy Reports, 2, 261–266. https://doi.org/10.1016/j.egyr.2016.10.004

Ayompe, L. M., Duffy, A., McCormack, S. J., & Conlon, M. (2011). Measured performance of a 1.72kW rooftop grid-connected photovoltaic system in Ireland. Energy Conversion and Management, 52(2), 816–825. https://doi.org/10.1016/j.enconman.2010.08.007

Babatunde, A. A., Abbasoglu, S., & Senol, M. (2018). Analysis of the impact of dust, tilt angle, and orientation on the performance of PV Plants. Renewable and Sustainable Energy Reviews, 90, 1017–1026. https://doi.org/10.1016/j.rser.2018.03.102

Bhattacharya, T., Chakraborty, A. K., & Pal, K. (2014). Effects of ambient temperature and wind speed on performance of monocrystalline solar photovoltaic module in Tripura, India. Journal of Solar Energy, 2014.

Buni, M. J., Al-Walie, A. A., & Al-Asadi, K. A. (2018). Effect of solar radiation on photovoltaic cell. International Research Journal of Advanced Engineering and Science, 3(3), 47-51.

Central Bank of Kenya (2014).https://www.centralbank.go.ke/

Chandra, S., Agrawal, S., & Chauhan, D. S. (2018). Effect of ambient temperature and wind speed on performance ratio of polycrystalline solar photovoltaic module: An experimental analysis. International Energy Journal, 18(2).

Chokmaviroj, S., Wattanapong, R., & Suchart, Y. (2006). Performance of a 500kWP grid-connected photovoltaic system at Mae Hong Son Province, Thailand. Renewable Energy, 31(1), 19–28. https://doi.org/10.1016/j.renene.2005.03.004

Dahmoun, M. E. H., Bekkouche, B., Sudhakar, K., Guezgouz, M., Chenafi, A., & Chaouch, A. (2021). Performance evaluation and analysis of grid-tied large scale PV plant in Algeria. Energy for Sustainable Development, 61, 181-195. https://doi.org/10.1016/j.esd.2021.02.004

Daut, I., Yusoff, M. I., Ibrahim, S., Irwanto, M., & Nsurface, G. (2012). Relationship between the solar radiation and surface temperature in Perlis. In Advanced Materials Research (Vol. 512, pp. 143-147). Trans Tech Publications Ltd.

de Lima, L. C., de Araújo Ferreira, L., & de Lima Morais, F. H. B. (2017). Performance analysis of a grid connected photovoltaic system in northeastern Brazil. Energy for Sustainable Development, 37, 79–85. https://doi.org/10.1016/j.esd.2017.01.004

Dogaheh and Puig (2019).Tilt Angle Optimization of Photovoltaic Panels.pdf.

Ekanem Dominic Ekanem, O. (2017). Determination of Optimal Tilt Angle for Biannual Seasonally Adjusted Flat-Plate Photovoltaic Modules Based on Perez Transposition Model. American Journal of Software Engineering and Applications, 6(3), 85. https://doi.org/10.11648/j.ajsea.20170603.15

Elhadj Sidi, C. E. B., Ndiaye, M. L., El Bah, M., Mbodji, A., Ndiaye, A., & Ndiaye, P. A. (2016). Performance analysis of the first large-scale (15 MWp) grid-connected photovoltaic plant in Mauritania. Energy Conversion and Management, 119, 411–421. https://doi.org/10.1016/j.enconman.2016.04.070

Energy Petroleum Regulatory Authority (2014).https://www.epra.go.ke/

Francis Olang, O., Francis Olang, L., & Strobl, J. (2017). Spatial Modelling of Solar Energy Potential in Kenya.

Gan, G. (2009). Effect of air gap on the performance of building-integrated photovoltaics. Energy, [online] 34(7), pp.913–921. Available at: [Accessed 20 Feb. 2020].

George, A., & Anto, R. (2012, December). Analytical and experimental analysis of optimal tilt angle of solar photovoltaic systems. In 2012 International Conference on Green Technologies (ICGT) (pp. 234-239). IEEE. https://doi.org/10.1109/ICGT.2012.6477978GoogleEarth.(2022). https://earth.google.com/web/data=MjIKMAouChwxVlFYc2hWdmNDRzAySXhpRWdGRUc5TnVabTNjEgwKCjNlNmYwNTAxXzAgAg?authuser=0

Hailu & Fung. (2019). Optimum Tilt Angle and Orientation of Photovoltaic Thermal System for Application in Greater Toronto Area, Canada. Sustainability, 11(22), 6443. https://doi.org/10.3390/su11226443

Haji, M. (2019). Performance Analysis of Installed Solar PV System Using Homer in Tanzania: A Case Study of Zanzibar and Arusha. American Journal of Electrical Power and Energy Systems, 8(1), 11. https://doi.org/10.11648/j.epes.20190801.12

Hammoud, M., Shokr, B., Assi, A., Hallal, J., & Khoury, P. (2019). Effect of dust cleaning on the enhancement of the power generation of a coastal PV-power plant at Zahrani Lebanon. Solar Energy, 184, 195-201. https://doi.org/10.1016/j.solener.2019.04.005

Herraiz, Á. H., Marugán, A. P., & Márquez, F. P. G. (2020). A review on condition monitoring system for solar plants based on thermography. Non-destructive testing and condition monitoring techniques for renewable energy industrial assets, 103-118. https://doi.org/10.1016/B978-0-08-101094-5.00007-1

Hioki, A. T., Silva, V. R. G. R. da, Vilela Junior, J. A., & Loures, E. de F. R. (2019). Performance Analysis of Small Grid Connected Photovoltaic Systems. Brazilian Archives of Biology and Technology, 62(spe), e19190018. https://doi.org/10.1590/1678-4324-smart-2019190018

International Electrotechnical Commission (1998). Photovoltaic system performance monitoring guidelines for measurement, data exchange and analysis. IEC 61724.

Jahn, U., Herz, M., Parlevliet, D., Paggi, M., Tsanakas, I., Stein, J. & Tanahashi, T. (2018). Review on infrared and electroluminescence imaging for PV field applications.

Kalogirou S. A., Agathokleous, R., & Panayiotou, G. (2013). On-site PV characterization and the effect of soiling on their performance. Energy, 51, 439-446.

Kerboua, A., Hacene, F. B., Goosen, M. F., & Ribeiro, L. F. (2022). Development of technical economic analysis for optimal sizing of a hybrid power system: a case study of an industrial site in Tlemcen Algeria. Results in Engineering, 16, 100675. https://doi.org/10.1016/j.rineng.2022.100675

Khasawneh, Q. A., Damra, Q. A., & Bany Salman, O. H. (2015). Determining the Optimum Tilt Angle for Solar Applications in Northern Jordan. Jordan Journal of Mechanical & Industrial Engineering, 9(3).

Khoo, Y. S., Nobre, A., Malhotra, R., Yang, D., Rüther, R., Reindl, T., & Aberle, A. G. (2013). Optimal orientation and tilt angle for maximizing in-plane solar irradiation for PV applications in Singapore. IEEE Journal of photovoltaics, 4(2), 647-653.

Khorasanizadeh, H., & Mohammadi, K. (2016). Diffuse solar radiation on a horizontal surface: Reviewing and categorizing the empirical models. Renewable and Sustainable Energy Reviews, 53, 338-362.

Kumar, A., & Thakur, N. S. (2011). OPTIMIZATION OF TILT ANGLE FOR PHOTOVOLTAIC ARRAY. International Journal of Engineering Science and Technology, 3(4), 9.

Kumar, K. A., Sundareswaran, K., & Venkateswaran, P. R. (2014). Performance study on a grid-connected 20 kWp solar photovoltaic installation in an industry in Tiruchirappalli (India). Energy for Sustainable Development, 23, 294–304. https://doi.org/10.1016/j.esd.2014.10.002

Kumar, N. M., Chopra, S. S., de Oliveira, A. K. V., Ahmed, H., Vaezi, S., Madukanya, U. E., & Castañón, J. M. (2020). Solar PV module technologies. In Photovoltaic Solar Energy Conversion (pp. 51-78). Academic Press.

Kumar, S., Upadhyaya, P., & Kumar, A. (2019). Performance Analysis of Solar Energy Harnessing System Using Homer Energy Software and PV Syst Software. 2019 2nd International Conference on Power Energy, Environment and Intelligent Control (PEEIC), 156–159. https://doi.org/10.1109/PEEIC47157.2019.8976665

Laith Mahmoud, M. H. (2017). Performance analysis of hybrid renewable energy systems used for rural electrification in Malaysia/Laith Mahmoud Mohammad Halabi (Doctoral dissertation, University of Malaya).

Lau, K. Y., Tan, C. W., & Yatim, A. H. M. (2018). Effects of ambient temperatures, tilt angles, and orientations on hybrid photovoltaic/diesel systems under equatorial climates. Renewable and Sustainable Energy Reviews, 81, 2625-2636. https://doi.org/10.1016/j.rser.2017.06.068

Leow, W. Z., Irwan, Y. M., Irwanto, M., Amelia, A. R., & Safwati, I. (2019). Influence of wind speed on the performance of photovoltaic panel. Indonesian Journal of Electrical Engineering and Computer Science, 15(1), 60-68.

Maghami, M. R., Hizam, H., Gomes, C., Radzi, M. A., Rezadad, M. I., & Hajighorbani, S. (2016). Power loss due to soiling on solar panel: A review. Renewable and Sustainable Energy Reviews, 59, 1307-1316.

Makenzi, M., Muguthu, J., & Murimi, E. (2020). Maximization of Site-Specific Solar Photovoltaic Energy Generation through Tilt Angle and Sun-Hours Optimization. Journal of Renewable Energy, 2020, 1–11. https://doi.org/10.1155/2020/8893891

Mamun, M. A. A., Islam, M. M., Hasanuzzaman, M., & Selvaraj, J. (2022). Effect of tilt angle on the performance and electrical parameters of a PV module: Comparative indoor and outdoor experimental investigation. Energy and Built Environment, 3(3), 278–290. https://doi.org/10.1016/j.enbenv.2021.02.001

Markam, K., & Sudhakar, K. (2016n.d.). Estimation of optimal tilt angle for solar photovoltaic installations in India. 03(05), 7.

Mensah, L. D., Yamoah, J. O., & Adaramola, M. S. (2019). Performance evaluation of a utility-scale grid-tied solar photovoltaic (PV) installation in Ghana. Energy for Sustainable Development, 48, 82–87. https://doi.org/10.1016/j.esd.2018.11.003

Miguel, A. D., Bilbao, J., Cazorro, J. R. S., & Martín, C. (2002). Performance Analysis of a Grid-Connected PV System in a Rural Site in the Northwest of Spain. 6.

Milosavljević, D. D., Pavlović, T. M., & Piršl, D. S. (2015). Performance analysis of A grid-connected solar PV plant in Niš, republic of Serbia. Renewable and Sustainable Energy Reviews, 44, 423–435. https://doi.org/10.1016/j.rser.2014.12.031

Mohammed, A. Y., Mohammed, F. I., & Ibrahim, M. Y. (2017, January). Grid connected Photovoltaic system. In *2017* international conference on communication, control, computing and electronics engineering (ICCCCEE) (pp. 1-5). IEEE.

Mousavi Maleki, S. A., Hizam, H., & Gomes, C. (2017). Estimation of hourly, daily and monthly global solar radiation on inclined surfaces: Models re-visited. *Energies*, *10*(1), 134.

Nabil, T., & Mansour, T. M. (2022). Augmenting the performance of photovoltaic panel by decreasing its temperature using various cooling techniques. Results in Engineering, 15, 100564. https://doi.org/10.1016/j.rineng.2022.100564

Nasrin, R., Hasanuzzaman, M., & Rahim, N. A. (2018). Effect of high irradiation on photovoltaic power and energy. International Journal of Energy Research, 42(3), 1115-1131. https://doi.org/10.1002/er.3907

Omkar, K., Srikanth, M. V., Swaroop, K. P., & PVV, R. R. (2015, May). Performance evaluation of 50KWp rooftop solar PV plant. In 2015 International Conference on Industrial Instrumentation and Control (ICIC) (pp. 761-765). IEEE. https://doi.org/10.1109/IIC.2015.7150844

Paul Gibbs, P. G. (2021). The 3 Best Ways to Optimize a Commercial PV System. The 3 Best Ways to Optimize a Commercial PV System | Greentech Media. https://www.greentechmedia.com/articles/read/the-3-best-ways-to-optimize-a-commercial-pv-system

Perez, R., Aguiar, R., Collares-Pereira, M., Dumortier, D., Estrada-Cajigal, V., Gueymard, C., & Ineichen, P. (2013). Solar resource assessment: A review. *Solar energy*, 515-594.

Peyvandi, M., Hajinezhad, A., & Moosavian, S. F. (2023). Investigating the intensity of GHG emissions from electricity production in Iran using renewable sources. Results in Engineering, 17, 100819. https://doi.org/10.1016/j.rineng.2022.100819

Plants, U. S. S. P. P. (2015). A Project Developer's Guide. International Finance Corporation, 34.

Prasad, B. K. K., Reddy, K. P., Rajesh, K., & Reddy, P. V. (2020). Design and simulation analysis of 12.4 kWp grid connected photovoltaic system by using PVsyst software. International Journal of Recent Technology and Engineering, 8(5), 2859-2864.

Qadourah, J. A. (2022). Energy and economic potential for photovoltaic systems installed on the rooftop of apartment buildings in Jordan. Results in Engineering, 16, 100642. https://doi.org/10.1016/j.rineng.2022.100642

Querikiol, E. M., & Taboada, E. B. (2018). Performance Evaluation of a Micro Off-Grid Solar Energy Generator for Islandic Agricultural Farm Operations Using HOMER. Journal of Renewable Energy, 2018, 1–9. https://doi.org/10.1155/2018/2828173

Renewables Provided 92.3% Of Kenya's Electricity Generation in 2020! (2021, November 4). CleanTechnicaCleanTechnica(2021). https://cleantechnica.com/2021/11/04/renewables-provided-92-3-of-kenyas-electricity-generation-in-2020/

Salih, S. M., & Kadim, L. A. (2014). Effect of tilt angle orientation on photovoltaic module performance. ISESCO Journal of Science and Technology, 10(17), 19-25.

Sathiracheewin, S., Sripadungtham, P., & Kamuang, S. (2020). Performance Analysis of Grid-Connected PV Rooftop, at Sakon Nakhon Province, Thailand. Advances in Science, Technology and Engineering Systems Journal, 5(4), 816–823. https://doi.org/10.25046/aj050496

Sathyanarayana, P., Ballal, R., Sagar, P. L., & Kumar, G. (2015). Effect of shading on the performance of solar PV panel. Energy and Power, 5(1A), 1-4.

Shah, A. (2020). Amorphous silicon solar cells. Solar Cells and Modules, 139-161.

Sharma, R., & Goel, S. (2017). Performance analysis of a 11.2 kW roof top grid-connected PV system in Eastern India. Energy Reports, 3, 76–84. https://doi.org/10.1016/j.egyr.2017.05.001

Sharma, S., Jain, K. K., & Sharma, A. (2015). Solar cells: in research and applications—a review. Materials Sciences and Applications, 6(12), 1145.

Singh, S., Kumar, R., & Vijay, V. (n.d.). Performance Analysis of 58 kW Grid-Connected Roof-top Solar PV System. 6.

Sreedhar, S., & Jagadeesh, D. (2016). A review on optimization algorithms for MPPT in solar PV system under partially shaded conditions. IOSR J. Electr. Electron. Eng, 23-32.

Srivastava, R., Tiwari, A. N., & Giri, V. K. (2020). An overview on performance of PV plants commissioned at different places in the world. Energy for Sustainable Development, 54, 51-59. https://doi.org/10.1016/j.esd.2019.10.004

Standardized baseline Grid Emission Factor for the Republic of Kenya (2020, December 29).. United Nations Framework Convention on Climate Change. https://cdm.unfccc.int/sunsetcms/storage/contents/stored-file-20201230125121808/ASB0050-2020_PSB0055.pdf

Sugirianta, I. B. K., Sunaya, I. G. A. M., & D Saputra, I. G. N. A. (2020). Optimization of tilt angle on-grid 300Wp PV plant model at Bukit Jimbaran Bali. Journal of Physics: Conference Series, 1450, 012135. https://doi.org/10.1088/1742-6596/1450/1/012135

Udoakah, Y., & Okpura, N. (2015). Determination of Optimal Tilt Angle for Maximum Solar Insolation for PV Systems in Enugu-Southern Nigeria. Nigerian Journal of Technology, 34(4), 838. https://doi.org/10.4314/njt.v34i4.24

Xiao, W., El Moursi, M. S., Khan, O., & Infield, D. (2016). Review of grid-tied converter topologies used in photovoltaic systems. *IET Renewable Power Generation, 10*(10), 1543-1551.

Ya'acob, M. E., Hizam, H., Khatib, T., & Radzi, M. A. M. (2014). A comparative study of three types of grid connected photovoltaic systems based on actual performance. Energy Conversion and Management, 78, 8-13.

Yadav, S. K., & Bajpai, U. (2018). Performance evaluation of a rooftop solar photovoltaic power plant in Northern India. Energy for Sustainable Development, 43, 130–138. https://doi.org/10.1016/j.esd.2018.01.006

APPENDICES

APPENDIX A: Journal Publication

Results in Engineering 19 (2023) 101302

Contents lists available at ScienceDirect

Results in Engineering

journal homepage: www.sciencedirect.com/journal/results-in-engineering

Performance analysis of 600 kWp grid-tied rooftop solar photovoltaic systems at strathmore university in Kenya

Emmanuel Ayora [d,*], Mathew Munji [a], Keren Kaberere [b], Bundi Thomas [c]

[a] Department of Physics, Kenyatta University, P. O. Box 43844 – 00100, Nairobi, Kenya
[b] Department of Electrical and Electronics Engineering, Jomo Kenyatta University of Agriculture and Technology, P.O. Box 62000 – 00200, Nairobi, Kenya
[c] Strathmore Energy Research Centre, P.O. BOX 59857-00200, Nairobi, Kenya
[d] Department of Energy ,Gas and Petroleum Engineering ,Kenyatta University,P.O Box 43844-00100, Nairobi, Kenya

ARTICLE INFO

Keywords:
Performance ratio
Capacity utilization factor
Performance analysis
Grid-tied solar PV system
Thermographic analysis

ABSTRACT

Kenya boasts of abundant solar irradiation potential across its expansive regions, averaging between 4.5 kWh/m^2 and 6 kWh/m^2 per day. Despite this advantageous condition, solar energy's contribution to the national energy mix remains relatively low. To boost solar energy contribution to the national grid, it is crucial to assess the performance of existing grid-tied solar PV systems and develop strategies to improve their energy yields and further help in designing and installing new plants. This paper presents a technical performance analysis of a 600-kWp grid-tied solar PV system at Strathmore University, monitored over one year between January and December 2019. Economic and thermographic analysis of the solar PV system is done. The performance indices studied according to IEC 61724 standard include performance ratio, capacity utilization factor, reference yield, final yield, total collection losses, and total energy yield. This solar plant generated 735 MWh in 2019. The annual average monthly performance ratio, capacity factor, and annual specific energy yield were 57.4%, 13.97%, and 1225 kWh/kWp, respectively. The annual average monthly final yield, array yield, reference yield, and total system collection losses were 3.37 kWh/kWp, 4.49 kWh/kWp, 5.9 kWh/kWp, and 2.53 kWh/kWp, respectively. The thermographic analysis done shows that the system exhibits healthy temperature distribution. The economic analysis demonstrated Levelized Cost of Energy (LCOE) and simple payback period of US$ 0.143/

APPENDIX B: Jinko PV Module Data sheet

SPECIFICATIONS

Module Type	JKM230P	JKM235P	JKM240P	JKM245P	JKM250P
Maximum Power at STC(Pmax)	230Wp	235Wp	240Wp	245Wp	250Wp
Maximum Power Voltage (Vmp)	29.6V	29.8V	30V	30.2V	30.4V
Maximum Power Current (Imp)	7.78A	7.89A	8.01A	8.12A	8.23A
Open-circuit Voltage (Voc)	36.8V	36.9V	37.2V	37.4V	37.6V
Short-circuit Current (Isc)	8.35A	8.47A	8.56A	8.69A	8.81A
Module Efficiency(%)	14.05%	14.35%	14.66%	14.97%	15.27%
Operating Temperature(℃)	-40℃~+85℃				
Maximum system voltage	600V (UL) /1000V (IEC) DC				
Maximum series fuse rating	15A				
Power tolerance	±3% / -0~+3% (Based on customer requirements and contract terms)				
Temperature coefficients of Pmax	-0.45%/℃				
Temperature coefficients of Voc	-0.27%/℃				
Temperature coefficients of Isc	0.05%/℃				
Nominal operating cell temperature (NOCT)	45±2℃				

STC: Irradiance 1000W/m² Module Temperature 25°C AM=1.5

APPENDIX C: Main simulations results for 4° tilted Solar PV modules at Kenyatta University

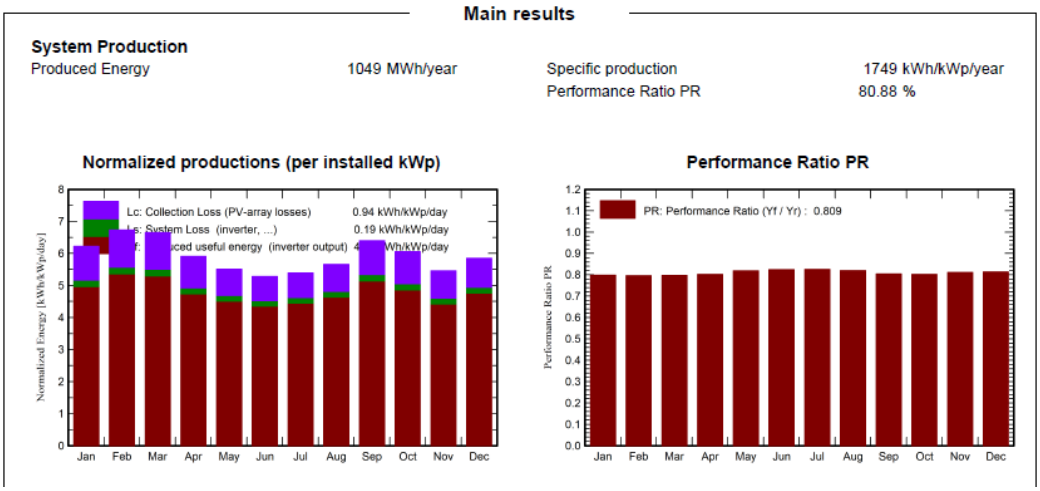

APPENDIX D: Loss diagram for 4° tilted Solar PV modules at Kenyatta University

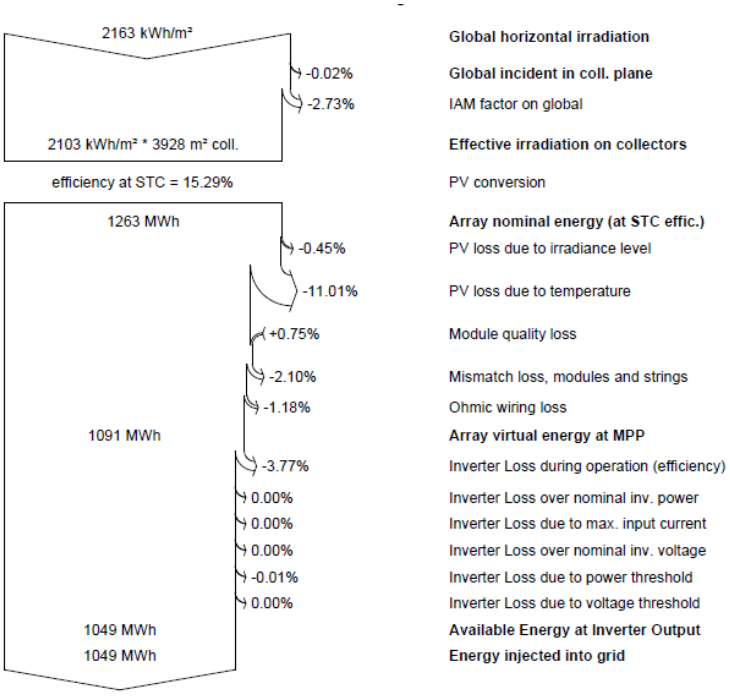

APPENDIX E: Main simulations results for 11° tilted Solar PV modules at Kenyatta University

Main results

System Production

Produced Energy	1041 MWh/year	Specific production	1735 kWh/kWp/year
		Performance Ratio PR	80.95 %

Normalized productions (per installed kWp)

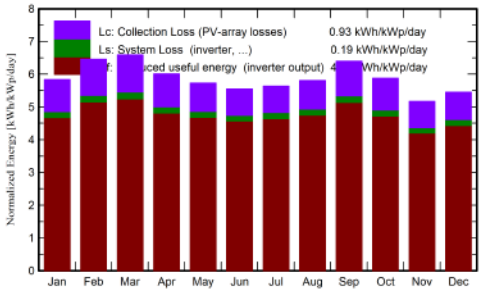

Performance Ratio PR

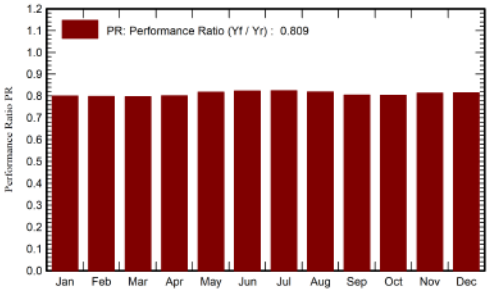

APPENDIX F: Loss diagram for 11° tilted Solar PV modules at Kenyatta University

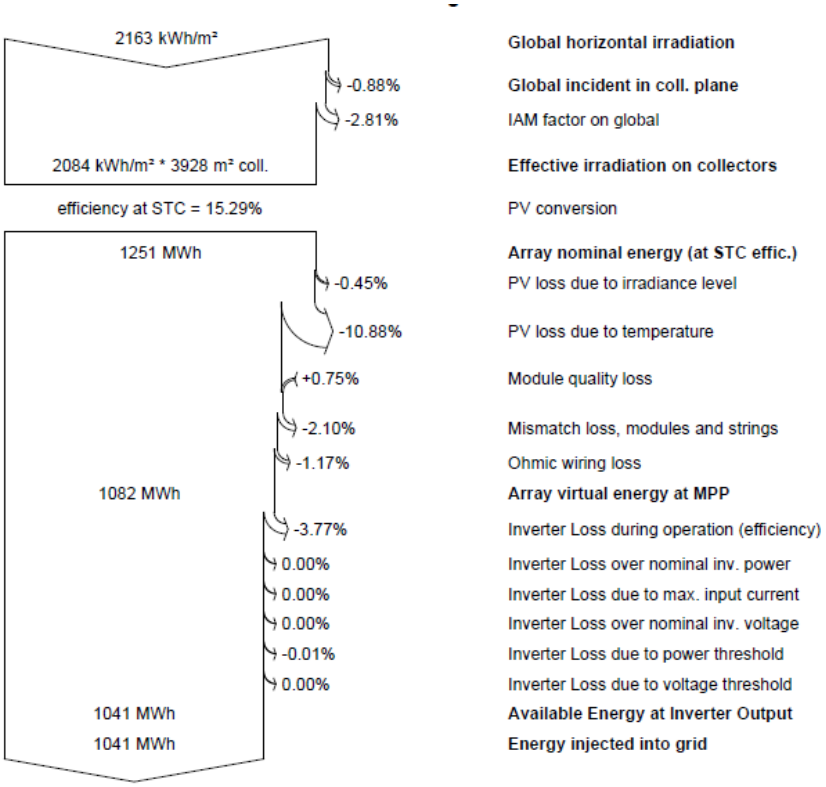

APPENDIX G: Main simulations results for 15° tilted Solar PV modules at Kenyatta University

Main results

System Production

Produced Energy	1031 MWh/year	Specific production	1718 kWh/kWp/year
		Performance Ratio PR	80.99 %

Normalized productions (per installed kWp)

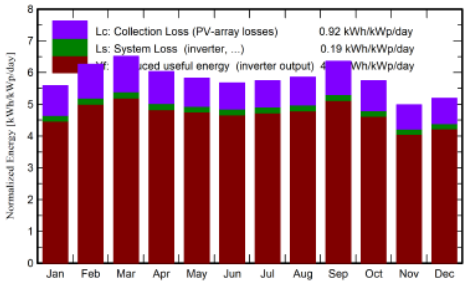

Performance Ratio PR

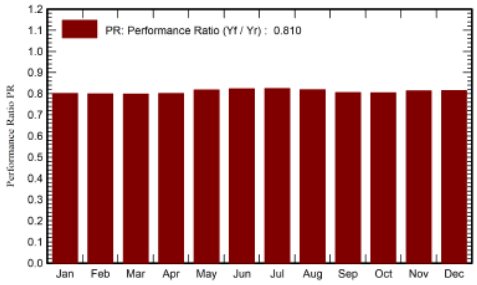

APPENDIX H: Optimized tilt angle simulations graph for Kenyatta University

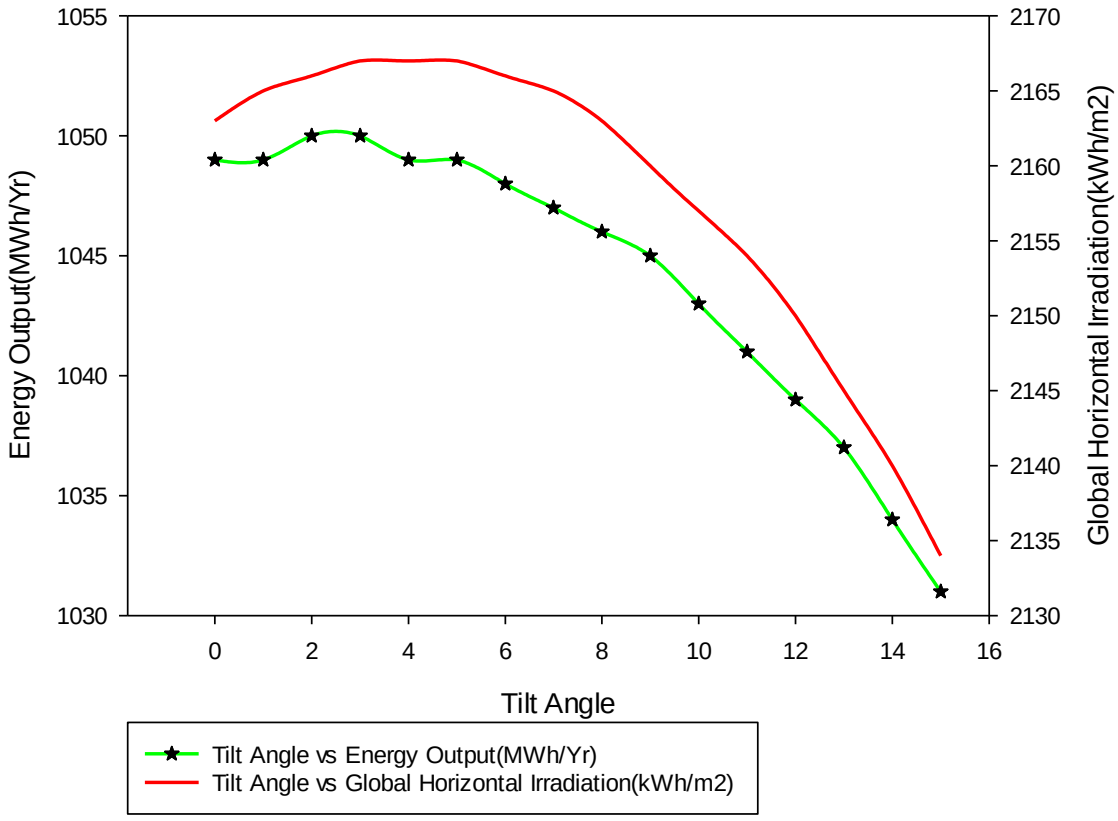

APPENDIX I: Loss diagram for 15° tilted Solar PV modules at Kenyatta University

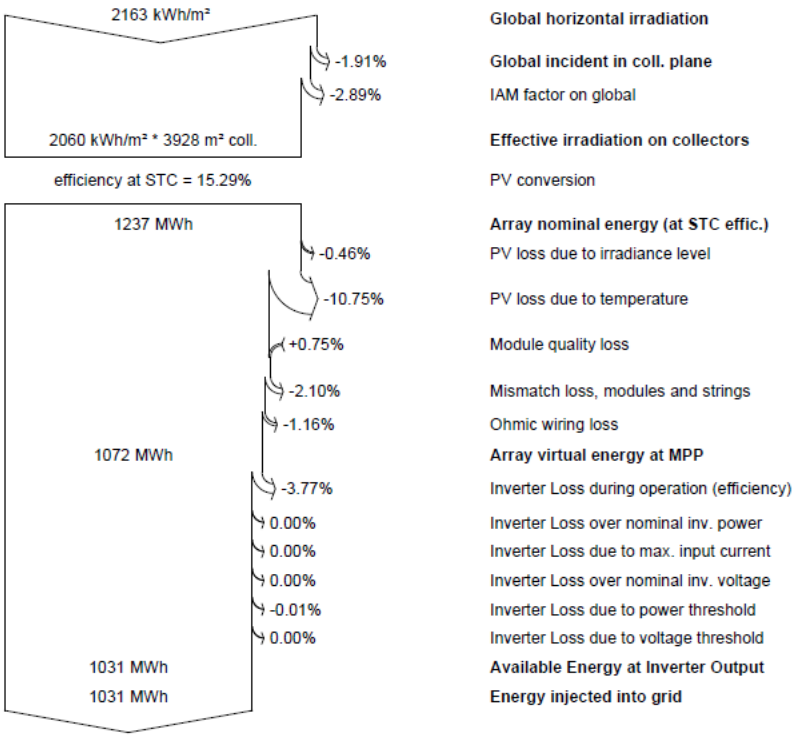

APPENDIX J: Table displaying Performance parameters for different grid-connected PV systems

Location	PV type	System size(kWp)	Specific Energy Yield (kWh/kWp)	Final yield (kWh/kWp)	Total Collection losses (kWh/kWp)	Performance Ratio (%)	Capacity Utilization Factor (%)	Reference yield (kWh/kWp)
Dublin, Ireland	Mc-si	1.72	885.1	2.4	-	81.5	-	-
India	P-si	11.2	-	3.67	-	78	-	
Brazil		2.2	1685.5	4.6	-	82.9	19.2	5.6
Strathmore, Nairobi	p-si	600	1225	3.37	2.51	57.4	13.97	5.9
India	p-si	5	1435.08	3.99	1.24	76.97	16.39	5.23
Morocco	p-si	5	1282.26	4.45	-	79	14.84	-
India		20	1507	-	-	82	17.2	-
India		50	1278.8	-	-	69.3	5.8	-
Ghana		2500	1419.12			70.6	16.2	
South Africa	p-si	8	2022.25	4.93	0.66	87.1	-	5.59
Serbia		2	1161.66	-	-	93.6	12.88	-
Mauritania		15000	-	-	2.05	68.6	16.14	5.875

APPENDIX K: Table illustrating Geographical site Solar Radiation and Ambient Temperature (NASA-SSE) for 2019

Month	Ambient Temp.(C)	Solar Radiation(kWh/m2)
Jan	21.64	6.66
Feb	23.56	7.09
Mar	25.18	7.27
Apr	24.38	6.49
May	21.30	5.44
Jun	19.92	4.36
Jul	20.64	5.25
Aug	21.63	5.59
Sep	22.89	6.11
Oct	21.5	5.83
Nov	20.77	5.94
Dec	19.93	5.79
Average	21.95	5.98

APPENDIX L: Table illustrating Energy generated by the Strathmore University Solar PV system for 2019

Year 2019	Energy (Wh)
January	75345776
February	74797904
March	83335328
April	69038144
May	53048572
June	41131656
July	44523644
August	51618884
September	59940820
October	58022944
November	63610296
December	60293752

APPENDIX M: Table showing the experimental design for the Kenyatta University Energy Technology Building site

Panel	Air gap(mm)	Tilt Angle (Degrees)
1	150	4
2	100	4
3	150	11
4	100	11
5	150	15
6	100	15

APPENDIX N: Approval of Research Proposal

KENYATTA UNIVERSITY
GRADUATE SCHOOL

E-mail: dean-graduate@ku.ac.ke
Website: www.ku.ac.ke

P.O. Box 43844, 00100
NAIROBI, KENYA
Tel. 020-8704150

Internal Memo

FROM: Dean, Graduate School

DATE: 16th August, 2019

TO: Mr. Ayora Emmanuel
C/o Department of Energy Technology

REF: J104/39125/2016

SUBJECT: APPROVAL OF RESEARCH PROPOSAL

This is to inform you that Graduate School Board, at its meeting on 7th August, 2019, approved your Research Proposal for the M.Sc. Degree entitled, **"Performance Evaluation and Optimization of Grid Tied Solar Photovoltaic Systems: A Case Study of Kenyatta University 100kw Solar Plant."**

You may now proceed with your Data collection, subject to clearance with the Director General, National Commission for Science, Technology & Innovation.

As you embark on your data collection, please note that you will be required to submit to Graduate School completed Supervision Tracking Forms per semester. The form has been developed to replace the Progress Report Forms. The Supervision Tracking Forms are available at the University's Website under Graduate School webpage downloads.

Thank you.

EDWIN OBUNGU
FOR: DEAN, GRADUATE SCHOOL

CC. Chairman, Department of Energy Technology

Supervisors:

1. Dr. Keren Kaberere
   Jomo Kenyatta University of Agriculture & Technology
   Department of Electrical and Electronics Engineering
   C/o Energy Technology Department
   Kenyatta University
2. Prof. Maurice Mangoli
   C/o Department of Electrical & Electronics Engineering
   Kenyatta University
3. Dr. Mathew Munji
   C/o Department of Physics
   Kenyatta University

APPENDIX O: Research Authorization

KENYATTA UNIVERSITY
GRADUATE SCHOOL

E-mail: dean-graduate@ku.ac.ke
Website: www.ku.ac.ke

P.O. Box 43844, 00100
NAIROBI, KENYA
Tel. 020-8704150

Our Ref: J104/39125/2016

DATE: 16th February, 2019

Director General,
National Commission for Science, Technology
and Innovation
P.O. Box 30623-00100
NAIROBI

Dear Sir/Madam,

RE: RESEARCH AUTHORIZATION FOR MR. AYORA EMMANUEL – REG. NO. J104/39125/2016

I write to introduce Mr. Ayora Emmanuel who is a Postgraduate Student of this University. He is registered for M.Sc. degree programme in the **Department of Energy Technology.**

Mr. Ayora intends to conduct research for a M.Sc. thesis Proposal entitled, **"Performance Evaluation and Optimization of Grid Tied Solar Photovoltaic Systems: A Case Study of Kenyatta University 100kw Solar Plant."**

Any assistance given will be highly appreciated.

Yours faithfully,

PROF. ELISHIBA KIMANI
DEAN, GRADUATE SCHOOL

APPENDIX P: Research Permit

REPUBLIC OF KENYA

NATIONAL COMMISSION FOR SCIENCE,TECHNOLOGY & INNOVATION

Ref No: 522911

Date of Issue: 26/August/2020

RESEARCH LICENSE

This is to Certify that Mr.. emmanuel ayora of Kenyatta University, has been licensed to conduct research in Nairobi on the topic: Performance Evaluation and Optimization of Grid Tied Solar Photovoltaic Systems: A Case Study of Kenyatta University 100kw Solar Plant for the period ending : 26/August/2021.

License No: NACOSTI/P/20/6370

522911

Applicant Identification Number

Director General
NATIONAL COMMISSION FOR SCIENCE,TECHNOLOGY & INNOVATION

Verification QR Code

NOTE: This is a computer generated License. To verify the authenticity of this document, Scan the QR Code using QR scanner application.